

Electronic Thesis and Dissertation Repository

---

10-14-2016 12:00 AM

## A Biomechanical Investigation of Scaphoid and Lunate Kinematics During Wrist Motion

Helen L. Stoesser  
*The University of Western Ontario*

Supervisor

Dr. James Johnson  
*The University of Western Ontario* Joint Supervisor

Dr. Graham King  
*The University of Western Ontario*

Graduate Program in Biomedical Engineering

A thesis submitted in partial fulfillment of the requirements for the degree in Master of Engineering Science

© Helen L. Stoesser 2016

Follow this and additional works at: <https://ir.lib.uwo.ca/etd>



Part of the [Biomechanics and Biotransport Commons](#)

---

### Recommended Citation

Stoesser, Helen L., "A Biomechanical Investigation of Scaphoid and Lunate Kinematics During Wrist Motion" (2016). *Electronic Thesis and Dissertation Repository*. 4360.  
<https://ir.lib.uwo.ca/etd/4360>

This Dissertation/Thesis is brought to you for free and open access by Scholarship@Western. It has been accepted for inclusion in Electronic Thesis and Dissertation Repository by an authorized administrator of Scholarship@Western. For more information, please contact [wlsadmin@uwo.ca](mailto:wlsadmin@uwo.ca).

## ***Abstract***

Carpal kinematics have been previously investigated, yet there remains no consensus regarding the relative contribution of each bone to total wrist motion. A more detailed understanding of carpal kinematics is essential in the effective diagnosis and treatment of injuries of the wrist, as many injuries manifest as an alteration in intercarpal kinematics. The scapholunate (SL) ligament is one of the most commonly injured intercarpal articulations resulting in a cascade of degenerative changes included cartilage wear and altered joint kinematics. The SL ligament is considered the primary stabilizer of the SL joint but is surrounded by a complex network of secondary ligamentous constraints, each contributing to the maintenance of normal SL kinematics. The ligamentous anatomy of the SL ligament and secondary stabilizers has been well established, although the functional and stabilizing role of each structure remains unclear. This work investigates the relative role and contribution of the scaphoid, lunate, and surrounding ligamentous restraints during planar wrist motions. An *in vitro* study examined the kinematics of the scaphoid, lunate, and capitate during planar motions of wrist flexion and extension. Scaphoid and lunate motion was found to correlate linearly with wrist motion throughout flexion and extension, with the scaphoid contributing at a greater degree throughout flexion-extension. Both the scaphoid and lunate were found to contribute more to wrist motion during flexion when compared to extension. A subsequent *in vitro* study examined the effect of the sequential sectioning of the SL ligament and two secondary stabilizers, the scaphotrapezium-trapezoid (STT) ligament and the radioscaphocapitate (RSC) ligament, on scaphoid and lunate kinematics during wrist flexion-extension and radial-ulnar deviation. The SL ligament was found to be the primary stabilizer of the SL joint, as sectioning caused the largest angular change in SL kinematics, and the STT and RSC ligaments are secondary stabilizers, as the additional sectioning induced further postural changes in SL kinematics. A more detailed understanding of role and stabilizing function of the SL ligament and secondary stabilizers may assist in the development of more effective treatment strategies following injury to the SL articulation.

**Keywords:** Wrist; Carpal Bones; Scaphoid; Lunate; Carpal Instability; Scapholunate Ligament

## ***Co-Authorship Statement***

**CHAPTER 1** Sole Authorship

**CHAPTER 2** ***Study Design*** – Masao Nishiwaki, Braden Gammon, Graham King, James Johnson

***Data Collection*** – Masao Nishiwaki, Braden Gammon

***Data Analysis*** – Helen Stoesser

***Technical Oversight*** – Daniel Langohr, Emily Lalone

***Statistical Analysis*** – Helen Stoesser

***Writing*** – Helen Stoesser

***Revisions*** – Helen Stoesser, Daniel Langohr, Emily Lalone, Graham King, James Johnson

**CHAPTER 3** ***Study Design*** – Helen Stoesser, Nina Suh, Graham King, James Johnson

***Data Collection*** – Helen Stoesser, Clare Padmore, Duncan Iglesias

***Data Analysis*** – Helen Stoesser

***Technical Oversight*** – Daniel Langohr

***Statistical Analysis*** – Helen Stoesser

***Writing*** – Helen Stoesser

***Revisions*** – Helen Stoesser, Daniel Langohr, Nina Suh, Graham King, James Johnson

**CHAPTER 4** Sole Authorship

**APPENDIX A** Sole Authorship

**APPENDIX B** Helen Stoesser, Jason Lockhart

**APPENDIX C** Helen Stoesser, Duncan Iglesias

## *Acknowledgments*

The completion of this thesis was possible with the support of numerous individuals. First and foremost, I express my sincere gratitude to my supervisors Dr. James Johnson and Dr. Graham King for their untiring support and guidance throughout this process. Their passion, dedication, and immense knowledge was invaluable to the success of this project. I am privileged to have studied under two such accomplished researchers.

My thanks to Dr. Nina Suh whose continual enthusiasm and commitment to this project is much appreciated. All of the hours committed to early morning specimen preparation and the long testing days did not go unnoticed. It was a joy to work alongside such a skilled surgeon.

I express my appreciation to all of my colleagues and lab mates at the HULC, especially Dr. Daniel Langohr, Dr. Emily Lalone, Duncan Iglesias, and Clare Padmore. Dan was instrumental in the completion of this thesis providing unwavering council, support, and guidance over the course of the past two years. Emily was a valuable resource throughout this process, always eager to help and so generous with her time. Duncan's hard work and dedication put into the Wrist Simulator along with the countless hours he devoted to testing made this thesis achievable. Clare was always my "tag-team" partner from day one and has made this process both manageable and fun. The rest of the HULC students, both past and present, have provided so many great memories over the last two years; working alongside such a knowledgeable group of individuals has been extremely rewarding.

Finally, I thank my parents for their unconditional love and encouragement over the last two years; they have always been my biggest supporters.

# *Table of Contents*

<b>Abstract</b> .....	i
<b>Co-Authorship Statement</b> .....	ii
<b>Acknowledgments</b> .....	iii
<b>Table of Contents</b> .....	iv
<b>List of Tables</b> .....	vii
<b>List of Figures</b> .....	viii
<b>List of Appendices</b> .....	xi
<b>List of Abbreviations</b> .....	xii
<b>Chapter 1</b> .....	1
1 Introduction.....	1
1.1 Anatomy of the Hand and Wrist.....	2
1.1.1 Bony Anatomy .....	2
1.1.2 Joints .....	15
1.1.3 Ligamentous Anatomy.....	19
1.1.4 Musculature.....	27
1.2 Wrist Kinematics .....	32
1.2.1 Range of Motion .....	32
1.3 Clinical Disorders of the Wrist.....	36
1.3.1 Fractures.....	37
1.3.2 Carpal Instability.....	39
1.3.3 Arthritis.....	41
1.4 Biomechanical Analyses.....	42
1.4.1 Wrist Motion Simulation .....	42

1.5 Thesis Rationale.....	49
1.6 Objectives and Hypotheses.....	51
1.6.1 Specific Objectives .....	51
1.6.2 Specific Hypotheses.....	52
1.7 Thesis Overview .....	53
1.8 References.....	54
<b>Chapter 2</b> .....	<b>59</b>
2 Biomechanical Evaluation of Carpal Kinematics During Simulated Wrist Motion .....	59
2.1 Introduction.....	60
2.2 Materials and Methods .....	61
2.2.1 Specimen Preparation .....	61
2.2.2 Testing Protocol .....	63
2.2.3 Outcome Variables and Data Analysis .....	63
2.2.4 Statistical Methods.....	64
2.3 Results.....	65
2.3.1 Flexion-Extension of the Scaphoid and Lunate .....	65
2.3.2 Ratio of Scaphoid and Lunate Rotation to Wrist Rotation .....	67
2.3.3 Direction of Motion .....	69
2.4 Discussion.....	70
2.5 Conclusions.....	73
2.6 References.....	74
<b>Chapter 3</b> .....	<b>78</b>
3 Biomechanical Evaluation of the Scapholunate Ligament and Secondary Stabilizers on Scaphoid and Lunate Kinematics.....	78
3.1 Introduction.....	79
3.2 Materials and Methods .....	81

3.2.1	Specimen Preparation .....	81
3.2.2	Testing Protocol .....	84
3.2.3	Outcome Variables and Data Analysis .....	86
3.2.4	Statistical Analysis.....	87
3.3	Results.....	88
3.3.1	Scaphoid and Lunate Kinematics During Wrist Flexion-Extension.....	88
3.3.2	Scaphoid and Lunate Kinematics During Wrist Radial-Ulnar Deviation.	95
3.4	Discussion.....	102
3.5	Conclusions.....	107
3.6	References.....	108
<b>Chapter 4</b>	.....	112
4	General Discussion and Conclusions .....	112
4.1	Summary.....	113
4.1.1	Chapter 2: Biomechanical Evaluation of Carpal Kinematics During Simulated Wrist Motion.....	114
4.1.2	Chapter 3: Biomechanical Evaluation of the Scapholunate Ligament and Secondary Stabilizers on Scaphoid and Lunate Kinematics .....	115
4.2	Strengths and Limitations .....	116
4.3	Current and Future Directions .....	118
4.4	Significance .....	119
<b>Appendices</b>	.....	120
Appendix A	– Glossary.....	120
Appendix B	– Carpal Tracker Mounts.....	122
Appendix C	– Carpal Coordinate System Constrution .....	125
Curriculum Vitae	.....	127

***List of Tables***

Table 3-1: Sequence of Incremental Sectioning of the Scapholunate Ligament and  
Secondary Stabilizers.....84



## ***List of Figures***

Figure 1-1: Bony Anatomy of the Radius .....	4
Figure 1-2: Bony Anatomy of the Ulna .....	6
Figure 1-3: Carpal Bones.....	7
Figure 1-4: Bony Anatomy of the Capitate.....	8
Figure 1-5: Bony Anatomy of the Scaphoid.....	9
Figure 1-6: Bony Anatomy of the Lunate.....	11
Figure 1-7: Metacarpals.....	12
Figure 1-8: Bony anatomy of the 3 <sup>rd</sup> Metacarpal.....	13
Figure 1-9: Joints of the Wrist .....	18
Figure 1-10: Volar Ligaments of the Wrist.....	25
Figure 1-11: Dorsal Ligaments of the Wrist.....	25
Figure 1-12: Scapholunate Interosseous Ligament.....	26
Figure 1-13: Muscles of the Wrist .....	28
Figure 1-14: Range of Wrist Motion: Flexion-Extension.....	33
Figure 1-15: Range of Wrist Motion: Radial-Ulnar Deviation.....	34
Figure 1-16: Range of Wrist Motion: Pronation-Supination .....	35
Figure 1-17: Scaphoid Fracture .....	38
Figure 1-18: Carpal Instability.....	40
Figure 1-19: Rheumatoid Arthritis in the Wrist.....	41

Figure 1-20: Nishiwaki’s Motion Wrist Simulator.....	44
Figure 1-21: Dunning’s Active Motion Wrist Simulator.....	46
Figure 1-22: Werner’s Active Motion Wrist Simulator.....	47
Figure 1-23: Iglesias’ Active Motion Wrist Simulator.....	48
Figure 2-1: <i>In Vitro</i> Passive Motion Wrist Simulator.....	62
Figure 2-2: Flexion-Extension of the Scaphoid and Lunate. ....	66
Figure 2-3: Ratio of Carpal Rotation to Wrist Rotation. ....	67
Figure 2-4: Average Ratio of Carpal Rotation to Wrist Rotation.....	68
Figure 2-5: Effect of Direction of Motion .....	69
Figure 3-1: Scaphoid and Lunate Tracker Placement.....	82
Figure 3-2: In Vitro Active Motion Simulator.....	83
Figure 3-3: Stages of Sectioning the Scapholunate Ligament and Secondary Stabilizers. ....	85
Figure 3-4: Scapholunate Intercarpal Motion.....	87
Figure 3-5: Scaphoid Flexion-Extension Following Sequential Ligament Sectioning During Wrist Flexion-Extension.....	89
Figure 3-6: Lunate Flexion-Extension Following Sequential Ligament Sectioning During Wrist Flexion-Extension.....	91
Figure 3-7: Mean Angular Change in Carpal Motion During Wrist Flexion-Extension....	92
Figure 3-8: Scapholunate Intercarpal Motion Following Sequential Ligament Sectioning During Wrist Flexion-Extension.....	94

Figure 3-9: Scaphoid Flexion-Extension Motion Following Sequential Ligament Sectioning During Wrist Radial-Ulnar Deviation.....	96
Figure 3-10: Lunate Flexion-Extension Motion Following Sequential Ligament Sections During Wrist Radial-Ulnar Deviation.....	98
Figure 3-11: Mean Angular Change in Carpal Motion During Wrist Radial-Ulnar Deviation.....	99
Figure 3-12: Scapholunate Intercarpal Motion Following Sequential Ligament Sections During Wrist Radial-Ulnar Deviation.....	101
Figure B-1: Scaphoid Tracker Mount.....	122
Figure B-2: Lunate Tracker Mount.....	123
Figure B-3: Carpal Tracker Mount.....	124
Figure C-1: Construction of the Neutral Carpal Frame .....	126

***List of Appendices***

Appendix A – Glossary..... 120

Appendix B – Carpal Tracker Mounts..... 122

Appendix C – Carpal Coordinate System Construction ..... 125

## *List of Abbreviations*

APL	Abductor Pollicis Longus
DOF	Degrees of Freedom
DRC	Dorsal Radiocarpal
DRU	Dorsal Radioulnar
DRUJ	Distal Radioulnar Joint
ECRB	Extensor Carpi Radialis Brevis
ECRL	Extensor Carpi Radialis Longus
ECU	Extensor Carpi Ulnaris
FCR	Flexor Carpi Radialis
FCU	Flexor Carpi Ulnaris
FEM	Flexion-Extension Motion
LRL	Long Radiolunate
PQ	Pronator Quadratus
PT	Pronator Teres
RUD	Radial-Ulnar Deviation
RSC	Radioscaphocapitate
RSL	Radioscapholunate
SC	Scaphocapitate
SL	Scapholunate
SRL	Short Radiolunate
STT	Scaphotrapezium-Trapezoid
UC	Ulnocapitate

# Chapter 1

## 1 *Introduction*

### *Overview*

*The purpose of this thesis is to evaluate the in-vitro kinematics of the capitate, scaphoid, and lunate during unconstrained simulated wrist motion. The role of the scapholunate ligament and the secondary stabilizers of the scapholunate joint will be analyzed with respect to scaphoid and lunate kinematics. As an introduction, this chapter will focus on the anatomy and kinematics of the wrist joint. The role and current state of previously implemented in-vitro simulators will be reviewed. The objective, hypothesis, rationale, and outline of the thesis are highlighted.*

## 1.1 **Anatomy of the Hand and Wrist**

The wrist is a complex joint structure linking the hand to the forearm. The wrist is comprised of numerous structures each with an essential role in maintaining function and mobility of the joint. The joint complex consists of multiple articulations between the bones of the distal forearm, the carpal bones, the metacarpals, the phalanges and each other. The wrist also is surrounded by a network of soft tissues including the tendons that cross or attach onto the carpus and the ligaments that connect carpal bones to one another and the bony structures of the hand and forearm.<sup>1</sup>

### 1.1.1 ***Bony Anatomy***

The hand consists of twenty-seven bones that articulate with the two bones of the distal forearm in order to provide the necessary structure to perform everyday tasks.<sup>2</sup> Bones are formed with two layers of tissue, a dense outer layer termed cortical or compact bone, and a porous inner layer termed trabecular or cancellous bone.<sup>2</sup> Bones are typically categorized into one of four groups: long, short, flat or irregular; with only long and short bones residing in the hand. Long bones consist of three regions, the shaft and the proximal and distal extremities.<sup>2</sup> The shaft or diaphysis spans the length of the bone and the extremities or epiphysis allows the bone to articulate with adjacent bones.<sup>2,3</sup> Short bones are cuboidal, equally wide as they are long, and provide support with little relative motion.<sup>4</sup>

#### 1.1.1.1 *Radius*

The radius is the shorter of the two parallel long bones that make up the forearm and is located on the lateral side of the ulna when placed in neutral anatomic position (Fig. 1-1).<sup>5</sup> The radial head is a cylindrical articular structure at the proximal end of the radius.<sup>2</sup> The cupped proximal surface, termed the articular dish, articulates with the capitellum of the distal humerus allowing for axial rotation of the forearm.<sup>5</sup> The articular circumference of the radial head articulates with the radial notch of the proximal ulna.<sup>5</sup> Coursing distally past the radial head the radius begins to narrow forming the radial neck and eventually the shaft of the bone.<sup>2</sup> The radial tuberosity is the rough projection found on the medial, anterior surface of the proximal radius and acts as the insertion site for the biceps brachii tendon.<sup>2,5</sup> The radial shaft bows laterally along the length of the bone with a prismoid cross sectional area forming four surfaces: dorsal, volar, medial and lateral.<sup>2</sup> At the distal end of the radius the diaphysis diverges forming two articulating surfaces: the ulnar notch, located on the medial side to articulate with the distal ulna, and the smooth concave groove on the distal surface to articulate with the proximal carpus.<sup>2</sup> The concave surface of the distal radius has two separate articular facets: the scaphoid and lunate fossa.<sup>6</sup> The fossae are separated by the cartilaginous sagittal ridge known as the interfacet prominence, forming a congruent articulation between the proximal scaphoid and lunate.<sup>6</sup> The lateral edge of the distal radius extends more distally forming the radial styloid process. This conical shaped osseous projection constrains the proximal pole of the scaphoid and is the site of attachment for the radioscaphocapitate ligament.<sup>2,6</sup>



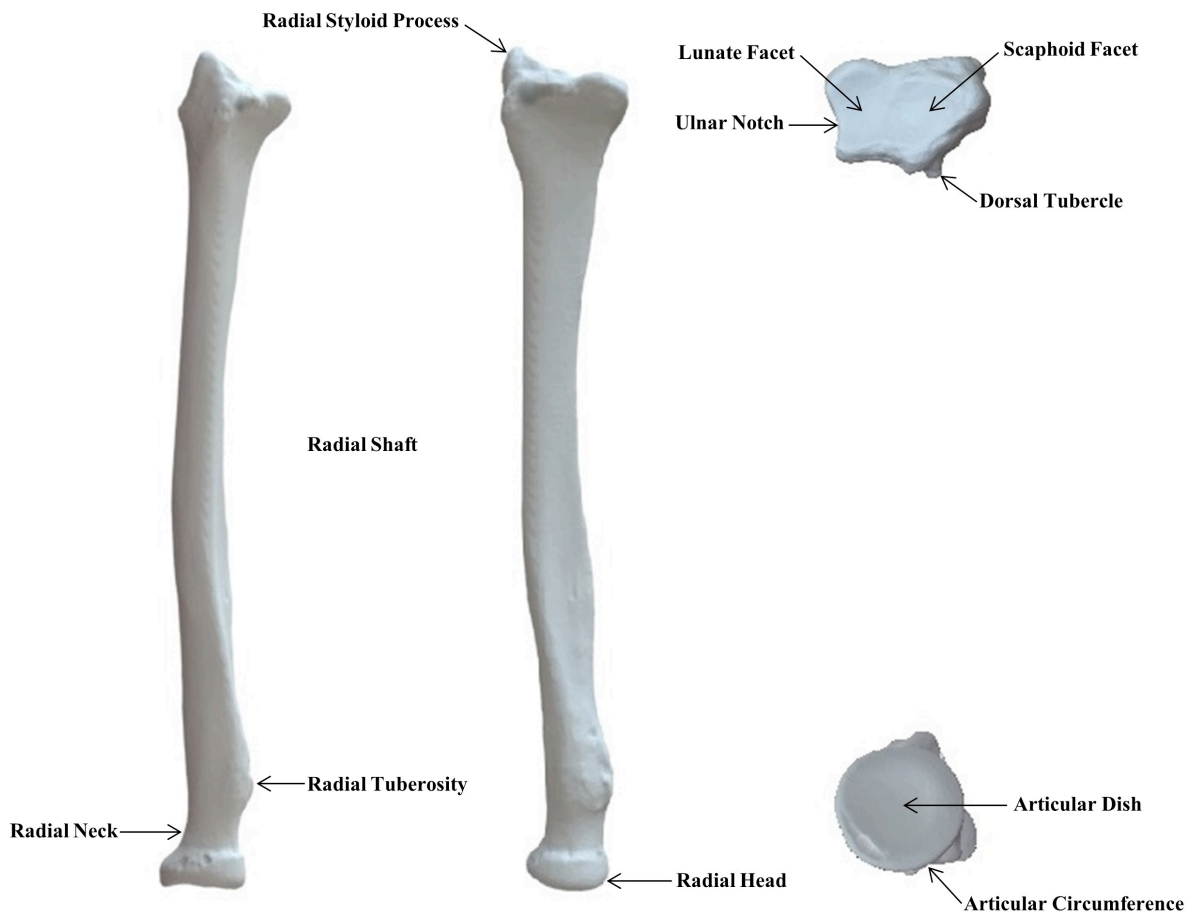


**Figure 1-1: Bony Anatomy of the Radius.** Bony anatomy of the left radius with important landmarks. (A) Lateral View, (B) Anterior View, (C) Distal Articular Surface, and (D) Proximal Articular Surface.

### 1.1.1.2 *Ulna*

The ulna is the longer of the two parallel long bones within the forearm located on the medial side of the radius when in neutral anatomic position (Fig. 1-2).<sup>5</sup> The ulna is formed by three segments: the proximal portion, the shaft, and the distal portion.<sup>2</sup> The ulna converges to a smaller head at the distal end of the diaphysis.<sup>2</sup> At the proximal end the ulna forms a cup like projection articulating with the trochlea of the humerus and the head of the radius.<sup>5</sup> This projection can be grouped into three different sections: the olecranon process, the trochlear notch, and coronoid process.<sup>2,5</sup> At the proximal most edge of the projection is the olecranon process with an anterior-inferior smoothed concave surface that forms the superior aspect of the trochlear notch.<sup>2</sup> At the distal end of the trochlear notch is the coronoid process characterized by a smooth anterior-superior surface which closes the cup like projection.<sup>2</sup> The trochlear notch is formed by the concave region residing between the two projections forming a hinge joint to articulate with the trochlea of the humerus.<sup>5</sup> A guiding ridge separates the medial and lateral facets of the sigmoid notch. The radial notch, located on the lateral side of the proximal ulna, is characterized by its concave groove which articulates with the radial head allowing rotation about the ulna during forearm pronation and supination.<sup>5</sup> The ulnar head has two distinct surfaces: on the lateral side a round surface to articulate with the sigmoid notch of the distal radius; and projecting distally on the medial side the ulnar styloid process.<sup>5,6</sup>

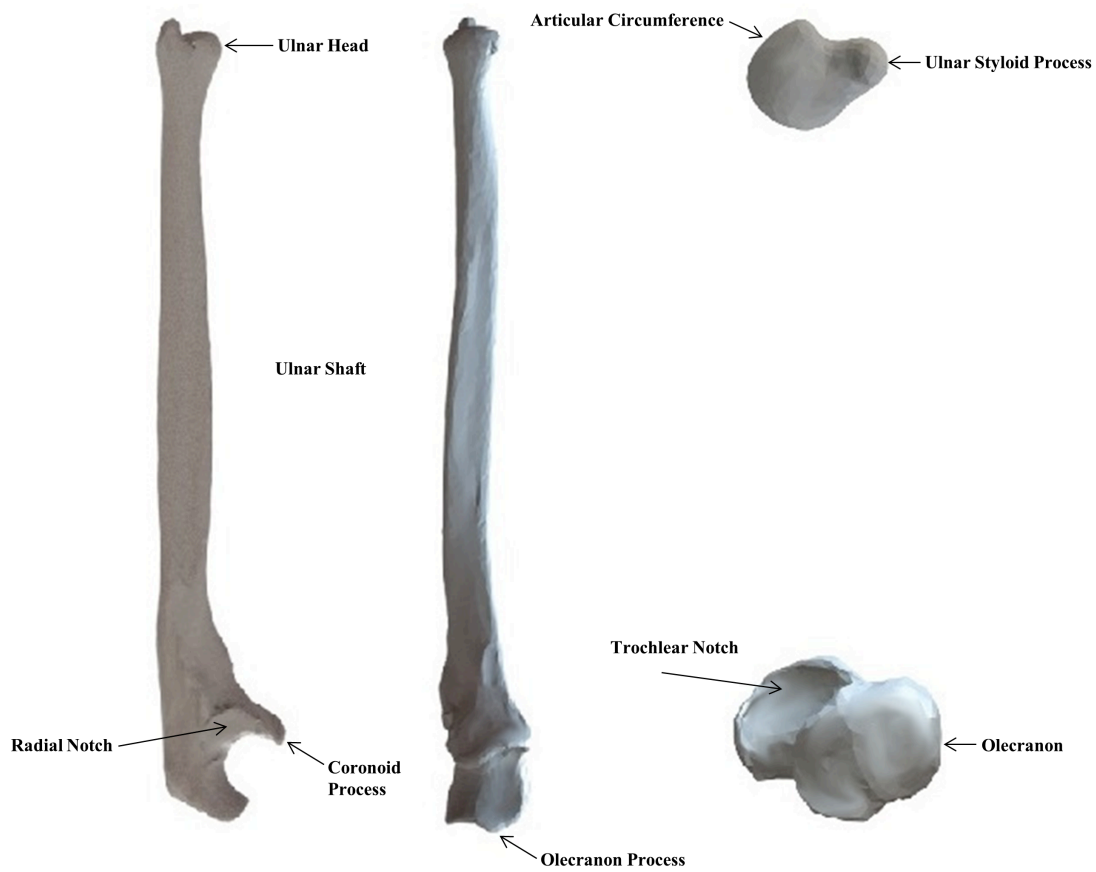


**Figure 1-2: Bony Anatomy of the Ulna.** Bony anatomy of the left ulna with important landmarks. (A) Lateral View, (B) Anterior View, (C) Distal Articular Surface, and (D) Proximal Articular Surface.

### 1.1.1.3 *Carpal Bones*

The carpus is composed of eight carpal bones which are conveniently divided into two anatomic rows, a proximal and distal carpal row (Fig. 1-3).<sup>2</sup> Moving radially, the proximal carpal row is composed of the scaphoid, lunate, triquetrum and pisiform, while the distal carpal row is formed by the trapezium, trapezoid, capitate and hamate.<sup>7</sup> As the pisiform is a sesamoid bone within the flexor carpi ulnaris tendon it is frequently excluded as being considered a true carpal bone.<sup>7</sup> Each carpal bone, with the exception of the pisiform, presents with six surfaces dedicated to articular contact or capsular attachment.<sup>2,7</sup> The structure of each bone remains similar, cancellous tissue enclosed by compact bone.<sup>2</sup> For the purpose of this thesis only the capitate, scaphoid and lunate will be discussed in detail.

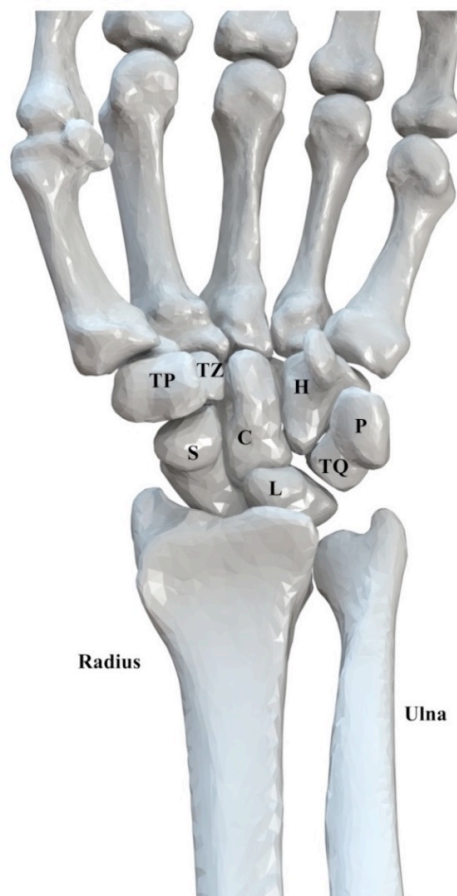


**Figure 1-3: Carpal Bones.** Volar view of the left hand showing the eight carpal bones and the distal radius and ulna. The proximal carpal row is formed by the scaphoid (S), lunate (L), triquetrum (TQ), and pisiform (P). The distal carpal row is formed by the trapezium (TP), trapezoid (TZ), capitate (C), and hamate (H).

### 1.1.1.3.1 *Capitate*

The capitate, positioned in the centre of the wrist, is the largest carpal bone and acts as the basis for the transverse carpal arch (Fig. 1-4).<sup>6</sup> The capitate has two nonarticular surfaces, volar and dorsal. The rough volar surface acts as an attachment site for the distal ligaments crossing over the midcarpal joint, while the dorsal surface contains foramina for blood vessels.<sup>6</sup> The head of the capitate is formed by the proximal one-third of the bone. This cartilage covered region is characterized by its spheroidal shape allowing for three different regions with differing radii of curvature for articular contact.<sup>6</sup> The lateral aspect is for the scaphoid, the proximal region for the lunate and the medial aspect, which is almost flat, for the hamate.<sup>6</sup> The radial portion of the distal aspect of the capitate, termed the body, is a flat cartilage covered region and contains an articular facet for the trapezoid.<sup>6</sup> The ulnar aspect of the capitate, not covered in cartilage, holds a distal volar depression which acts as the attachment site of the capitolunate interosseous ligament.<sup>6</sup> The distal articular surface of the capitate has two facets, one slightly concave facet which articulates with the base of the third metacarpal and one small lateral facet which articulates with the styloid process of the second metacarpal.<sup>6</sup>

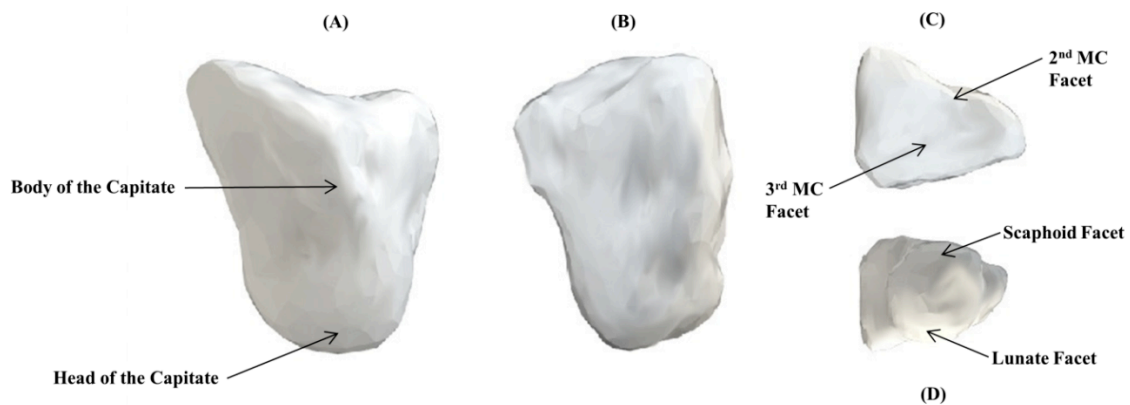


**Figure 1-4: Bony Anatomy of the Capitate.** Bony anatomy of the left capitate with important landmarks. (A) Lateral View, (B) Volar View, (C) Distal Articular Surface, and (D) Proximal Articular Surface.

### 1.1.1.3.2 *Scaphoid*

The scaphoid is the largest carpal bone of the proximal row and is located on the radial side of the carpus (Fig. 1-5).<sup>2</sup> The scaphoid plays a critical stabilizing link between the proximal and distal carpal rows.<sup>6</sup> The scaphoid has four articular facets covering the majority of its surface: a proximal-lateral convex facet, articulates with the scaphoid fossa and distal radius; a medial semilunar facet, articulates with the lateral region of the lunate; a distal-medial concave oval facet, articulates with the lateral surface of the head of the capitate; and a distal convex articular surface, commonly separated by a smooth sagittal ridge, for the trapezoid and trapezium.<sup>6</sup> The scaphoid tubercle or tuberosity, located between the proximal and articular surfaces on the volar aspect of the bone provides an attachment point for ligaments.<sup>6</sup> This non articular surface continues laterally along the surface of the scaphoid forming the waist of the bone, where the majority of the vascular elements enter.<sup>6</sup> The dorsal surface of the scaphoid is narrower and shorter than the opposing volar surface.<sup>6</sup> The proximal margin of the medial surface contains the articulation for the lunate as well as a roughened edge as the point of attachment for the scapholunate interosseous ligament.<sup>6</sup> The long axis of the scaphoid is obliquely orientated in both the sagittal and coronal planes with the wrist in the neutral anatomic position.<sup>6</sup>

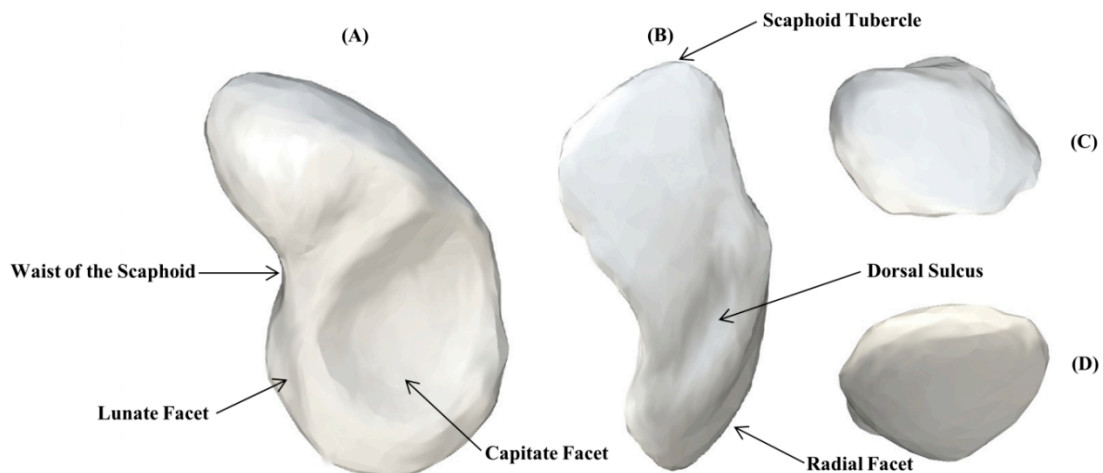


**Figure 1-5: Bony Anatomy of the Scaphoid.** Bony anatomy of the left scaphoid with important landmarks. (A) Medial View, (B) Dorsolateral View, (C) Distal Articular Surface, and (D) Proximal Articular Surface.

#### 1.1.1.3.3 *Lunate*

The lunate is characterized by its moon-shaped structure, larger volarly than dorsally (Fig. 1-6). The lunate is positioned in the center of the proximal row between the scaphoid, on the radial side, and the triquetrum, on the ulnar side.<sup>2</sup> The lunate consists of four articular surfaces: proximal, distal, lateral and medial; and two non-articular sides: volar and dorsal.<sup>6</sup> The distal biconcave articular surface of the lunate, houses the midcarpal condyle formed by the head of the capitate and the proximal pole of the hamate.<sup>6</sup> For the majority of the population the distal region of the lunate forms two facets: a larger lateral facet for the capitate and a smaller more medial facet for the hamate.<sup>6</sup> In some patients there is no articulation of the lunate with the hamate. Through its flat semilunar articular surfaces the lunate articulates laterally with the scaphoid and medially with the triquetrum.<sup>6</sup> The roughened edges on the proximal margins of both the lateral and medial facets allow for the scapholunate and lunotriquetral interosseous ligaments to insert.<sup>6</sup> The proximal biconvex articular surface of the lunate has a larger radius of curvature than that of the adjacent scaphoid.<sup>6</sup> When the wrist is in the neutral anatomic position roughly two-thirds of the proximal region articulates with the distal radius while the remaining portion articulates with the triangular fibrocartilage, a structure that connects the distal radius and ulna.<sup>6</sup> The non articular volar region of the lunate is roughened containing a large number of vascular foramina and is the site of attachment for numerous ligaments.<sup>6</sup> The smaller, non articular dorsal region of the lunate is triangular and is the attachment site for important stabilizing ligaments.<sup>6</sup> The volar and dorsal poles of the lunate are formed via the distal edge of the two non articular surfaces and have an important stabilizing role during wrist flexion and extension.<sup>6</sup>

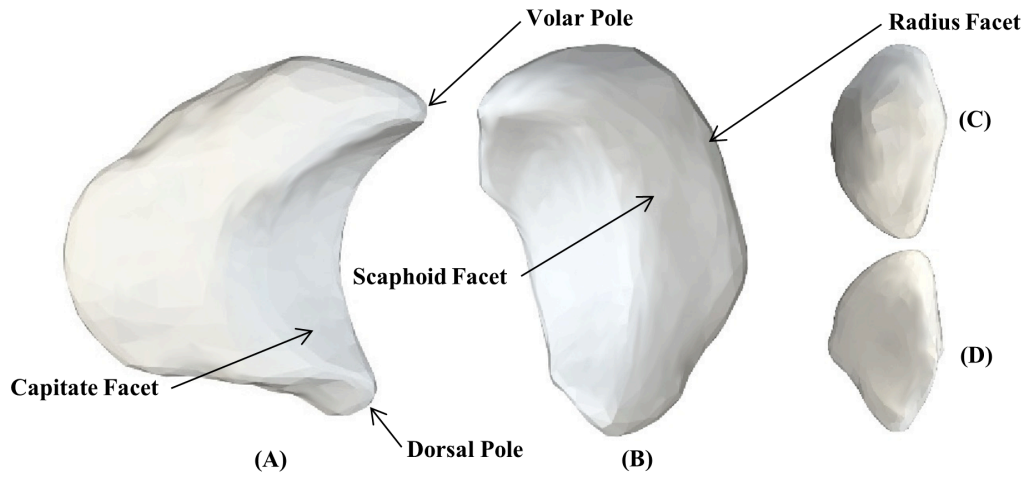


**Figure 1-6: Bony Anatomy of the Lunate.** Bony anatomy of the left lunate with important landmarks. (A) Distal Articular Surfaces, (B) Proximal Articular Surfaces, (C) Medial View, and (D) Lateral View.



#### 1.1.1.4 *Metacarpals*

The metacarpals comprise five long cylindrical bones that make up the structure of the palm and hand (Fig. 1-7). Moving radially, the naming convention starts with the thumb termed the first metacarpal and the small finger the fifth metacarpal.<sup>2</sup> Each metacarpal is composed of a proximal metaphysis, a diaphysis, and a distal metaphysis (Fig. 1-8).<sup>2</sup> The proximal metaphyses of the metacarpal bones are cuboidal and articulate with one another via flat mediolateral facets.<sup>6</sup> The concave proximal portion of each metacarpal articulates closely with the corresponding carpal(s) in the distal row of the wrist.<sup>2</sup> Whereas, the distal metaphysis of each metacarpal is convex and articulates with the base of the corresponding proximal phalange.<sup>2</sup> The diaphysis of each metacarpal consists of four non articular surfaces: medial, lateral, volar and dorsal. The medial and lateral surfaces of the bone are concave acting as an attachment site for interosseous muscles, while the dorsal aspect of the bone is broad and flattened allowing for extensor tendon insertion.<sup>2</sup>

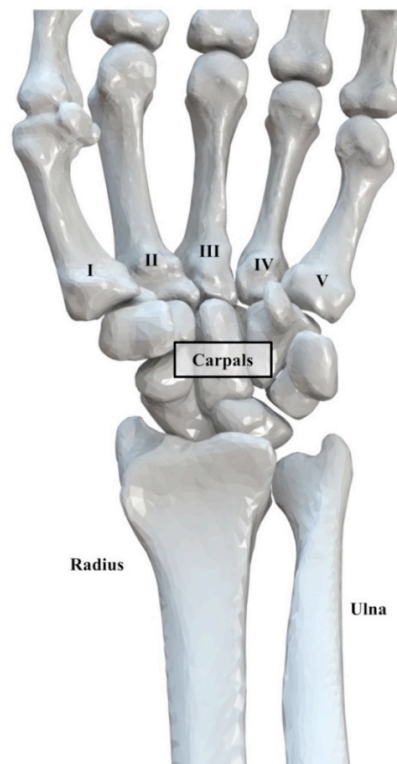


**Figure 1-7: Metacarpals.** Volar view of the left hand showing the distal radius and ulna, the carpals, and the metacarpals. Moving radially the thumb is termed the first metacarpal (I) and the small finger is termed the fifth metacarpal (IV).

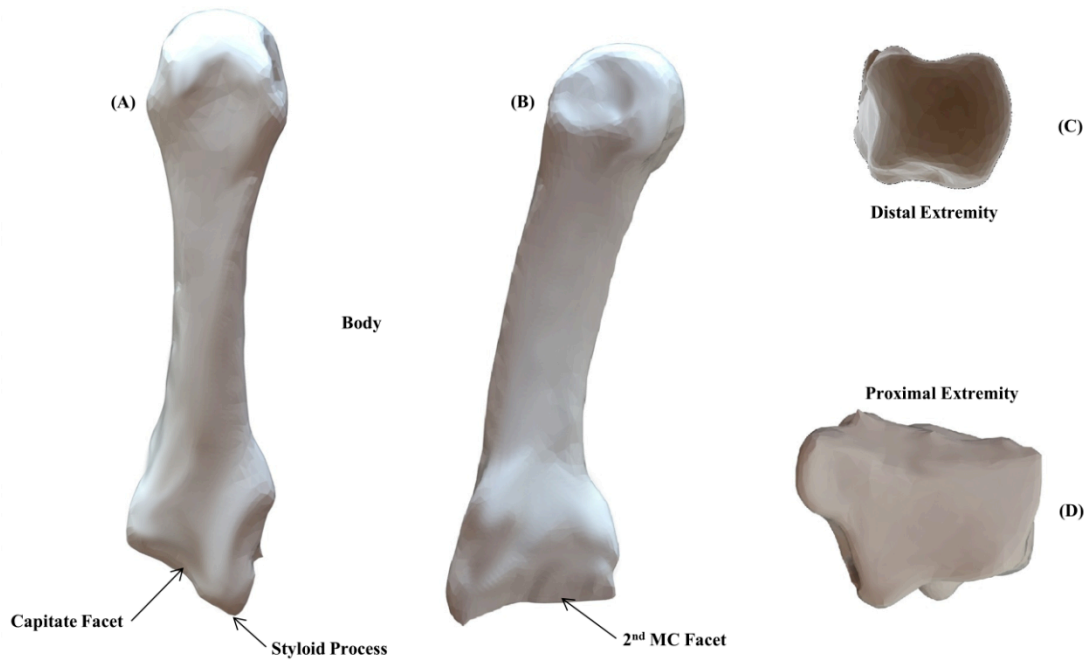


**Figure 1-8: Bony anatomy of the 3<sup>rd</sup> Metacarpal.** Bony anatomy of the left 3<sup>rd</sup> metacarpal with important landmarks. (A) Dorsal View, (B) Lateral View, (C) Distal Articular Surface, and (D) Proximal Articular Surface.

#### 1.1.1.5 *Phalanges*

The phalanges account for the remaining fourteen bones of the hand and make up the digits. With the exception of the thumb with only two, each digit is composed of three phalanges termed after their relative anatomic position: proximal, medial, and distal.<sup>2</sup> Like the metacarpals, each phalange is made up of a proximal metaphysis, a diaphysis, and a distal metaphysis.<sup>2</sup> The proximal metaphysis of the phalange is oval with concave articular surfaces.<sup>2</sup> The distal metaphyses are smaller than the proximal metaphyses with the end of the bone diverging into two condyles separated by a shallow groove.<sup>2</sup> Tapering downwards the diaphysis of each phalange is concave on the volar surface and convex on the dorsal surface.<sup>2</sup> The dorsal and volar surfaces of the diaphysis are rough allowing for the attachment of the flexor tendons.

### 1.1.2 *Joints*

The bones of the hand and wrist articulate with one another, each with different, but interdependent kinematic behaviors.<sup>6</sup> The synovial joints within the wrist include the: distal radioulnar joint (DRUJ), radiocarpal joint, midcarpal joint, pisotriquetral joint, trapeziometacarpal joint, and the carpometacarpal joints (Fig. 1-9). Articular cartilage, composed of hyaline cartilage, covers the joint surface of the fifteen bones that link the hand to the distal forearm including: the distal radius and ulna, the eight carpals, and the five proximal metacarpals.<sup>1</sup> Articular cartilage provides flexibility, support, and smooth surfaces allowing joints to track efficiently.<sup>1</sup>

#### 1.1.2.1 *Distal Radioulnar Joint*

The DRUJ is an L-shaped cavity formed by two separate articulations: vertically, between the distal ulna and the sigmoid notch of the radius and horizontally, between the ulnar dome and the proximal aspect of the articular disc (Fig. 1-9).<sup>6</sup> The articular disc is a semicircular fibrocartilaginous structure filling the joint space between the distal aspect of the ulna to the proximal carpal bones.<sup>6</sup> DRUJ stability is maintained via the dorsal and volar radioulnar ligaments.<sup>6</sup> In contrast, in order for the forearm to pronate and supinate the dorsal and volar DRUJ capsule are lax.<sup>6</sup>

### 1.1.2.2 *Radiocarpal Joint*

The radiocarpal joint is the articulation formed between the proximal carpal row and the distal articulating surface of the radius with the triangular fibrocartilage complex (Fig. 1-9).<sup>7</sup> The proximal articulating surface of the scaphoid has a larger radius of curvature than the lunate, shown by the differences in curvature on the distal articulating surface of the radius.<sup>7</sup> The proximal articular aspect of the triquetrum is relatively flat and does not articulate with another bone rather rests against the triangular fibrocartilage complex.<sup>7</sup> The radiocarpal joint is anatomically isolated from communicating with the DRUJ and midcarpal joint due to the interosseous ligaments of the proximal carpal row and the triangular fibrocartilage complex.<sup>7</sup>

### 1.1.2.3 *Midcarpal Joint*

The midcarpal joint is the articulation between the proximal and distal carpal rows (Fig. 1-9).<sup>7</sup> The midcarpal joint is formed through three different components: laterally, the convex aspect of the distal scaphoid articulates with the concavity formed by the trapezium, trapezoid, and lateral aspect of the head of the capitate; centrally, the convex aspect of the capitate and proximal pole of the hamate articulates with the concavity of the scaphoid and lunate; and medially, the convex proximal aspect of the hamate articulates with the concavity on the distal triquetrum.<sup>6</sup> The majority of the stabilizing ligaments of the midcarpal joint insert laterally and volarly onto the carpus, leaving the dorsal capsule hypermobile.<sup>6</sup>

### 1.1.2.4 *Pisotriquetral Joint*

The pisotriquetral joint is the large synovial cavity formed within the space of the flexor carpi ulnaris tendon and the volar aspect of the ulnocarpal ligamentous complex.<sup>6</sup> As the joint capsule has no secondary stabilizing ligaments it is lax allowing the pisiform to be relatively mobile throughout wrist flexion and extension.<sup>6</sup>

#### 1.1.2.5 *Trapeziometacarpal Joint*

The trapeziometacarpal joint is the articulation of distal aspect of the trapezium and the proximal base of the first metacarpal (Fig. 1-9). This reciprocal joint is formed through the two saddle-shaped articular surfaces, the distal concavity articulating with the proximal convexity and vice versa.<sup>6</sup> This relatively loose joint capsule is constrained by four capsular reinforcing ligaments inserted onto the medial and volar aspects of the first metacarpal.<sup>6</sup>

#### 1.1.2.6 *Carpometacarpal Joint*

The carpometacarpal joints are formed via the tight ligamentous complex, inserted onto the dorsal and volar aspects of the carpus, linking the base of second to fifth metacarpal with the corresponding bone in the distal carpal row (Fig. 1-9).<sup>6</sup> The carpometacarpal joint cavities extend distally to the intermetacarpal facets.<sup>6</sup>

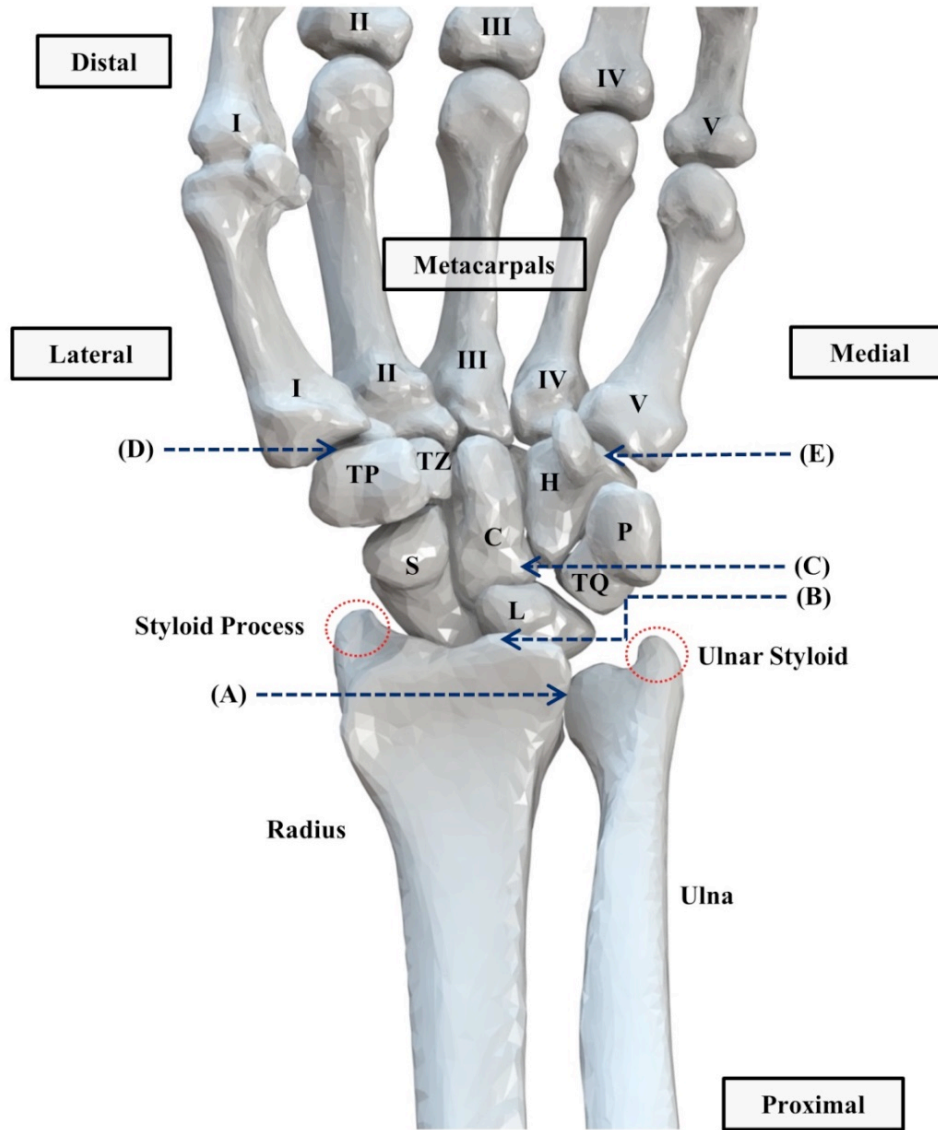


**Figure 1-9: Joints of the Wrist.** Volar view of the left hand illustrating the articulation between the eight carpal bones with the distal radius, distal ulna, metacarpals, and each other. Carpal bones shown: scaphoid (S), lunate (L), triquetrum (TQ), pisiform (P), trapezium (TP), trapezoid (TZ), capitate (C), and hamate (H). Metacarpals and phalanges shown: moving radially the thumb (I) to the small finger (IV). The arrows indicate the different joints within the hand: (A) distal radial-ulnar joint, (B) radiocarpal joint, (C) midcarpal joint, (D) trapeziometacarpal joint, and (E) carpometacarpal joint. The radial styloid process and ulnar styloid are also highlighted.

### 1.1.3 *Ligamentous Anatomy*

Ligaments are bundles of fibrous connective tissues which act to bind bone to bone across and articulation providing joint stability.<sup>8</sup> The wrist joint is surrounded by a complex configuration of ligaments connecting the bones both dorsally and volarly in order to provide carpal stability (Fig. 1-10,1-11, 1-12).<sup>8</sup> The ligaments of the wrist are categorized into two categories: intrinsic and extrinsic ligaments. Intrinsic carpal ligaments originate and insert only onto carpal bones, providing a rigid framework for the wrist joint.<sup>8</sup> Whereas, extrinsic ligaments bridge carpal bones to the metacarpals or the distal radius.<sup>8</sup> The principle name of each ligament typically stems with the bone of origin as the prefix and the bone of insertion as the suffix. In addition to being grouped into the two aforementioned categories the ligaments of the hand and wrist are also classified into groups by their location within the carpus and their organization within the joint capsule.<sup>6</sup> The sub grouping of ligaments include: radiocarpal, ulnocarpal, distal radioulnar, intercarpal, and carpometacarpal ligaments. Only the specific ligaments of interest for this thesis will be discussed in detail.

#### 1.1.3.1 *Radiocarpal Ligaments*

There are four extrinsic volar radiocarpal ligaments originating from the distal lateral rim of the radial styloid and coursing ulnarly and distally onto the adjacent carpals: radioscapocapitate (RSC), long radiolunate (LRL), short radiolunate (SRL) and radioscapolunate (RSL) (Fig. 1-10).<sup>9</sup> These ligaments work to bridge the link between the distal radius and proximal carpal row providing joint stability during functional wrist extension. On the dorsal surface there is the dorsal radiocarpal (DRC) ligament originating from the dorsal rim of the distal radius and attaches onto the proximal tubercle of the triquetrum.<sup>8</sup> The DRC provides the wrist joint lateral support during flexion.



#### 1.1.3.1.1 *Radioscaphocapitate Ligament*

The RSC ligament is the radial most positioned of the volar radiocarpal ligaments, attaching proximally to the radial styloid process as well as the radial region of the volar margin on the distal radius (Fig. 1-10).<sup>6</sup> In part, the RSC ligament aids in the formation of both the volar floor and radial wall of the radiocarpal joint capsule.<sup>6</sup> Moving distally from the radius the RSC ligament courses ulnarly towards the scaphoid, first inserting onto the lateral aspect of the waist. The second insertion point of the RSC ligament on the scaphoid is from the radial aspect of the waist and volarly, throughout the region of the margin of the proximal pole.<sup>6</sup> The remaining portion of the ligament continues ulnarly and distally passing the the volar and proximal aspects of the scaphocapitate (SC) joint space and attached on the volar aspect of the head of the capitate.<sup>6</sup> The distalmost fibers of the RSC ligament integrate with the SC ligament to insert onto the volar surface of the waist of the capitate.<sup>6</sup>

#### 1.1.3.1.2 *Long Radiolunate Ligament*

The LRL ligament originates along the volar margin of the distal radius and spans the majority of the length of the scaphoid fossa (Fig. 1-10, 1-12).<sup>6</sup> The most radial and superficial fibers of the LRL ligament overlap with the ulnar and superficial fibers of the RSC ligament forming a continuous capsule.<sup>6</sup> At the joint surface there is a deep longitudinal division between the RSC and LRL, defined as the interligamentous sulcus, which extends the length of the ligaments and allows for arthroscopic identification. The LRL ligament then passes volar to the proximal pole of the scaphoid with no considerable attachment but the synovial lining surrounding the proximal pole and joint surface.<sup>6</sup> Moving ulnarly, the LRL ligament passes volarly over the volar portion of the scapholunate (SL) ligament.<sup>6</sup> The LRL ligament then concludes by inserting into the radial aspect on the the volar surface of the lunate.<sup>6</sup>

#### 1.1.3.1.3 *Short Radiolunate Ligament*

The SRL ligament originates along the volar rim of the distal radius, proximal to the articular surface of the lunate fossa (Fig. 1-10, 1-12).<sup>6</sup> Forming the floor of the radiolunate joint space, the SRL ligament moves distally and insert into the lunate at the junction of the proximal articular surface and the nonarticular volar pole.<sup>6</sup> As the lunate dorsiflexes the fibers in the SRL ligament become relatively collinear in a tightly packed horizontal orientation.<sup>6</sup> When the lunate extends, the SRL fibers delaminate leaving the proximal fibers orientated vertically and the the distal fibers orientated obliquely.<sup>6</sup> The SRL ligament is thought to be one of the primary stabilizers of the lunate.

#### 1.1.3.1.4 *Dorsal Radiocarpal Ligament*

The DRC ligament originates along the dorsal rim of the distal radius, commencing just radial to Lister's tubercle and spans ulnarly to the origin of the dorsal portion of the dorsal radioulnar (DRU) ligament.<sup>6</sup> The deep fibers of the DRC ligament attach to the dorsal pole of the lunate and the more superficial fibers attach to the dorsal surface of the triquetrum.<sup>6</sup> There are no organized capsular ligaments between the proximal-ulnar margins of the DRC ligament and the distal margin of the DRU ligament.<sup>6</sup> Rather, the joint capsule consists of synovial and fibrous lamina while remaining relatively compliant allowing functional flexion of the radiocarpal joint.<sup>6</sup> Likewise, there are no ligaments between the distal-radial margins of the DRC and the proximal margin of the DIC producing a compliant bilaminar joint capsule which accommodates for midcarpal joint flexion.<sup>6</sup>

### 1.1.3.2 *Ulnocarpal Ligaments*

The extrinsic ulnocarpal ligaments originate from the volar radioulnar ligament, forming the volar extent of the triangular fibrocartilage complex (TFCC).<sup>6</sup> There are three ulnocarpal ligaments including the ulnolunate (UL), ulnotriquetral (UT), and ulnocapitate (UC) with few distinguishable characteristics other than the individual points of origin and insertion (Fig. 1-10).<sup>6</sup> The grouping of ulnocarpal ligaments form the volar and ulnar walls of the ulnar region of the radiocarpal joint space, providing medial support to the joint during extension.<sup>6</sup>

### 1.1.3.3 *Distal Radioulnar Ligaments*

The role of the distal radioulnar ligaments is to maintain congruity between the ulnar head and sigmoid notch providing dynamic stability to the distal radioulnar joint (DRUJ) throughout forearm rotation.<sup>10</sup> The distal volar radioulnar ligament originates on the anterior surface of the ulnar notch of the radius and courses to insert onto the anterior head on the ulna (Fig. 1-11).<sup>6</sup> The origin of the distal dorsal radioulnar ligament is on the dorsal surface of the ulnar notch of the radius and courses to insert onto the dorsal margin of the ulnar head.<sup>6</sup>

### 1.1.3.4 *Intercarpal Ligaments*

The intrinsic intercarpal ligaments of the wrist maintain the congruity between bones and play a critical role in stabilizing the carpus during movements of the hand (Fig. 1-10).<sup>6</sup> The rigid attachment between carpal bones allow limited movement between bones. The intercarpal ligaments include: scaphotrapezium-trapezoid (STT), scapholunate (SL), scaphocapitate (SC), lunotriquetral, triquetrocipitate, ulnotriquetral, trapeziotrapezoid, capitotrapezoid, capitoamate, dorsal intercarpal, triquetroamate, triquetrocipitate, and pisohamate.

#### 1.1.3.4.1 *Scaphotrapezium-Trapezoid Ligament*

The origin of the STT ligament is distal to the attachment site of the RSC ligament on the lateral cortex of the distal pole of the scaphoid (Fig. 1-10).<sup>6</sup> Moving distally the STT diverges to form two distinct bands, the scaphotrapezoid and the scaphotrapezium ligaments.<sup>6</sup> Forming the dorsolateral STT joint capsule, both bands course distally attaching to the dorsal cortical surfaces of the trapezoid and trapezium.<sup>6</sup> Before attaching to the respective bones the fibers from each ligament interdigitate with surrounding ligaments attaching in the same region, with no clear divisions between them. Forming the volar STT joint capsule, the fibers of the STT ligament appear as a flat sheet of longitudinally oriented fibers.<sup>6</sup>

#### 1.1.3.4.2 *Scaphocapitate Ligament*

The SC ligament is a large capsular ligament originating at the distal pole of the scaphoid (Fig. 1-10).<sup>6</sup> The origin of the SC ligament is directly adjacent with the origin of the STT ligament and the course of the SC ligament is just distal to the course of the RSC ligament.<sup>6</sup> The SC ligament moves distally and ulnarly towards the body of the capitate, inserting onto the radial portion of the volar surface.<sup>6</sup>

#### 1.1.3.4.3 *Scapholunate Interosseous Ligament*

The scapholunate (SL) interosseous ligament is uniquely “C” shaped and spans the interval between the dorsal, volar and proximal edges of the scapholunate (SL) joint surface (Fig. 1-12).<sup>6</sup> This arrangement allows the distal portion of the SL joint surface to be directly exposed to the midcarpal joint space whereas the proximal interosseous component of the SL ligament isolates the surfaces from the radiocarpal joint.<sup>6</sup> The three sub-regions of the SL ligament each have different material and anatomic properties.<sup>11</sup> The dorsal component of the SL ligament is the most critical stabilizer of the SL joint acting as the primary restraint to distraction as well as torsional and translational moments.<sup>11</sup> It is a true ligament characterized by its thick transversely oriented collagen fibers.<sup>11</sup> The volar component of the SL ligament, although considerably thinner than the dorsal component, plays a role in the rotational stability of the SL joint.<sup>11</sup> The proximal or membranous component of the SL ligament provides little restraint to abnormal carpal motion as it is histologically defined as a fibrocartilaginous structure.<sup>11</sup>

#### 1.1.3.5 *Carpometacarpal Ligaments*

The carpometacarpal ligaments are responsible for binding the distal carpal row to the proximal metacarpals on both the volar and dorsal side of the hand in order to maintain the congruency of the carpometacarpal articulation.

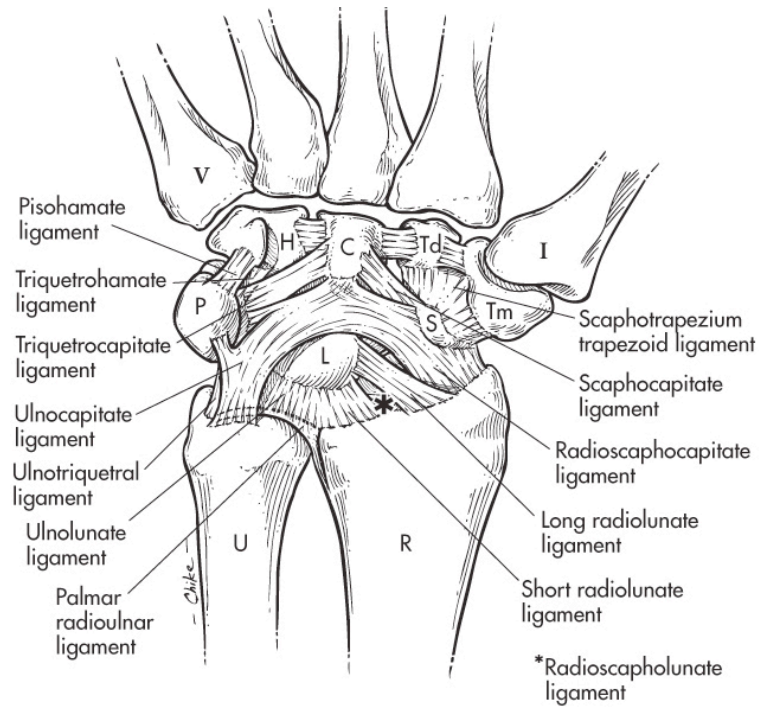


**Figure 1-10: Volar Ligaments of the Wrist.** Schematic of the volar ligaments of the right hand. (Reprinted with permission from Wolters Kluwer: The Wrist: Diagnosis and Operative Treatment).

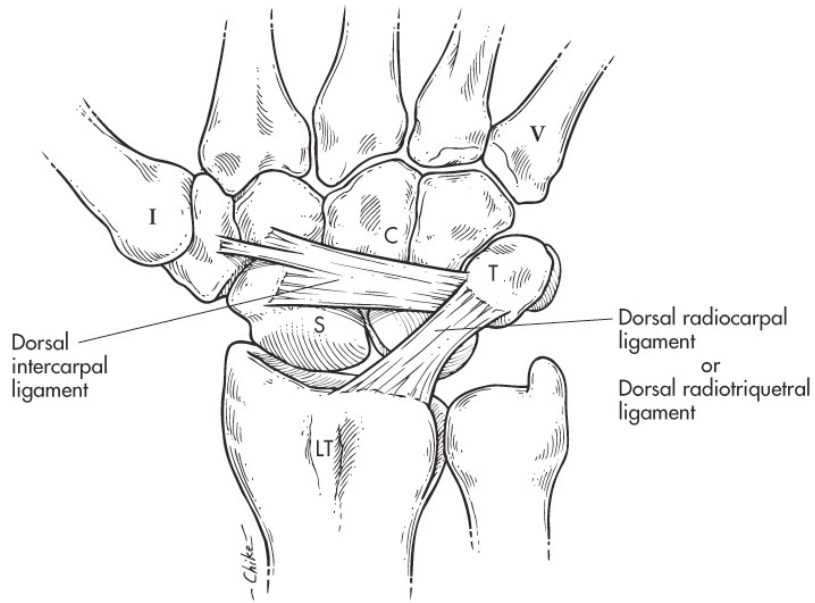


**Figure 1-11: Dorsal Ligaments of the Wrist.** Schematic of the dorsal ligaments of the right hand including the dorsal radiocarpal and dorsal intercarpal ligaments (Reprinted with permission from Wolters Kluwer: The Wrist: Diagnosis and Operative Treatment).

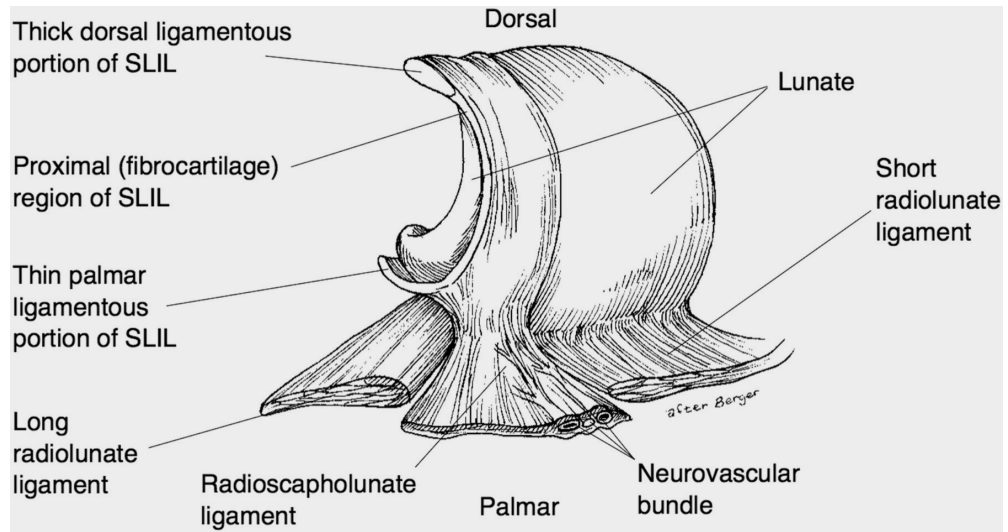


**Figure 1-12: Scapholunate Interosseous Ligament.** Volar view of the right scapholunate ligament highlighting the dorsal, proximal, and volar aspects of the ligament. The short and long radiolunate ligaments are also shown (Reprinted with permission from The Journal of Bone & Joint Surgery: Scapholunate Ligament Reconstruction).

#### 1.1.4 *Musculature*

The essential function of muscle is the ability to contract making it possible to produce joint motion. Muscles of the human body are classified as one of three types of tissue: smooth, cardiac, or skeletal. Skeletal muscle fibers are tubular, multinucleated, striated and unlike smooth and cardiac muscle contract voluntarily under nerve control.<sup>13</sup> Skeletal muscles are attached to the skeleton via fibrous connective tissues known as tendons.<sup>14</sup> The fibers within the muscle generate tension across a joint by contracting, shortening in length, and producing a moment arm in order to manipulate the position of the joint.<sup>14</sup> The magnitude of force is dependent on the size, type, and insertion point from the joint center of the muscle. As skeletal muscles contract the bone of origin remains stationary while the bone of insertion is manipulated.<sup>14</sup> Tendons do not actively change length as the muscle contracts however may undergo slight alterations due to their viscoelastic nature.

The majority of the time a single muscle is not solely accountable for joint motion, rather a group of synergistic muscles aid in the motion with the muscle applying the greatest load being termed the primary mover.<sup>14</sup> Additionally, as muscles contract they typically have antagonists pairs which bring about joint motion in opposite direction.<sup>14</sup>

Motion of the wrist is primarily achieved via six muscles: the flexor carpi radialis (FCR), flexor carpi ulnaris (FCU), abductor pollicis longus (APL), extensor carpi radialis brevis (ECRB), extensor carpi radialis longus (ECRL), and extensor carpi ulnaris (ECU) (Fig. 1-13).<sup>6</sup> The wrist flexors are found in the volar component of the forearm and the extensors in the dorsal component. Wrist rotation is primarily controlled via two muscles, the biceps brachii and the pronator quadratus (PQ).<sup>14</sup>



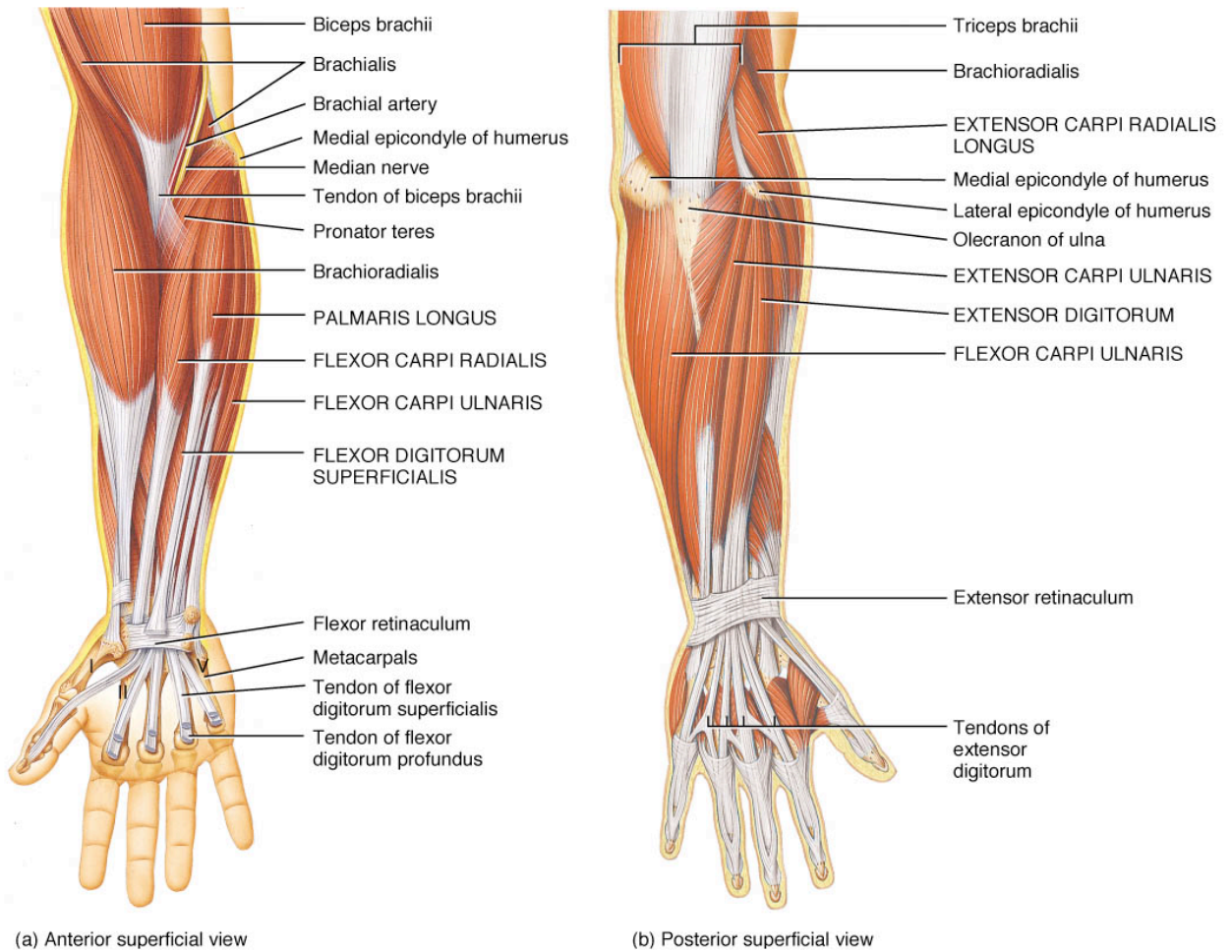


**Figure 1-13: Muscles of the Wrist.** The muscles of the anterior (volar compartment) and posterior (dorsal compartment) forearm.<sup>15</sup>

#### 1.1.4.1 *Volar Compartment*

The volar compartment of the forearm contains the FCU, FCR and APL muscles (Fig. 1-13). These superficial muscles work synergistically to assist in flexion as well as ulnar and radial deviation of the wrist joint.

##### *Flexor Carpi Ulnaris*

The FCU originates at the medial epicondyle of the humerus and inserts onto the dorsal surfaces of the pisiform, hamate and proximal end of the fifth metacarpal.<sup>2</sup> The FCU is the primary wrist flexor and acts synergistically during ulnar deviation.

##### *Flexor Carpi Radialis*

The FCR originates at the medial epicondyle of the humerus and inserts onto the base of the second and third metacarpals.<sup>2</sup> The FCR is a synergistic muscle aiding in both wrist flexion and radial deviation.<sup>6</sup>

##### *Abductor Pollicis Longus*

Unlike the other two wrist flexors the APL originates at the dorsal aspect of the radius and ulna and inserts onto the dorsal surface of the trapezium and the base of the first metacarpal.<sup>2</sup> The APL is the primary wrist abductor and extends the thumb.

#### 1.1.4.2 *Dorsal Compartment*

The dorsal compartment of the forearm contains the ECRB, ECRL, and ECU muscles which assist in extension, adduction and abduction of the wrist (Fig. 1-13). The wrist extensors are antagonistic to the flexors.

##### *Extensor Carpi Radialis Brevis*

The ECRB originates at the lateral epicondyle of the humerus and inserts onto the base of the third metacarpal, opposing the FCR.<sup>2</sup> The ECRB is a synergistic muscle aiding in both wrist extension and abduction in addition to stabilizing the wrist during finger flexion.

##### *Extensor Carpi Radialis Longus*

The ECRL originates at the lateral epicondyle of the humerus and inserts onto the base of the second metacarpal, also opposing the FCR.<sup>2</sup> The ECRL is a synergistic muscle assisting in functional wrist extension and abduction.

##### *Extensor Carpi Ulnaris*

The ECU originates at the lateral epicondyle of the humerus and inserts onto the dorsal base of the fifth metacarpal, opposing the FCU which inserts onto the volar base. The ECU is the primary muscle utilized in wrist extension and abduction.

#### 1.1.4.3 *Forearm Rotators*

Wrist rotation is controlled by four major muscles in the forearm. The biceps brachii and supinator are the primary supinator muscles and the pronator teres (PT) and pronator quadratus PQ are the primary pronator muscles of the forearm (Fig. 1-13).

##### *Biceps Brachii*

The biceps brachii is formed via two proximal heads that originate from the supraglenoid tubercle and the coracoid process of the scapula and converges to a single head that inserts onto the radial tuberosity of the distal forearm.<sup>2</sup> The biceps brachii is the primary muscle utilized in forearm supination and is synergistic during elbow flexion.

##### *Supinator*

The supinator originates on the lateral epicondyle of the humerus and the proximal ulna and inserts mid shaft onto the lateral radius.<sup>2</sup> The supinator muscle works synergistically with the biceps brachii assisting in forearm supination.

##### *Pronator Teres*

The PT originates from the medial epicondyle of the humerus and the proximal ulna and inserts mid shaft onto the lateral aspect of the radius.<sup>2</sup> It is a pronator of the forearm.

##### *Pronator Quadratus*

The PQ originates on the anteromedial surface of the ulna and inserts onto distal anterolateral surface of the radius.<sup>2</sup> The PQ works synergistically with the PT assisting in forearm pronation and elbow flexion.

## 1.2 Wrist Kinematics

### 1.2.1 *Range of Motion*

The wrist is a hypermobile joint capable of multi-planar motions including flexion-extension, radial-ulnar deviation, pronation supination, and in combination circumduction (Fig. 1-14, 1-15, 1-16). In order to accurately describe the complex movements of the wrist it is necessary to understand the anatomical neutral position in which these motions are defined. The neutral position of the wrist relative to the radius is defined as the long axis of the third metacarpal parallel to the long axis of the radius.<sup>16</sup> Neutral forearm rotation is defined as the position of the radius relative to the ulna with the elbow at 90 degrees of flexion and the thumb point to the shoulder.<sup>16</sup> Range of motion depends on several factors included but not limited to gender, age, injury, or disease.

### 1.2.1.1 *Flexion-Extension Motion*

Planar wrist flexion-extension motion (FEM) occurs around the sagittal axis of the hand (Fig. 1-14).<sup>17</sup> The wrist joint can typically reach anywhere from 65 to 90 degrees of flexion and 55 to 75 degrees of extension, demonstrating a 160 degree motion arc.<sup>1,17</sup> The total range of planar wrist FEM is a result of the combination of motion between the radiocarpal and midcarpal joints.<sup>18</sup> Wrist FEM is limited by the dorsal radiocarpal ligaments during wrist flexion and a combination of the volar ligaments and dorsal aspect of the radius during extension.<sup>6</sup>

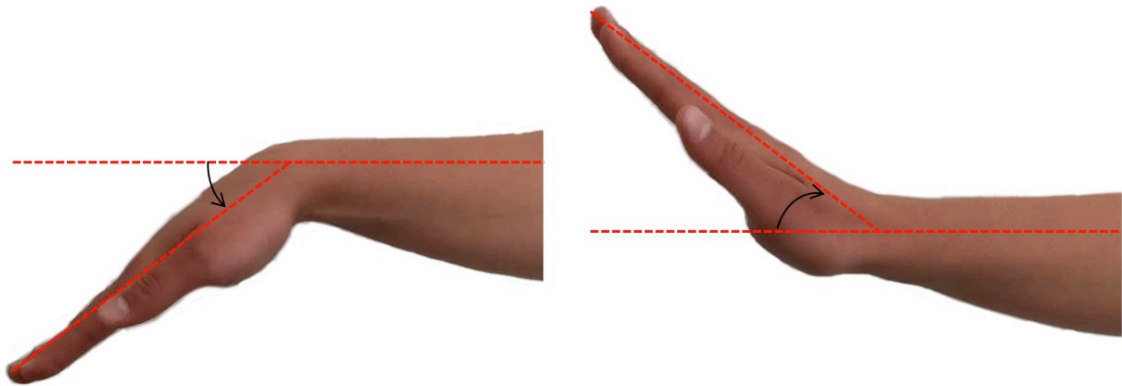


**Figure 1-14: Range of Wrist Motion: Flexion-Extension.** Motion of the wrist joint in flexion (left) and extension (right).

### 1.2.1.2 *Radial-ulnar Deviation*

Planar wrist radial-ulnar deviation (RUD) occurs around the medial-lateral axis of the wrist (Fig. 1-15).<sup>17</sup> On average the wrist has a 60 degree range of motion, deviating radially between 15 and 25 degrees and ulnarly between 30 and 45 degrees.<sup>1,17</sup> RUD motion is limited through carpal interaction with the radial styloid and the tightening of the ulnar collateral ligaments in radial deviation and the tightening of the radial collateral ligaments in ulnar deviation.<sup>6</sup>

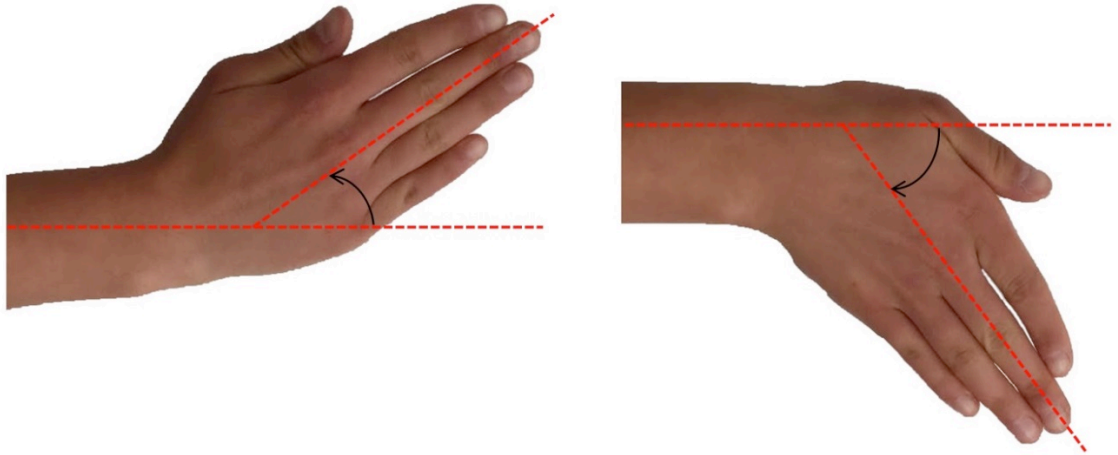


**Figure 1-15: Range of Wrist Motion: Radial-Ulnar Deviation.** Motion of the wrist joint in radial deviation (left) and ulnar deviation (right).

### 1.2.1.3 *Pronation Supination*

Pronation supination motion largely occurs at the proximal and distal radioulnar joints of the forearm (Fig. 1-16).<sup>1</sup> On average the wrist and forearm can exhibit 150 degrees of motion, pronating anywhere between 60 and 80 degrees and supinating between 60 to 85 degrees.<sup>1</sup> The pronation supination axis lies obliquely through the center of the humeral capitulum and the midpoint of the ulnar head.<sup>1</sup> The radioulnar ligaments at the DRUJ are the principal constraint to wrist supination while wrist pronation is limited by the crossing of the radial and ulnar shafts.<sup>19</sup>

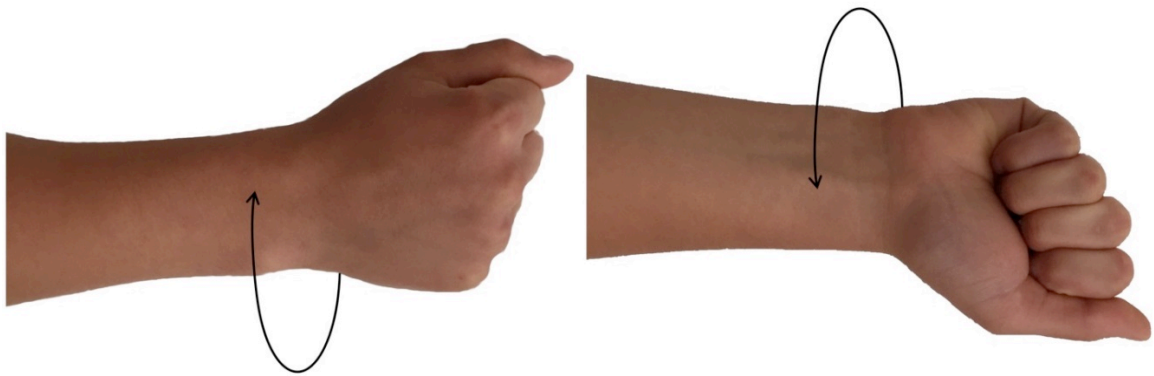


**Figure 1-16: Range of Wrist Motion: Pronation-Supination.** Motion of the forearm in pronation (left) and supination (right).



### 1.3 Clinical Disorders of the Wrist

The wrist joint bears considerable load during daily activities leaving it vulnerable to injury. In the native state, the intricate balance of joint geometry and tendon forces across the wrist prevents the ligaments and capsular structures from carrying excessive loads.<sup>6</sup> Any disruption to this balance, as a result of an injury or disease, may result in abnormal force transmission and altered kinematics across the wrist joint.<sup>6</sup> As a result, the joint often becomes unstable due to the progressive stretching of the surrounding capsule and stabilizing ligaments.<sup>6</sup>

Wrist pain is one of the most common complaints heard by clinicians. Often times the principal cause of pain is obvious but a complete examination is necessary in order to diagnose the critical underlying pathologies.<sup>20</sup> Wrist pain may occur as a result of injury, either repetitive stress or sudden impact, or as a result of a degenerative disease. A comprehensive understanding of the intricate anatomy and kinematics of the hand is necessary in order to effectively diagnose and treat injuries of the wrist.

### 1.3.1 *Fractures*

Wrist fractures are one of the most common injuries occurring to the skeletal system and account for a large portion of wrist pain complaints. There is a wide variety of fracture patterns depending on the mechanism of injury. Fractures at the distal radius and ulna are the most common, accounting for 44 percent of wrist fractures, while individual carpal fractures account for only 14 percent.<sup>21</sup> Fractures of the distal forearm commonly occur as a result of axial loading on the outstretched hand and extended wrist, generally termed a Colles' Fracture.<sup>6,21</sup> Often times fractures of the distal forearm result in malunion and misalignment of the adjacent carpal bones leading to further degenerative changes within the joint.<sup>22</sup> These injuries may increase the laxity of the wrist joint thereby influencing the individual carpal kinematics and the overall range of motion of the wrist. Scaphoid fractures are the most common carpal fracture, representing 60 to 70 percent of all carpal bone fractures (Fig. 1-17).<sup>21</sup> Fractures of the scaphoid commonly occur at the anatomic waist due to compression tension loads, torsional stress, or rotational forces.<sup>21</sup> As the scaphoid plays a large role in linking the proximal and distal carpal rows, upon fracture the integrity of the scaphoid is lost generating an imbalance leaving the wrist joint unstable.<sup>21</sup> There is no single treatment available for all forms of wrist fractures but rather depends on the severity and type of injury presented as well as the patient's age and activity level. Some common treatment techniques include but are not limited to: splinting, casting, pin fixation, external fixation, and open reduction and internal fixation.<sup>6,23,24</sup>



**Figure 1-17: Scaphoid Fracture.** Anteroposterior view of a common fracture at the anatomical waist of the scaphoid (Reprinted with Permission from AFP: Diagnosis and Management of Scaphoid Fractures).

### 1.3.2 *Carpal Instability*

Carpal instability is another major cause of wrist pain. Carpal instability is defined as the wrist joint's inability to transfer loads without subsequent changes in stress on the surrounding ligaments and articular cartilage, and the inability to maintain a functional range of motion without changes in intercarpal alignment.<sup>6</sup> Instability generally occurs due to ligament disruption, articular cartilage damage, or as a sequelae of a carpal fracture.<sup>26</sup> The most common cause of carpal instability is injury to the scapholunate ligament within the proximal row (Fig. 1-18).<sup>6,11</sup> The proximal carpal row is considered an intercalated segment with no direct control mechanisms attached to it, causing its motion to be entirely dependent on the mechanical signals of the surrounding articulations and vascular elements.<sup>11</sup> Isolated injury to the SL ligament, although insufficient to cause abnormal carpal alignment, is often a precursor to abnormal joint kinematics, cartilage wear, and further degenerative changes.<sup>11</sup> SL instabilities are typically initiated through a fall on an outstretched hand, resulting in a partial tear or attenuation of the SL ligament.<sup>11</sup> If not managed a partial SL tear may lead to a complete tear eventually causing SL dissociation, a dorsal intercalated segmental instability (DISI), or a pattern of wrist arthritis termed scapholunate advanced collapse (SLAC).<sup>11</sup> Currently there is no gold standard in the management of carpal instabilities but rather the treatment strategy is tailored to the stage and degree of injury present. Some typical treatment options include: splinting, casting, arthroscopic debridement, reduction, pinning, direct repair with or without dorsal capsulodesis, and arthrodesis.<sup>6,11,27</sup>

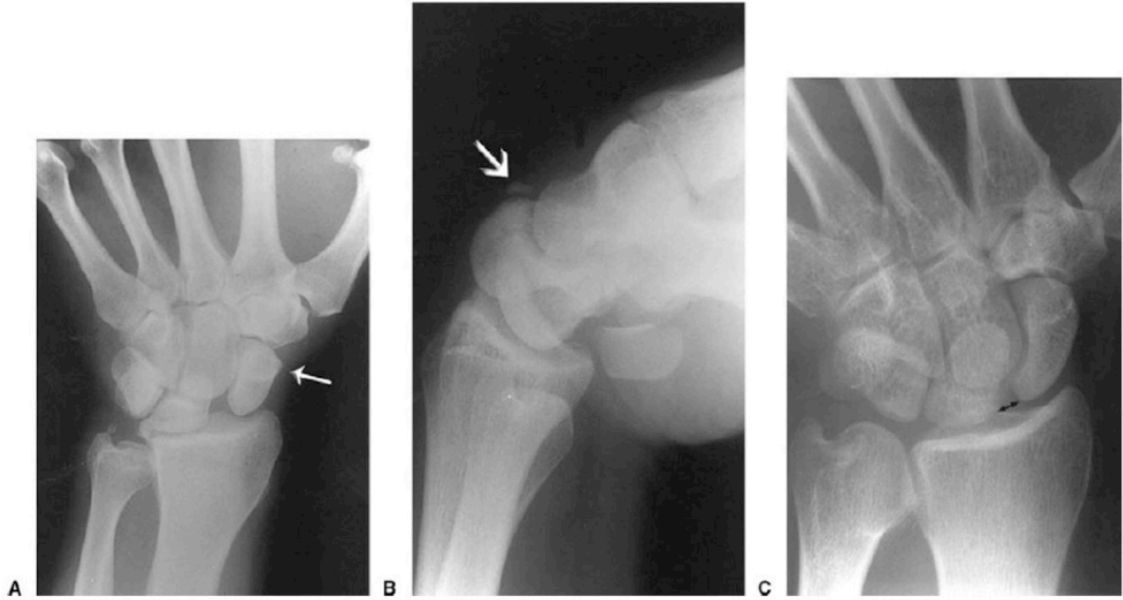


**Figure 1-18: Carpal Instability.** Radiographic evidence of scapholunate instability: (A) Anteroposterior view of the scaphoid abnormally flexed, (B) full flexion with abnormal scaphoid subluxation, and (C) ulnar deviation shows characteristic gapping of the scapholunate interval (Reprinted with Permission from The Journal of Hand Surgery: Scapholunate Instability Current Concepts in Diagnosis and Management).

### 1.3.3 *Arthritis*

Arthritis may occur with age or as a result of a previous injury and can cause the healthy articular cartilage to erode triggering painful bone on bone contact (Fig. 1-19). The most common types of arthritis to affect the hand and wrist are osteoarthritis, rheumatoid arthritis, and post-traumatic arthritis.<sup>6,29</sup> Osteoarthritis is a degenerative disease, most commonly affecting the elderly, which causes cartilage deterioration, pain and joint stiffness.<sup>29</sup> Rheumatoid arthritis is an autoimmune disease causing chronic inflammation, pain, stiffness, and swelling of multiple joints. This disease commonly affects the radioulnar articulation causing damage to the articular cartilage, bone, and surrounding tendons and ligaments.<sup>29</sup> Post-traumatic arthritis occurs following injury to the wrist, such as a fracture or torn ligament. It can either effect the articular cartilage directly or cause a delayed onset of cartilage loss.<sup>29</sup> There is currently no cure for arthritis, but depending on the severity of the disease there are numerous non-surgical and surgical treatment strategies including: steroid injections, anti-inflammatory medications, proximal row carpectomy, carpal fusion, and total wrist arthroplasty.<sup>6,29</sup>



**Figure 1-19: Rheumatoid Arthritis in the Wrist.** Advanced rheumatoid arthritis within the wrist joint causing carpal bone malalignment and collapse (Reprinted with Permission from AAOS: Arthritis of the Wrist).

## 1.4 Biomechanical Analyses

### 1.4.1 *Wrist Motion Simulation*

The wrist is a complex joint consisting of multiple intricate articulations that work together in producing a functional range of motion. Loss or limited range of motion at the wrist joint is a direct result of tissue damage occurring due to a degenerative disease, such as arthritis, or an injury, such as a fracture or ligament tear. In order to examine wrist joint mechanics, it is first necessary to understand the normal kinematics of the carpal bones. This knowledge is critical when considering surgical procedures, designing prosthetic devices, and in investigating the various different pathologies of the wrist joint.

Surgical repair techniques of the wrist are often tested and validated using *in vitro* cadaveric models. A variety of different *in vitro* testing devices and simulators have been developed in order to investigate the kinematics of the wrist joint and can be classified as passive or active motion simulators. Both testing methods have associated strengths and limitations that determine the validity of the results and whether they will be an optimal pre-clinical testing strategy.

#### 1.4.1.1 *Passive Motion Simulators*

Wrist joint kinematics can be simulated via passive motion through the use of external forces, either from an investigator or a mechanical apparatus, influencing the position of the hand relative to the position of the forearm. External forces may incorrectly simulate joint motion if the true line of action of the muscle is not reproduced generating joint laxity. Passive motion simulators that incorporate muscle tone loads provide more clinically relevant results, however these are still subject to errors in the magnitude of load added. Human manipulation of a specimen could potentially result in varied movements and also introduce externally applied forces and moments, thereby affecting the quality of the results.



*Nishiwaki et al.* developed a wrist simulator capable to reproducing planar wrist motions both passively and forearm rotation actively. Upper limb cadaveric forearms were amputated mid-humerus and fixated to the base of the simulator. Pneumatic actuators maintained a minimum tone load on the ECU, ECRL, FCU, PT, and bicep brachii muscle groups (Fig. 1-20).<sup>30</sup> Optical trackers were inserted into the radius, ulna, third metacarpal, scaphoid, and lunate. Passive motion was simulated by the investigator moving the Steinmann pin, inserted into the third metacarpal, through the simulator's passive motion arc.<sup>30</sup> Active forearm pronation and supination was simulated by connecting the biceps brachii and PT sutures to either a servomotor, the primary mover, or a pneumatic actuator, the synergistic muscle mover.<sup>30</sup>

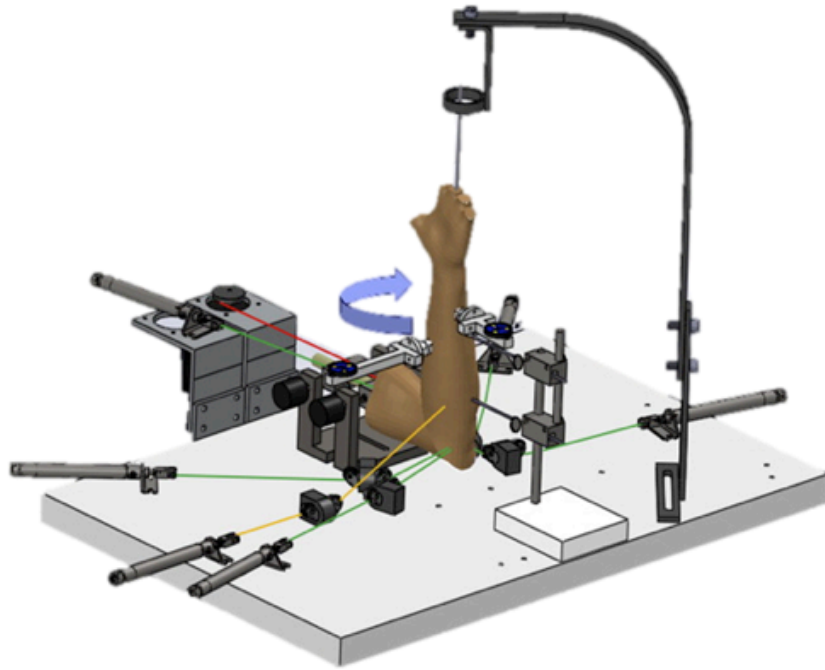


**Figure 1-20: Nishiwaki's Motion Wrist Simulator.** Wrist motion simulator developed by *Nishiwaki et al.* to test the effect of dorsal angulation deformities on DRUJ kinematics (Reprinted with Permission from *The Journal of Hand Surgery: Effect of Volarly Angulated Distal Radius Fractures on Forearm Rotation and Distal Radioulnar Joint Kinematics*).

#### 1.4.1.2 *Active Motion Simulators*

Active motion simulators recreate motion by applying force directly to the muscle tendon of interest in order to produce joint position. Force-position algorithms are designed using antagonistic relationships between opposing muscles in order to effectively reproduce an *in vivo* loading scenarios. The primary mover muscle group, for the desired action, is position controlled to maintain a continuous angular velocity while the antagonistic muscle group holds a desired tone load. In order to reverse the direction of motion, the force-position algorithm interchanges the two muscle groups. The muscle group that was previously position controlled now maintains a constant load and the opposing muscle group is used to manipulate the position of the joint.

*Dunning et al.* simulated active motion on cadaveric specimens using a custom controlled loading apparatus. A manifold of pneumatic actuators delivered computer controlled forces to the nine muscles of interest generating finger and wrist motions (Fig. 1-21).<sup>24</sup> Specimens were amputated mid humerus and mounted to the simulator with the elbow at 90 degrees of flexion. Cables were sutured at the musculotendinous junction and attached to the pneumatic actuators, electromagnetic receivers (Flock of Birds, Ascension Technologies, Burlington, VT) were used to track the relative motion of unstable extra-articular distal radial fractures.<sup>24</sup> Although this method of actuation does model *in vivo* loading scenarios, it is an open loop control system with no positional feedback from the trackers making it less repeatable. Prior to testing the loading apparatus must be extensively tuned with respect to the tendon forces necessary to perform the desired motion, leaving it susceptible to variations in inter-specimen loading conditions.

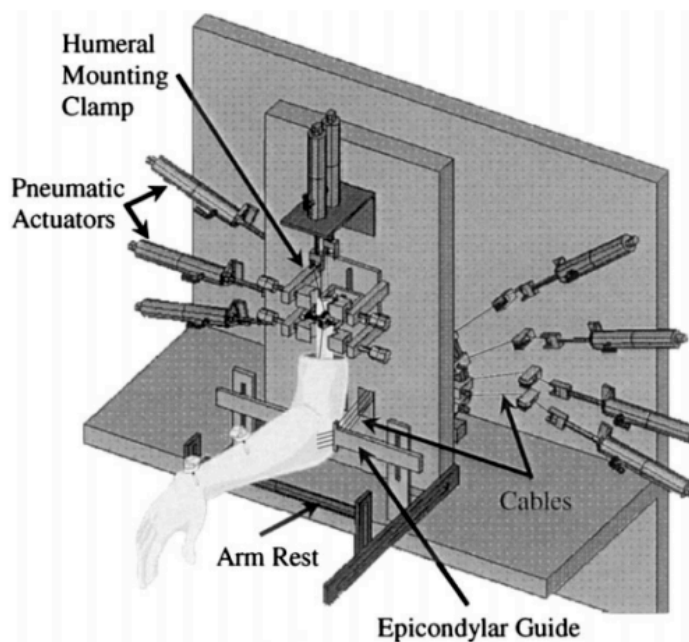


**Figure 1-21: Dunning's Active Motion Wrist Simulator.** Active wrist motion simulator developed by *Dunning et al.* to test the stability of external fixation used in the treatment of distal radius fractures (Reprinted with Permission from *The Journal of Hand Surgery: Supplemental Pinning Improves the Stability of External Fixation in Distal Radius Fractures during Simulated Finger and Forearm Rotation*).

*Werner et al.* developed the first reported active motion wrist simulator capable of producing repeatable planar and non planar wrist motions (Fig. 1-22).<sup>31</sup> The simulator is described as a multichannel servohydraulic system which attached to the six major wrist flexors and extensors: ECU, ECRL, ECRB, FCU, FCR, and APL. The system utilized electromagnetic spatial trackers to record the position of the ulna, third metacarpal, and lunate with real time feedback to control the desired motion path of the wrist.<sup>31</sup> The cadaveric specimens were amputated distal to the elbow and cemented into the base of the simulator. All soft tissue structures with the exception of the tendons and ligaments of interest were excised.<sup>31</sup> More recent simulators have used optical tracking for recording spatial position as it allows surgical procedures using ferromagnetic metals to be evaluated without the risk of interference.

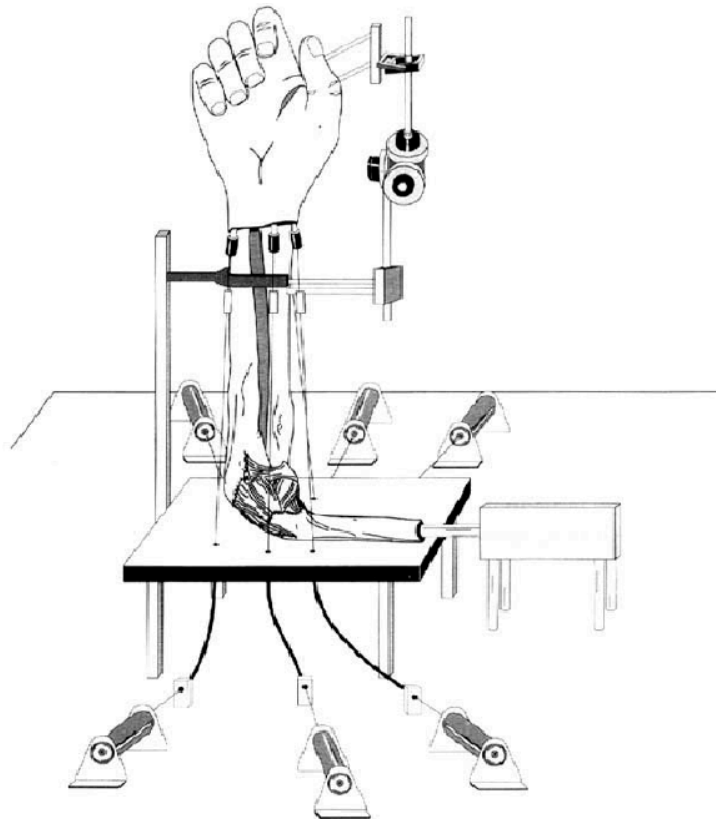


**Figure 1-22: Werner's Active Motion Wrist Simulator.** Active wrist simulator developed by *Werner et al.* capable of producing repeatable planar and non-planar motion paths (Reprinted with Permission from The Journal of Orthopaedic Research: Wrist Joint Motion Simulator).

Recently *Iglesias et al.* developed a wrist motion simulator capable of performing both passive and active *in vitro* motion in multiple gravity loaded positions (Fig. 1-23). The simulator used a manifold of seven electric servomotors connected via cables to the musculotendinous junction of: the ECU, ECRL, ECRB, FCU, FCR, PT, and biceps brachii.<sup>32</sup> Each servomotor was instrumented with a strain gauge in order to provide muscle force feedback throughout testing. The simulator was capable of maintaining target tendon tone loads effectively producing repeatable active wrist motion.<sup>32</sup> The simulator was able to replicate active wrist flexion-extension as well as forearm rotation. The system utilized optical tracking methods to record the position of the radius, ulna, and third metacarpal to provide real time feedback to the system. A minimum tone load of 8.9 Newtons was used to produce the desired wrist motion pathways.<sup>32</sup>

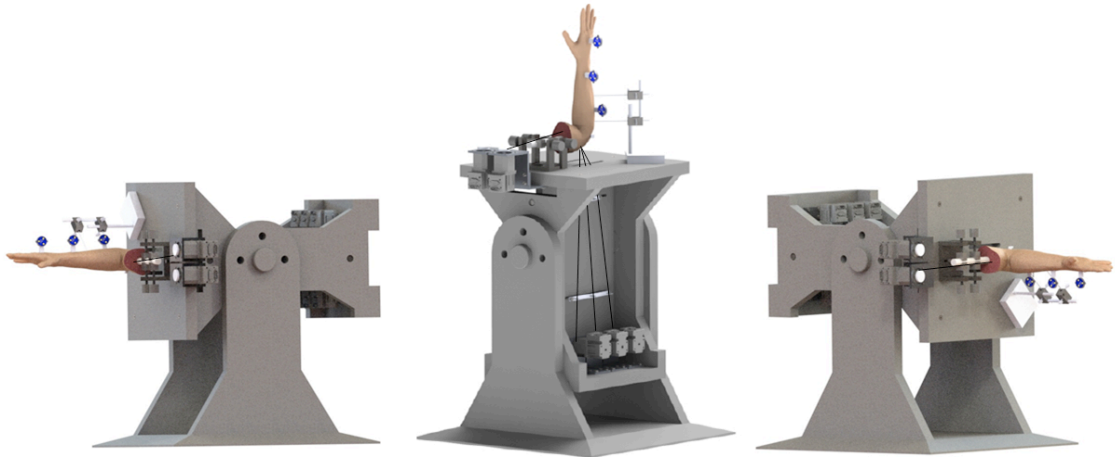


**Figure 1-23: Iglesias' Active Motion Wrist Simulator.** Active motion wrist simulator developed by *Iglesias et al.* highlighting the different gravity loaded positions (Reprinted with Permission from *Iglesias et al.*: Development of an in-vitro passive and active motion Simulator for the investigation of wrist function and Kinematics).

## 1.5 Thesis Rationale

As previously noted, the wrist is comprised of numerous bones with multiple articular surfaces, ligaments, tendons and neurovascular bundles with intimate interactions. Normal wrist kinematics are dependent on the intricate interplay between the loading applied and the carpal bone morphology and ligamentous constraints of the joint. The kinematics of the wrist joint have been studied extensively both *in vitro* and *in vivo*, yet there remains no consensus regarding individual carpal kinematics and their respective contributions to total wrist motion. The resulting discrepancies in data have led to numerous theories depicting normal carpal kinematics occurring within the wrist joint including: row, column, intercalated segment, and oval ring concepts.<sup>33-36</sup> A more comprehensive understanding of normal and abnormal carpal kinematics is necessary in order to effectively diagnose and treat the subtle injuries of the hand and wrist.

Ligamentous injuries are one of the most common sources of wrist pain and discomfort. The ligaments of the wrist are typically injured following trauma to the hand or wrist with the most frequently injured intercarpal ligament being the scapholunate (SL).<sup>11,37-39</sup> The SL ligament plays a critical role in preserving wrist joint stability joining the scaphoid and lunate allowing them to move synergistically throughout wrist motion.<sup>38</sup> Damage to the SL ligament and surrounding articular joint space often causes carpal instability, causing the scaphoid and lunate to rotate and dissociate from their native alignment.<sup>38</sup> The SL ligament is considered the primary stabilizer of the SL joint, but is surrounded by a complex configuration of secondary stabilizers, each playing a role in the maintenance of normal SL kinematics.<sup>11</sup> Following SL ligament injury, the secondary stabilizers are often vulnerable to secondary attenuation.<sup>11</sup> Although the ligamentous anatomy of the wrist is well documented, the functional and stabilizing role of these secondary restraints remains unclear. Clinically, the void of information regarding the stabilizing role of each of these ligaments results in confusion as to which structures should be repaired following injury. As the etiology of SL instability remains unknown, treatment recommendations vary and often result in poor clinical outcomes for patients.

As injuries arising in the wrist often manifest as alterations in intercarpal motion, a better understanding of individual carpal kinematics and the ligamentous stabilizers, will allow for improved examination of the wrist joint under normal and pathological conditions and lead to advances in techniques and the outcome of partial wrist fusions, ligament reconstructions, and prosthetic devices.

## 1.6 Objectives and Hypotheses

### 1.6.1 *Specific Objectives*

The objectives of this thesis are as follows:

1. To determine the normal kinematics of the capitate, scaphoid, and lunate during unconstrained wrist flexion-extension;
2. To determine the effect of the scapholunate ligament sectioning on scaphoid and lunate kinematics throughout planar wrist flexion-extension and radial-ulnar deviation and;
3. To determine the effect of the secondary stabilizers including the: scaphotrapezium-trapezoid ligament and radioscaphocapitate ligament on scaphoid and lunate kinematics throughout planar wrist flexion-extension and radial-ulnar deviation.



### 1.6.2 *Specific Hypotheses*

Based on the above objectives, these hypotheses have been generated:

1. The capitate, scaphoid, and lunate will move synergistically throughout planar wrist flexion-extension but will contribute at differing levels between wrist flexion and extension.
2. The scapholunate ligament is the primary stabilizer of the scapholunate joint and following sectioning will alter the native kinematics of the scaphoid and lunate during wrist motion.
3. The sectioning of the secondary stabilizers will further alter the native kinematics of the scaphoid and lunate. The scaphoid will become more flexed and the lunate will become more extended following the sectioning of the secondary stabilizers.

## 1.7 Thesis Overview

**Chapter 2:** Investigates the normal kinematics of the capitate, scaphoid, and lunate during unconstrained planar wrist flexion-extension.

**Chapter 3:** Investigates the kinematics of the scaphoid and lunate following the sequential sectioning of the scapholunate ligament and secondary stabilizers during unconstrained planar wrist flexion-extension and radial-ulnar deviation.

**Chapter 4:** Provides a general discussion, summary, and potential areas of future work.

## 1.8 References

1. Bajuri MN, Abdul Kadir MR. The Wrist Joint. In: Springer Berlin Heidelberg; 2013:1-12.
2. Gray H. *Anatomy of the Human Body*. 20th ed. (Philadelphia: Lea & Febiger, ed.). New York, NY; 1918.
3. Silverstein J, Moeller J, Hutchinson M. Common Issues in Orthopedics. In: *Textbook of Family Medicine*. 8th ed. Philadelphia : Saunders Elsevier; 2011.
4. Lieberman J. Bone and Joint Biology. In: *AAOS Comprehensive Orthopaedic Review*. Rosemont, IL: American Academy of Orthopaedic Surgeons; 2009.
5. White TD, Black MT, Folkens PA, White TD, Black MT, Folkens PA. Chapter 9 – Arm: Humerus, Radius, and Ulna. In: *Human Osteology*. ; 2012:175-198.
6. Cooney WP. *The Wrist: Diagnosis and Operative Treatment*. Vol 8. 2nd ed. (Kluwer W, ed.). Philadelphia, Baltimore, New York, London, Buenos Aires, Hong Kong, Sydney, Tokyo; 2011.
7. An K-N, Berger RA, Cooney WP, eds. *Biomechanics of the Wrist Joint*. New York, NY: Springer New York; 1991.
8. Phillips B, Schmidt S. Wrist Joint Anatomy. Published 2013.
9. Wheelless C. *Wheelless' Textbook of Orthopaedics*. (Wheelless C, Thompson D, Burge P, et al., eds.). Durham, NC: Data Trace Internet Publishing; 2014.
10. Ward LD, Ambrose CG, Masson M V., Levaro F. The role of the distal radioulnar ligaments, interosseous membrane, and joint capsule in distal radioulnar joint stability. *J Hand Surg Am*. 2000;25(2):341-351.
11. Kitay A, Wolfe SW. Scapholunate instability: current concepts in diagnosis and management. *J Hand Surg Am*. 2012;37(10):2175-2196.

12. Pappou IP, Basel J, Deal DN. Scapholunate ligament injuries: a review of current concepts. *Hand (N Y)*. 2013;8(2):146-156.
13. Schlossberg L, Zuidema G. *The Johns Hopkins Atlas of Human Functional Anatomy*. 4th ed. Baltimore: Johns Hopkins University Press; 1997.
14. Mader S. *Understanding Human Anatomy And Physiology*. 5th ed. (McGraw-Hill Higher Education, ed.). Burr Ridge, IL; 2005.
15. Anatomy Medicine. The Muscles of the Arm and Hand. Published 2016.
16. Wu G, van der Helm FCT, Veeger HEJD, et al. ISB recommendation on definitions of joint coordinate systems of various joints for the reporting of human joint motion--Part II: shoulder, elbow, wrist and hand. *J Biomech*. 2005;38(5):981-992.
17. Lippert L. Clinical Kinesiology and Anatomy of the Upper Extremities. In: *Clinical Kinesiology and Anatomy*. 5th ed. F.A. Davis; 2011.
18. Ruby LK, An KN, Linscheid RL, Cooney WP, Chao EY. The effect of scapholunate ligament section on scapholunate motion. *J Hand Surg Am*. 1987;12(5 Pt 1):767-771.
19. Acosta R, Hnat W, Scheker LR. Distal radio-ulnar ligament motion during supination and pronation. *J Hand Surg Br*. 1993;18(4):502-505..
20. Forthman CL, Segalman KA. Lesions and Tumors of the Carpus. *Hand Clin*. 2006;22(4):435-446.
21. Morhart M, Ghahary A, Tredget E, Jarman A. Wrist Fractures and Dislocations. Published 2015.
22. De Smet L, Verhaegen F, Degreeef I. Carpal Malalignment in Malunion of the Distal Radius and the Effect of Corrective Osteotomy. *J Wrist Surg*. 2014;03(03):166-170.

23. Osada D, Viegas SF, Shah MA, Morris RP, Patterson RM. Comparison of different distal radius dorsal and volar fracture fixation plates: A biomechanical study. *J Hand Surg Am.* 2003;28(1):94-104.
24. Dunning CE, Lindsay CS, Bicknell RT, Patterson SD, Johnson JA, King GJ. Supplemental pinning improves the stability of external fixation in distal radius fractures during simulated finger and forearm motion. *J Hand Surg Am.* 1999;24(5):992-1000.
25. Phillips TG, Reibach AM, Slomiany WP. Diagnosis and management of scaphoid fractures. *Am Fam Physician.* 2004;70(5):879-884.
26. Muminagic S, Kapidzic T. Wrist instability after injury. *Mater Sociomed.* 2012;24(2):121-124.
27. Mathoulin CL, Dauphin N, Wahegaonkar AL. Arthroscopic dorsal capsuloligamentous repair in chronic scapholunate ligament tears. *Hand Clin.* 2011;27(4):563-572, xi.
28. Kitay A, Wolfe SW. Scapholunate instability: current concepts in diagnosis and management. *J Hand Surg Am.* 2012;37(10):2175-2196.
29. Brubacher J, Fischer S. American Academy of Orthopaedic Surgeons - Arthritis of the Wrist. Published 2016.
30. Nishiwaki M, Welsh M, Gammon B, Ferreira LM, Johnson JA, King GJW. Distal radioulnar joint kinematics in simulated dorsally angulated distal radius fractures. *J Hand Surg Am.* 2014;39(4):656-663.
31. Werner FW, Palmer AK, Somerset JH, et al. Wrist joint motion simulator. *J Orthop Res.* 1996;14(4):639-646.
32. Iglesias D. Development of an in-vitro passive and active motion Simulator for the investigation of wrist function and Kinematics. *Electron Thesis Diss Repos.* 2015.

33. Weber ER. Concepts governing the rotational shift of the intercalated segment of the carpus. *Orthop Clin North Am.* 1984;15(2):193-207.
34. Landsmeer JM. Studies in the anatomy of articulation. I. The equilibrium of the “intercalated” bone. *Acta Morphol Neerl Scand.* 1961;3:287-303.
35. Navarro A. Luxacuiones del carpo. *Anal Fac Med.* 1921:113-141.
36. von Bonin G. A Note on the Kinematics of the Wrist-Joint. *J Anat.* 1929;63(Pt 2):259-262.
37. Lee SK, Zlotolow DA, Sapienza A, Karia R, Yao J. Biomechanical comparison of 3 methods of scapholunate ligament reconstruction. *J Hand Surg Am.* 2014;39(4):643-650.
38. Dimitris C, Werner FW, Joyce DA, Harley BJ. Force in the Scapholunate Interosseous Ligament During Active Wrist Motion. *J Hand Surg Am.* 2015;40(8):1525-1533.
39. Kuo CE, Wolfe SW. Scapholunate Instability: Current Concepts in Diagnosis and Management. *J Hand Surg Am.* 2008;33(6):998-1013.
40. Lavernia CJ, Cohen MS, Taleisnik J. Treatment of scapholunate dissociation by ligamentous repair and capsulodesis. *J Hand Surg Am.* 1992;17(2):354-359.
41. Blatt G. Capsulodesis in reconstructive hand surgery. Dorsal capsulodesis for the unstable scaphoid and volar capsulodesis following excision of the distal ulna. *Hand Clin.* 1987;3(1):81-102.
42. Weiss A-PC. Scapholunate ligament reconstruction using a bone-retinaculum-bone autograft. *J Hand Surg Am.* 1998;23(2):205-215.
43. Watson H, Weinzweig J, Guidera PM, Zeppieri J, Ashmead D. One Thousand Intercarpal Arthrodeses. *J Hand Surg J Br Soc Surg Hand.* 1999;24(3):307-315.

44. Kleinman WB, Carroll C. Scapho-trapezio-trapezoid arthrodesis for treatment of chronic static and dynamic scapho-lunate instability: a 10-year perspective on pitfalls and complications. *J Hand Surg Am.* 1990;15(3):408-414.
45. Wyrick JD, Youse BD, Kiefhaber TR. Scapholunate ligament repair and capsulodesis for the treatment of static scapholunate dissociation. *J Hand Surg Br.* 1998;23(6):776-780.
46. Wyrick JD, Stern PJ, Kiefhaber TR. Motion-preserving procedures in the treatment of scapholunate advanced collapse wrist: Proximal row carpectomy versus four-corner arthrodesis. *J Hand Surg Am.* 1995;20(6):965-970.
47. Short WH, Werner FW, Green JK, Masaoka S. Biomechanical evaluation of ligamentous stabilizers of the scaphoid and lunate. *J Hand Surg Am.* 2002;27(6):991-1002.
48. Short WH, Werner FW, Green JK, Masaoka S. Biomechanical evaluation of the ligamentous stabilizers of the scaphoid and lunate: Part II. *J Hand Surg Am.* 2005;30(1):24-34.
49. Short WH, Werner FW, Green JK, Sutton LG, Brutus JP. Biomechanical evaluation of the ligamentous stabilizers of the scaphoid and lunate: part III. *J Hand Surg Am.* 2007;32(3):297-309.

## Chapter 2

### 2 *Biomechanical Evaluation of Carpal Kinematics During Simulated Wrist Motion*

#### *Overview*

*The kinematics of the wrist have been previously investigated although there remains no agreement regarding the influence of each carpal bone on total wrist motion. This chapter presents a study that examines the normal kinematics of the capitate, scaphoid, and lunate during unconstrained planar wrist flexion and extension. This study also examined the effect of motion direction (i.e. flexion or extension) on carpal kinematics.*

*A version of this work was presented at the 2016 Annual Meeting of the Orthopaedic Research Society, the 2016 Biennial Canadian Bone and Joint Conference, and at the 2016 Annual Meeting of the Canadian Orthopaedic Research Society.*

*A version of this work has been accepted for publication in The Journal of Wrist Surgery.*



## 2.1 Introduction

As described in Chapter 1 (Section 1.5) normal wrist kinematics rely on the intricate interplay between the articular geometry and ligamentous constraints. The wrist joint is frequently subdivided into the radiocarpal and midcarpal joints based on the functional grouping of the bones in the proximal and distal rows.<sup>1</sup> The midcarpal joint is formed by the articulation of the scaphoid, lunate and triquetrum, with the trapezium, trapezoid, capitate and hamate.<sup>2</sup> The radiocarpal joint is formed by the articulation between the bones of the proximal carpal row the scaphoid, lunate and triquetrum with the distal radius. The combination of midcarpal and radiocarpal joint relative motion is responsible for the total range of wrist motion in flexion and extension.<sup>3</sup>

Carpal kinematics have been previously studied as highlighted in Chapter 1 (Section 1.5), yet there remains no consensus regarding each carpal bone's contribution to wrist motion. This disparity has led to numerous theories depicting the normal kinematics of the wrist including: row, column, intercalated segment and oval ring concepts.<sup>1,4-6</sup> In addition, previous kinematic studies have investigated the contribution of the radiocarpal and midcarpal joints during wrist motion, however there is disagreement regarding the role of each joint throughout flexion and extension.<sup>3,7-10</sup> A more detailed understanding of normal carpal bone kinematics during wrist motion is necessary to effectively diagnose and treat ligamentous injuries of the wrist. This information is also clinically beneficial as many injuries arising in the wrist often manifest as an alteration of intercarpal motion.<sup>11</sup> Furthermore, a better understanding carpal kinematics allows for evaluation of the wrist joint under normal and pathological conditions, and should lead to improvements in the outcome of partial wrist fusions, ligament reconstructions and prosthetic devices.<sup>12</sup>

The objective of the present *in vitro* biomechanical study was to determine the kinematics of the scaphoid, lunate and capitate during planar motions of unconstrained wrist flexion and extension. In addition, this study emphasizes the ratio of carpal bone rotation to total wrist rotation in flexion and extension. Further, this study examined the effect of motion direction (*i.e.* flexion or extension) on kinematics and the contribution of scaphoid and lunate rotation to overall wrist flexion and extension.

## 2.2 Materials and Methods

### 2.2.1 *Specimen Preparation*

Seven (7) fresh frozen cadaveric upper limb specimens (average age: 67 years; range 37-91; 5 male; 4 left) amputated at the mid-humerus were used. CT scans of each wrist were examined beforehand to rule out and underlying wrist pathologies. There was no history of trauma or wrist disease in any of the specimens used. The upper limbs were thawed overnight at room temperature and the fingers were disarticulated at the metacarpophalangeal joints. The tendons of the abductor pollicis longus (APL), extensor carpi radialis brevis (ECRB), extensor carpi radialis longus (ECRL), extensor carpi ulnaris (ECU), flexor carpi radialis (FCR) and flexor carpi ulnaris (FCU) were exposed and sutured at the musculotendinous junction (Ethicon, Somerville, NJ). The specimens were mounted in a custom wrist motion simulator by rigidly securing the humerus in a clamp (Fig.2-1). Two threaded pins were used to fix the ulna to the simulator with the elbow aligned at 90° flexion. A Steinmann pin was inserted into the proximal radius securing the forearm in neutral rotation (Fig.2-1).

The neutral position of the wrist in flexion-extension was defined by visually aligning the third metacarpal with the forearm. As the capitate-third metacarpal joint is rigid, the position of the capitate was used to represent wrist position.<sup>13</sup> A Steinmann pin was inserted longitudinally into the shaft of the third metacarpal and placed into the arc of the simulator as a guide for passive wrist motion (Fig.2-1). Muscle tone loads were produced using pneumatic actuators via cables routed through a system of pulleys and connected to the tendon sutures (Airport Corporation, Norwalk, CT). Optical tracking markers (Optotrak Certus; Northern Digital, Waterloo, Ontario, Canada) were secured to the lunate, scaphoid, capitate and radius under fluoroscopic control to capture the kinematics throughout testing. The radial marker was attached to the distal shaft of the radius. The lunate marker was inserted dorsally through a small arthrotomy along the distal edge of the dorsal radiocarpal ligament; the scaphoid marker was inserted through a small volar incision over the tuberosity; and the capitate marker was placed dorsally into the body of the bone.

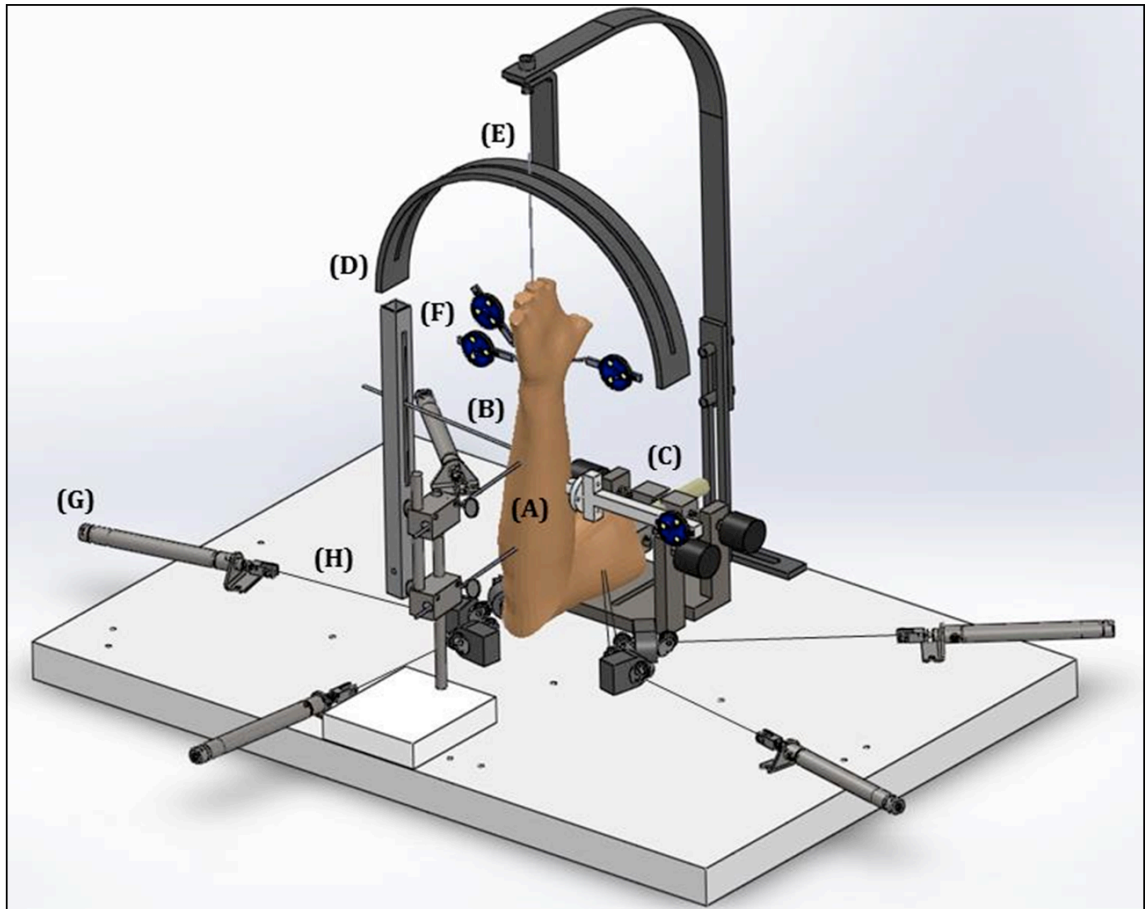


**Figure 2-1: *In Vitro* Passive Motion Wrist Simulator.** This device is capable of loading six muscle groups of interest while simulating passive flexion-extension of the wrist: (A) ulna fixed with the elbow at 90° flexion, (B) radius fixed with the forearm in neutral rotation, (C) rigidly fixed humerus, (D) flexion-extension motion arc, (E) Steinmann pin inserted into 3<sup>rd</sup> metacarpal; passive motion guide, (F) Optotrack six DOF tracking markers, (G) pneumatic actuators, and (H) cables connecting actuators and corresponding muscle sutures.

### 2.2.2 *Testing Protocol*

Passive flexion and extension motion of the wrist was simulated by one investigator moving the Steinmann pin along the flexion-extension motion arc of the simulator at a speed of approximately 5°/sec. Tone loads of 10 N were applied to the APL, ECRB, ECRL, ECU, FCR and FCU. Each specimen was subjected to two extension and two flexion trials and data was analyzed from the second trial of each.

Extension trials were defined as moving the wrist from flexion to extension, and flexion trials were defined as extension to flexion. Kinematic data was extracted in 5° increments. The specimens were irrigated with saline and the skin was closed throughout the testing protocol in an effort to maintain specimen hydration. Data was analyzed from 35° of extension to 35° of flexion due to variable specimen range of motion and impingement of the trackers in some specimens at the extremes of motion. Following the testing protocol, the joints were dissected, and the landmarks on the radius, scaphoid, lunate and capitate were digitized using a pointed stylus. All tracker mounts were inspected following dissection to ensure there was no visible movement that occurred throughout testing. The neutral position of the wrist, as defined by the International Society of Biomechanics (ISB), served to form the coordinate systems and was used to calculate the angle of wrist flexion and extension.<sup>14</sup>

### 2.2.3 *Outcome Variables and Data Analysis*

The angulation of the scaphoid and lunate relative to the distal radius was evaluated for both flexion and extension trials. Extension trials and flexion trials were averaged over the tested range of motion in order to calculate the contribution of the lunate and scaphoid to global wrist motion. Wrist flexion-extension angle was defined as the angle between the long axis of the radius and the long axis of the third metacarpal with respect to the distal radius coordinate system. The coordinate systems for each bone employed ISB recommendations with the exception of the origin of each of the carpal coordinate systems located at the proximal pole in contrast to the suggested volumetric centroid.<sup>14</sup>

However, the orientation of the carpal coordinate systems remained in parallel with the radial coordinate system while the wrist was in neutral position.<sup>14</sup>

#### 2.2.4 *Statistical Methods*

A 3-way repeated measures analysis of variance (ANOVA) was completed using SPSS 17.0 (SPSS Inc., Chicago, IL, USA). The factors (*viz.* independent variables) included: direction of motion (flexion [-35° to 0°], extension [0° to 35°]), bone (capitate, scaphoid, lunate), and wrist flexion-extension angle (in 5° increments). The outcome variables were the rotation angles of the carpal bones about the physiologic axes of motion (flexion/extension). A paired t-test analysis was also performed for the scaphoid and lunate rotational data to assess differences between flexion and extension motion pathways. Statistical significance was set at  $p < 0.05$ .

## 2.3 Results

### 2.3.1 *Flexion-Extension of the Scaphoid and Lunate*

The rotation of the scaphoid and lunate were found to correlate linearly with wrist motion during flexion trials ( $R^2=0.99$  for both) (Fig. 2-2). Scaphoid rotation was on average  $95\pm 20\%$  ( $p=1.0$ ) of wrist flexion, and lunate rotation was an average  $70\pm 12\%$  of wrist flexion ( $p=0.007$ ). The motion between the scaphoid and lunate was  $25\pm 17\%$  of global wrist flexion. For  $60^\circ$  of capitate flexion, the scaphoid flexed  $57\pm 12^\circ$ , and the lunate flexed  $42\pm 7^\circ$ , thus yielding scapholunate intercarpal motion of  $15\pm 14^\circ$ .

During extension trials both the scaphoid and lunate were found to correlate linearly with wrist motion ( $R^2=0.99$  and  $0.97$  respectively). Scaphoid rotation was  $83\pm 19\%$  ( $p=0.033$ ) of wrist extension, and lunate rotation was  $37\pm 18\%$  ( $p=0.001$ ) of wrist extension. The motion between the scaphoid and lunate was  $46\pm 15\%$  of global wrist extension. For  $60^\circ$  of capitate extension, the scaphoid extended  $50\pm 11^\circ$ , the lunate extended  $22\pm 11^\circ$ , and the scapholunate intercarpal motion was  $28\pm 16^\circ$ .

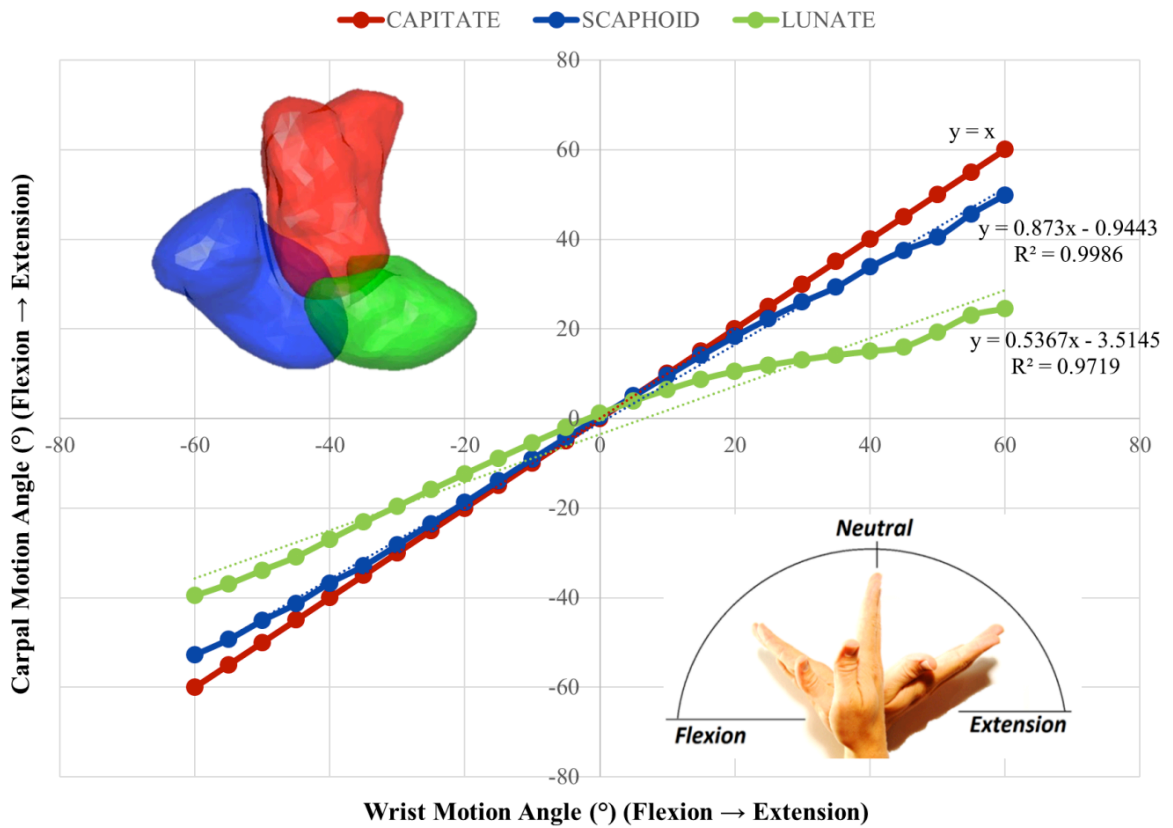


**Figure 2-2: Flexion-Extension of the Scaphoid and Lunate.** The mean relative rotation of the scaphoid, lunate and capitate (with respect to the radius) from 60° of wrist flexion to 60° of extension. Standard deviations were omitted for clarity (Scaphoid range: ±2.20° to ±5.25°; Lunate range: ±1.01° to ±5.15°).

### 2.3.2 *Ratio of Scaphoid and Lunate Rotation to Wrist Rotation*

The ratio of scaphoid and lunate rotation to global wrist rotation decreased as the wrist was moved from flexion to extension (Fig. 2-3). There was no significant difference in scaphoid rotation between flexion and extension of the wrist ( $p=0.15$ ) (Fig. 2-3). However, there was a significant decrease in lunate rotation compared to wrist rotation from flexion to extension ( $p=0.004$ ). Significant differences were found between the rotation of the lunate when compared to both the scaphoid and capitate throughout flexion and extension (Fig.2-4). The lunate rotated on average  $46\pm 25\%$  less than the capitate, and  $35\pm 31\%$  less than the scaphoid during wrist flexion and extension ( $p=0.001$ ). The scaphoid rotated on average  $11\pm 19\%$  less than the capitate during wrist flexion and extension, however this was not statistically significant ( $p=0.066$ ).

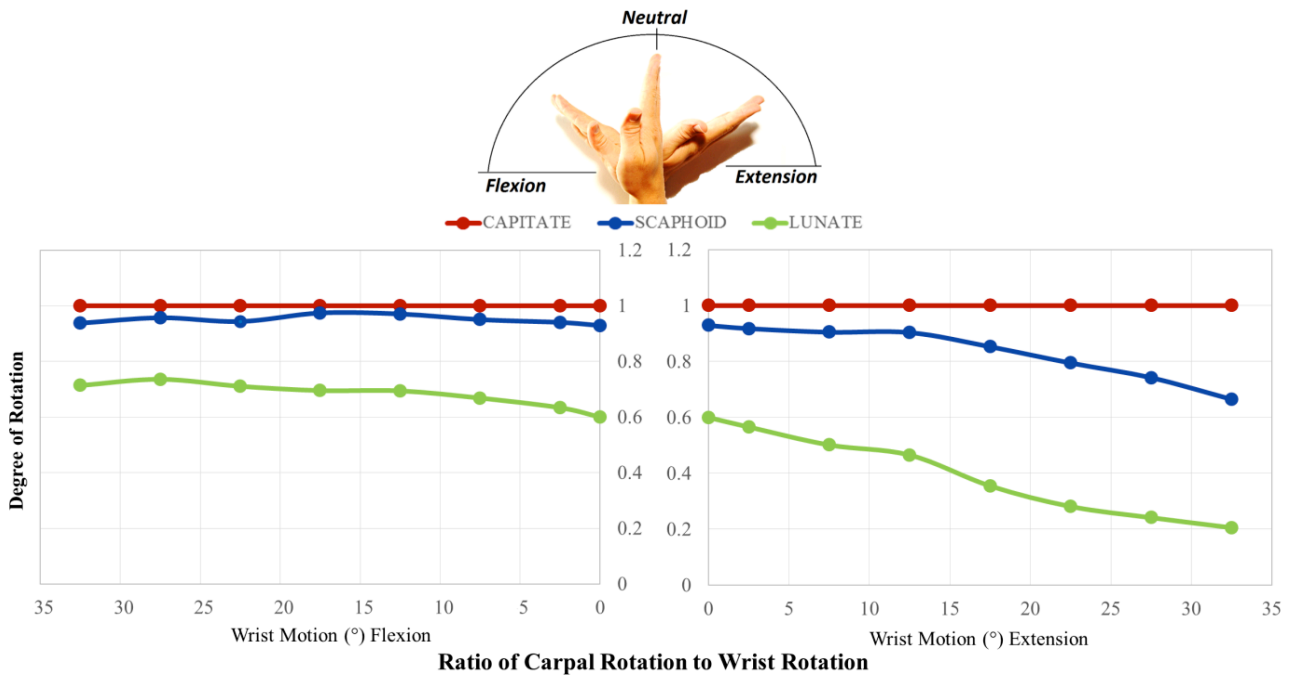


**Figure 2-3: Ratio of Carpal Rotation to Wrist Rotation.** The ratio of scaphoid and lunate rotation respect to wrist rotation. Standard deviations were omitted for clarity (Scaphoid range:  $\pm 0.08^\circ$  to  $\pm 0.24^\circ$ ; Lunate range:  $\pm 0.10^\circ$  to  $\pm 0.26$ ).



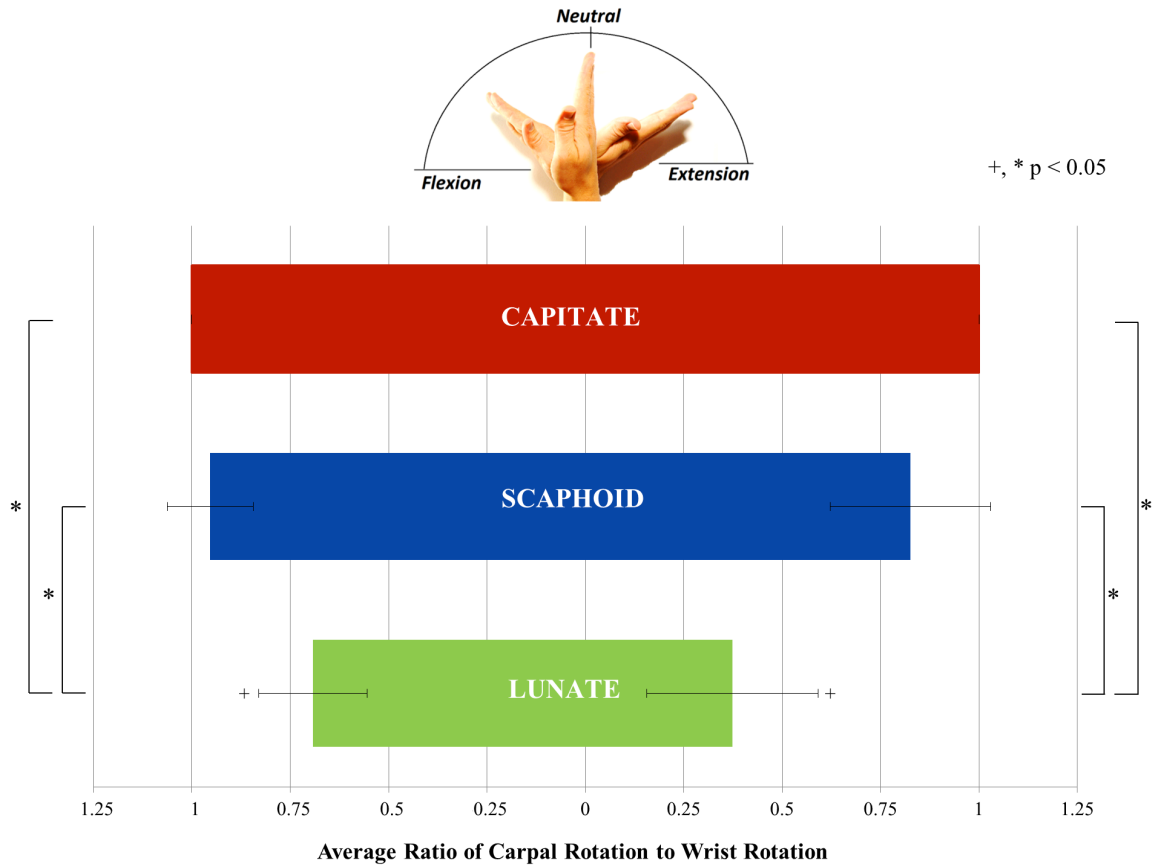


**Figure 2-4: Average Ratio of Carpal Rotation to Wrist Rotation.** The ratio of scaphoid and lunate motion with respect to wrist rotation during flexion and extension. The capitate demonstrates a 1:1 ratio with global wrist rotation, as it is directly in line with the wrist flexion-extension axis. The data is the mean and the error bars indicate the standard deviation of each carpal bone for both flexion and extension.

### 2.3.3 *Direction of Motion*

Direction of motion did not have a statistically significant effect on carpal kinematics for wrist flexion and extension motions with mean differences less than 6.4% between directions. There was no difference in scaphoid and lunate contributions to wrist flexion or extension ( $p=0.26$  and  $0.77$ , respectively) for the two directions of motion (Fig. 2-5).

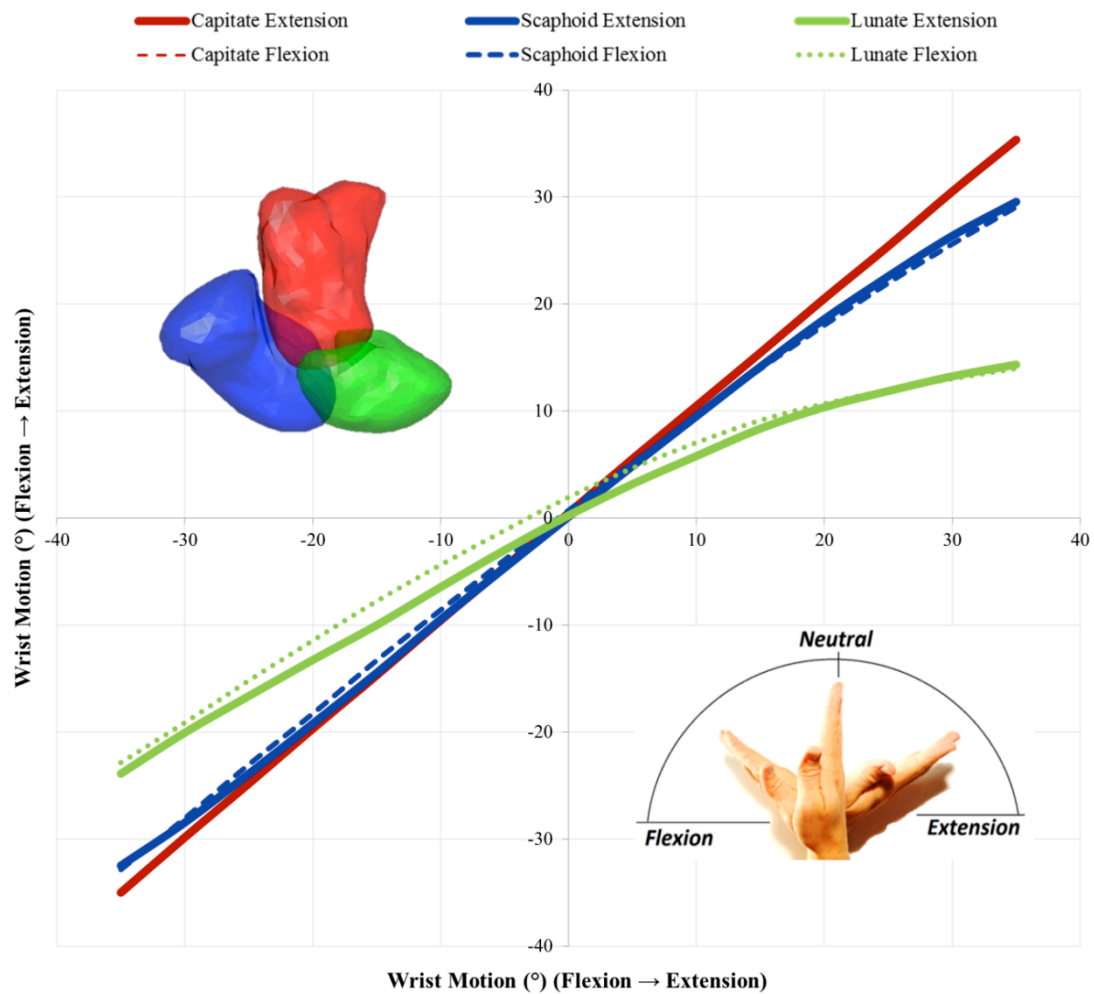


**Figure 2-5: Effect of Direction of Motion.** The mean rotation of the scaphoid and lunate compared to wrist rotation, for both flexion and extension trials.

## 2.4 Discussion

Planar wrist flexion-extension is achieved via rotation at the radiocarpal and midcarpal joints and is defined by the motion of the capitate as it moves with respect to the radius. Carpal kinematics have been studied *in vivo* and *in vitro*, yet there remains no unanimity regarding the contribution of each carpal bone to wrist motion. Consequently, numerous theories have been developed due to the inconsistencies in data representing the kinematics of the native wrist joint. This study investigated capitate, scaphoid and lunate kinematics during unconstrained planar wrist flexion-extension. Our results found that at the radiocarpal joint the scaphoid contributes at a greater extent to wrist motion throughout flexion and extension when compared to the lunate. Scaphoid and lunate motion was found to correlate linearly with capitate motion throughout the tested range of motion, both contributing more to total wrist motion during flexion. In addition, our results found that the ratio of scaphoid and lunate rotation to wrist rotation decreases from flexion to extension, suggesting that the radiocarpal joint plays a more critical role in flexion. The relatively large magnitude of scapholunate differential rotation, averaging  $10\pm 4^\circ$  at  $35^\circ$  of wrist flexion and  $15\pm 5^\circ$  at  $35^\circ$  of wrist extension, may explain the high incidence of scapholunate ligament injuries relative to other intercarpal joints.<sup>15</sup>

At all wrist positions, we found the scaphoid contributed a greater extent to wrist motion compared to the lunate, consistent with previous *in vivo* and *in vitro* studies.<sup>16-21</sup> Our results confirm the synergistic motion between the capitate, lunate and scaphoid throughout motion. Agreeing with *Wolfe et al.*<sup>20</sup>, the present data indicates that the scaphoid and lunate correlate linearly with the capitate throughout wrist flexion-extension (Fig. 2-2). Our findings are also consistent with *Werner et al.*<sup>19</sup> who showed that the scaphoid and lunate do not contribute equally to wrist flexion and extension, each producing a unique arc of motion (Fig. 2-2). Despite finding a small magnitude of interspecimen variability, we confirmed wrist motion during flexion and extension follows a similar trend. This supports the hypothesis by *Kobayashi et al.*<sup>16</sup> that the underlying mechanism that governs carpal kinematics in the uninjured state is uniform within subject population.

Contrasting the majority of published studies, we found the scaphoid contributed more to flexion compared to extension (Flexion - 95%, Extension - 83% vs. Flexion - 86%, Extension - 69%).<sup>17</sup> Likewise, our results for the lunate contrast the range of contributions found within literature for flexion, which are greater than the average of previously reported contributions (70% vs. 50%)<sup>17</sup>, but agree for extension. As shown by *Moojen et al.* a large variability exists in previously reported scaphoid and lunate contributions to wrist motion due to methodologies limitations (Scaphoid Extension Range[58-99%], Flexion Range [61-88%]; Lunate Extension Range [22-68%], Flexion Range[36-63%]).<sup>17</sup> Previous *in vitro* studies<sup>3,12,19,22</sup> were limited to less than  $\pm 60^\circ$  flexion-extension due to tracking constraints and assumed a linear relationship within these positions similar to the present study. The *in vivo* study performed by *Wolfe et al.*<sup>21</sup> utilized static positioning at four positions of flexion-extension, while an *in vivo* study by *Moojen et al.*<sup>17</sup> imitated continuous motion using  $5^\circ$  increments. The present investigation provides new information on continuous wrist motion compared to interpolating between wrist angles.<sup>23</sup>

Previous kinematic studies have reported varying results regarding the relative contribution of the radiocarpal and midcarpal joints to wrist motion, with few studies showing equal radiocarpal and midcarpal contribution during flexion with the radiocarpal joint contributing more in extension.<sup>24-26</sup> Other studies suggested that the radiocarpal joint contributes a greater degree in wrist extension and the midcarpal joint more in flexion.<sup>3,8,18,27,28</sup> Agreeing with our study, several investigators showed that the radiocarpal joint contributed more in wrist flexion and the midcarpal joint more in extension.<sup>22,29-31</sup> This variability may stem from how carpal angles were represented; either relative to a starting position, or similar to this study, as an angle relative to another bone.<sup>23</sup> Reporting carpal angles with respect to the distal radius gave an anatomical reference throughout the tested range of motion.

Currently a range of surgical options exist for wrist arthritis including partial carpal fusions<sup>32</sup>, however it is unclear as to which method of fusion has superior biomechanical potential optimizing the range of wrist motion. Our results provide a better representation of potential outcomes of partial wrist fusions with respect to wrist motion. When

performing a midcarpal fusion, the lunate should be fixed in a slightly flexed position allowing for functional wrist extension. Similarly, when performing a radioscapolunate fusion the lunate should be fixed in a slightly extended position allowing for functional wrist extension.

The work of this chapter has limitations. In addition to only analyzing wrist motion from  $\pm 35^\circ$  of wrist flexion-extension, motion testing was performed in one anatomic plane to maintain reproducibility, not incorporating the complex multiplanar motions of the wrist. Carpal kinematics were considered in one anatomic plane not considering the rotational and translational movements of the bones throughout flexion-extension. Although wrist motion was performed passively, balanced tendon loading was applied across the wrist to mimic physiologically relevant forces which may occur clinically with active motion. Future work will investigate the effect of dynamic stabilizers and varied tone loads during active motion on carpal kinematics. Our study deviated from the ISB suggested volumetric centroid coordinate system, although we only reported joint angles which would be unaffected by origin definition.

This study has several strengths. A highly accurate optical motion capture system facilitating real time kinematic measurements was employed. Additionally, this study analyzed normal kinematics of the native wrist in the flexion-extension plane throughout continuous motion compared to interpolating static positions which may not effectively represent dynamic motion, nor does it recreate normal kinematics.<sup>23</sup>

## 2.5 Conclusions

Overall, these findings support a relative collaboration of the scaphoid, lunate and capitate during wrist flexion and extension. It was found that the scaphoid and lunate both rotated more during wrist flexion compared to extension, suggesting the radiocarpal joint has a greater influence during flexion and the midcarpal joint is more important for extension. The large magnitude of differential rotation observed between the scaphoid and lunate averaging  $10\pm 4^\circ$  at  $35^\circ$  of wrist flexion and  $15\pm 5^\circ$  at  $35^\circ$  of wrist extension may explain, in part, the high incidence of scapholunate ligament injuries relative to other intercarpal ligaments. A detailed understanding of normal and abnormal carpal kinematics may assist in the future design and development of wrist arthroplasty, assist surgeons in positioning the carpal bones when performing partial wrist fusions, and help develop better techniques for scapholunate ligament repair and reconstruction.

## 2.6 References

1. Weber ER. Concepts governing the rotational shift of the intercalated segment of the carpus. *Orthop Clin North Am.* 1984;15(2):193-207.
2. Moritomo H, Murase T, Goto A, Oka K, Sugamoto K, Yoshikawa H. Capitate-based kinematics of the midcarpal joint during wrist radioulnar deviation: an in vivo three-dimensional motion analysis. *J Hand Surg Am.* 2004;29(4):668-675.
3. Sarrafian SK, Melamed JL, Goshgarian GM. Study of wrist motion in flexion and extension. *Clin Orthop Relat Res.* (126):153-159.
4. Landsmeer JM. Studies in the anatomy of articulation. I. The equilibrium of the “intercalated” bone. *Acta Morphol Neerl Scand.* 1961;3:287-303.
5. Navarro A. Luxacuiones del carpo. *Anal Fac Med.* 1921:113-141.
6. von Bonin G. A Note on the Kinematics of the Wrist-Joint. *J Anat.* 1929;63(Pt 2):259-262.
7. Ruby LK, An KN, Linscheid RL, Cooney WP, Chao EY. The effect of scapholunate ligament section on scapholunate motion. *J Hand Surg Am.* 1987;12(5 Pt 1):767-771.
8. Berger RA, Crowninshield RD, Flatt AE. The three-dimensional rotational behaviors of the carpal bones. *Clin Orthop Relat Res.* 1982;(167):303-310.
9. Gellman H, Kauffman D, Lenihan M, Botte MJ, Sarmiento A. An in vitro analysis of wrist motion: the effect of limited intercarpal arthrodesis and the contributions of the radiocarpal and midcarpal joints. *J Hand Surg Am.* 1988;13(3):378-383.
10. Volz RG, Lieb M, Benjamin J. Biomechanics of the wrist. *Clin Orthop Relat Res.* 1980;(149):112-117.

11. An K-N, Berger RA, Cooney WP, eds. *Biomechanics of the Wrist Joint*. New York, NY: Springer New York; 1991.
12. Ishikawa J, Cooney WP, Niebur G, An KN, Minami A, Kaneda K. The effects of wrist distraction on carpal kinematics. *J Hand Surg Am*. 1999;24(1):113-120.
13. Lichtman DM, Schneider JR, Swafford AR, Mack GR. Ulnar midcarpal instability--clinical and laboratory analysis. *J Hand Surg Am*. 1981;6(5):515-523.
14. Wu G, van der Helm FCT, Veeger HEJD, et al. ISB recommendation on definitions of joint coordinate systems of various joints for the reporting of human joint motion--Part II: shoulder, elbow, wrist and hand. *J Biomech*. 2005;38(5):981-992.
15. Goto A, Moritomo H, Murase T, et al. In vivo three-dimensional wrist motion analysis using magnetic resonance imaging and volume-based registration. *J Orthop Res*. 2005;23(4):750-756.
16. Kobayashi M, Berger RA, Nagy L, et al. Normal kinematics of carpal bones: A three-dimensional analysis of carpal bone motion relative to the radius. *J Biomech*. 1997;30(8):787-793.
17. Moojen TM, Snel JG, Ritt MJPF, Venema HW, Kauer JMG, Bos KE. In vivo analysis of carpal kinematics and comparative review of the literature. *J Hand Surg Am*. 2003;28(1):81-87.
18. Savelberg HH, Otten JD, Kooloos JG, Huijkes R, Kauer JM. Carpal bone kinematics and ligament lengthening studied for the full range of joint movement. *J Biomech*. 1993;26(12):1389-1402.
19. Werner FW, Short WH, Fortino MD, Palmer AK. The relative contribution of selected carpal bones to global wrist motion during simulated planar and out-of-plane wrist motion. *J Hand Surg Am*. 1997;22(4):708-713.



20. Wolfe SW, Crisco JJ, Katz LD. A non-invasive method for studying in vivo carpal kinematics. *J Hand Surg Br.* 1997;22(2):147-152.
21. Wolfe SW, Neu C, Crisco JJ. In vivo scaphoid, lunate, and capitate kinematics in flexion and in extension. *J Hand Surg Am.* 2000;25(5):860-869.
22. Patterson RM, Nicodemus CL, Viegas SF, Elder KW, Rosenblatt J. High-speed, three-dimensional kinematic analysis of the normal wrist. *J Hand Surg Am.* 1998;23(3):446-453.
23. Moojen T., Snel J., Ritt MJP., Kauer JM., Venema H., Bos K. Three-dimensional carpal kinematics in vivo. *Clin Biomech.* 2002;17(7):506-514.
24. Bunnell S. *Surgery of the Hand.* 3rd ed. (Lippencott J, ed.). Philadelphia; 1956.
25. Fisk GR. The wrist. *J Bone Joint Surg Br.* 1984;66(3):396-407.
26. Garcia-Elias M, Cooney WP, An KN, Linscheid RL, Chao EY. Wrist kinematics after limited intercarpal arthrodesis. *J Hand Surg Am.* 1989;14(5):791-799.
27. Sommer HJ, Miller NR. A technique for kinematic modeling of anatomical joints. *J Biomech Eng.* 1980;102(4):311-317.
28. Youm Y, McMurthy RY, Flatt AE, Gillespie TE. Kinematics of the wrist. I. An experimental study of radial-ulnar deviation and flexion-extension. *J Bone Joint Surg Am.* 1978;60(4):423-431.
29. de Lange A, Kauer JM, Huiskes R. Kinematic behavior of the human wrist joint: a roentgen-stereophotogrammetric analysis. *J Orthop Res.* 1985;3(1):56-64.
30. Seradge H, Owens W, Seradge E. The effect of intercarpal joint motion on wrist motion: are there key joints? An in vitro study. *Orthopedics.* 1995;18(8):727-732.
31. Smith DK, An KN, Cooney WP, Linscheid RL, Chao EY. Effects of a scaphoid waist osteotomy on carpal kinematics. *J Orthop Res.* 1989;7(4):590-598.

32. Got C, Vopat BG, Mansuripur PK, Kane PM, Weiss APC, Crisco JJ. The effects of partial carpal fusions on wrist range of motion. *J Hand Surg Eur Vol.*

## Chapter 3

### ***3 Biomechanical Evaluation of the Scapholunate Ligament and Secondary Stabilizers on Scaphoid and Lunate Kinematics***

#### ***Overview***

*The stabilizing influence of the scapholunate ligament and secondary ligamentous restraints on scaphoid and lunate kinematics have been previously investigated, however, their role remains inconclusive. This chapter presents a study that examines the effect of sequential sectioning of the scapholunate ligament and two of the secondary stabilizers, the scaphotrapezium-trapezoid and radioscaphocapitate ligaments on scaphoid and lunate kinematics during simulated active planar wrist flexion-extension and radial-ulnar deviation. In order to generate physiologic motions, a novel wrist testing apparatus was employed for the studies of this chapter.*

*A version of this work was accepted to the 2017 Annual Meeting of the Orthopaedic Research Society.*

### 3.1 Introduction

As described in Chapter 1 (Section 1.5), ligamentous injuries of the wrist often lead to chronic pain and discomfort. The wrist joint is surrounded by a complex configuration of ligaments connecting adjacent carpal bones allowing for subtle alterations in kinematic behaviors.<sup>1,2</sup> Ligamentous injuries have the potential to disrupt the delicate balance within the wrist joint leading to altered kinematics, abnormal joint loading, and secondary degenerative changes.<sup>2</sup> The most commonly injured intercarpal ligament is the scapholunate (SL) ligament.<sup>2-5</sup> The SL ligament plays an important role in the stability of the wrist joining the scaphoid and lunate, allowing them to rotate in relative unison throughout wrist motion.<sup>2,4</sup> Damage to the SL ligament and the secondary restraints causes the scaphoid to flex and the lunate to extend with dissociation of the carpal bones from their native alignment.<sup>4,6</sup> Although the etiology of SL instability remains unclear it often leads to a pattern of secondary osteoarthritis termed scapholunate advanced collapse (SLAC).<sup>7</sup>

The scaphoid, lunate, and triquetrum of the proximal carpal row are considered an intercalated segment as no tendons insert directly on them.<sup>2,8</sup> The motion of the bones is dependent on the geometry and contact from surrounding articulations, linked by an intricate system of intrinsic and extrinsic carpal ligaments.<sup>2,9</sup> The SL ligament is considered the primary ligamentous restraint of the scaphoid and lunate (Fig. 1-10).<sup>2,9</sup> The SL ligament is C-shaped and attaches along the dorsal, proximal, and volar margins of the articulating surfaces, leaving an intercarpal space between the bones distally (Fig. 1-12).<sup>2,9</sup> The three anatomical regions of the SL ligament have different material and anatomic properties, where the dorsal portion is the thickest and most critical of the SL stabilizers.<sup>2,10,11</sup> There are a number of secondary stabilizers of the SL joint. The radioscapnocapitate (RSC) ligament, on the volar-radial side of the articulation, originates at the palmar aspect of the radial styloid and inserts onto the palmar aspect of the scaphoid and capitate (Fig. 1-10).<sup>9</sup> The scaphotrapezium-trapezoid (STT) ligament connects the distal pole of the scaphoid with the palmar aspect of the trapezium and trapezoid (Fig. 1-10).<sup>9</sup> Although the ligamentous anatomy of these structures has been well documented the stabilizing role of each structure remains unknown.

Numerous biomechanical studies have evaluated the effect of sectioning the SL ligament and secondary stabilizers yet there remain no conclusive results regarding the influence of each structure on scaphoid and lunate kinematics.<sup>2,12-16</sup> Clinically, the void of information results in uncertainty to as which stabilizers should be repaired following SL injury. As the cause of scapholunate instability remains unknown treatment strategies vary and often result in poor long term clinical outcomes for patients.<sup>12,15,17-24</sup>

The objective of this *in vitro* biomechanical study was to quantify changes in scaphoid and lunate alignment in the flexion-extension plane during wrist flexion-extension and radial-ulnar deviation following the sequential sectioning of the SL ligament and secondary stabilizers. In addition, the intercarpal angle between the scaphoid and lunate was quantified in the flexion-extension plane following the sequential sectioning of the ligaments.

## 3.2 Materials and Methods

### 3.2.1 *Specimen Preparation*

Eight (8) fresh frozen cadaveric upper limb specimens (average age: 74 years; range 54-90; 8 male; 8 right) amputated mid-humerus were used. CT scans of each wrist were examined to rule out any underlying wrist pathology. SL ligament integrity was confirmed via fluoroscopy and subsequently by direct inspection in each of the specimens. The upper limb specimens were thawed eighteen hours at room temperature prior to testing and all soft tissue structures were left intact.

Optical tracking markers as described in Chapter 2 (Optotrak Certus; Northern Digital, Waterloo, Ontario, Canada) were secured to the lunate, scaphoid, third metacarpal, ulna, and radius to capture the kinematics throughout testing. Two cortical bone screws ( $\text{\O}2.7\text{mm}$ ) were inserted into the scaphoid and lunate under fluoroscopic control ensuring proper tracker fixation. The lunate screws were inserted through a dorsal incision on the midpoint of the osseous body and aimed towards the volar rim; the scaphoid screws were inserted through a volar incision over the tuberosity. Each specimen was subjected to a full range of wrist flexion-extension and radial-ulnar deviation under fluoroscopic control to ensure that there was no screw impingement on wrist motion (Fig. 3-1). The tracker mounts were secured to the carpal screws and the optical trackers oriented for an optimal line of sight during testing. The third metacarpal tracker was inserted through a dorsal incision on the distal diaphysis; the ulnar tracker was inserted into the proximal one-third of the shaft; and the radial tracker was secured into the distal two-thirds of the shaft using cortical bone screws ( $\text{\O}3.5\text{mm}$ ).

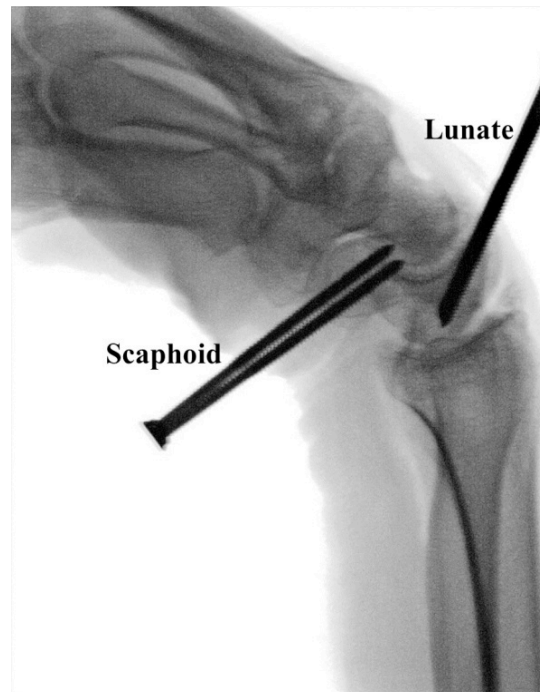


**Figure 3-1: Scaphoid and Lunate Tracker Placement.** Two cortical screws ( $\varnothing$  2.7mm) inserted into the scaphoid and lunate showing no impingement in full flexion.

Following a similar protocol described in Chapter 2, the tendons of the biceps brachii, pronator teres (PT), extensor carpi radialis brevis (ECRB), extensor carpi radialis longus (ECRL), extensor carpi ulnaris (ECU), flexor carpi radialis (FCR) and flexor carpi ulnaris (FCU) were exposed and sutured at the musculotendinous junction (Ethicon, Somerville, NJ). Epicondyle blocks were fixated onto the lateral and medial epicondyles of the humerus to guide the suture lines and maintain the physiological line of action of the tendons. The specimens were mounted in a custom wrist motion simulator capable of active motion by rigidly securing the humerus in a clamp. This was a more advanced simulator than the system employed in Chapter 2 (Fig. 3-2). Two threaded pins were used to fix the shaft of the ulna to the support tower aligning the elbow at 90° flexion (Fig. 3-2). The suture lines were linked to their corresponding SmartMotor (SM2316D-PLS2, SMI Animatics Corp., CA) at the base of the simulator platform (Fig. 3-2). The digits of each specimen were manipulated into full flexion and immobilized using Coban Self-Adherent Wrap (3M, Elyria, OH).

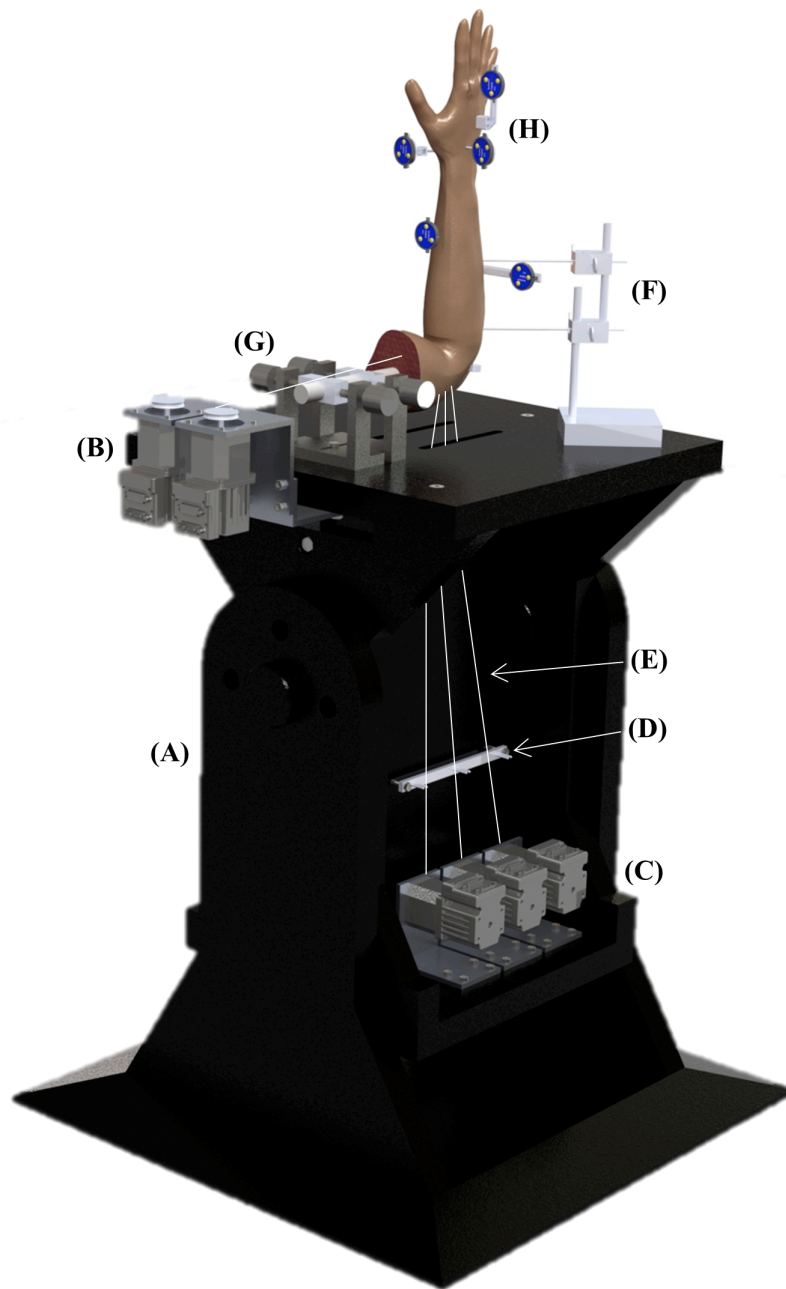


**Figure 3-2: In Vitro Active Motion Simulator.** This device is capable of loading the seven muscle groups of interest to simulate active wrist flexion-extension and radial-ulnar deviation: (A) simulator platform; (B) biceps brachii SmartMotor; (C) motor manifold used to control the magnitude of forces applied to the muscle group of interest; (D) cable guide rail used to converge the suture lines from the motor manifold the specimen; (E) suture cables connecting SmartMotors to the muscle group of interest; (F) ulnar support tower fixing the specimen at 90° of flexion; (G) humeral clamp rigidly fixing the specimen to the simulator; and (H) Optotrak six DOF tracking markers.



### 3.2.2 *Testing Protocol*

Clinically relevant coordinate systems were established for the radius, ulna, and third metacarpal in order to track joint angles. The neutral position of the wrist, as defined by the International Society of Biomechanics (ISB), served to construct the coordinate systems and was used to calculate the angle of wrist flexion-extension and radial-ulnar deviation throughout motion.<sup>25</sup> In order to maintain neutral forearm rotation during all wrist motion trials, 45N of tone load was applied to the biceps brachii and PT muscles.<sup>25</sup>

Five cyclic motion trials of planar wrist flexion-extension and radial-ulnar deviation were performed for each stage of the sectioning protocol (Table 3-1). Motion trials were performed at approximately 5°/sec where flexion-extension trials ranged from 50° of extension to 50° of flexion while radial-ulnar deviation trials ranged from 10° radial deviation to 20° ulnar deviation. Data was analyzed from the fifth trial of each cycle.

**Table 3-1: Sequence of Incremental Sectioning of the Scapholunate Ligament and Secondary Stabilizers.**

<b>Sequence of Ligament Sectioning</b>	
<b>Stage I</b>	Intact State
<b>Stage II</b>	Dorsal SL Cut
<b>Stage III</b>	Complete SL Cut
<b>Stage IV</b>	SL + STT Cut
<b>Stage V</b>	SL, STT, + RSC Cut

The dorsal portion and dorsal half of the membranous portion of the SL ligament was sectioned by inserting a #11 scalpel blade into the SL joint space through a dorsal incision on the wrist. The scalpel was passed through the dorsal capsular structures just radial to the dorsal radiocarpal ligament. The remainder of the SL ligament was sectioned through a volar incision on the specimen passing the scalpel through the volar capsuloligamentous and remaining membranous portions of the ligament. The STT ligament was sectioned by inserting the scalpel blade into the STT joint space and running the blade from the volar surface of the trapezium and trapezoid proximally to the lateral aspect of the distal pole of the scaphoid. The RSC ligament was sectioned inserting the blade through the volar incision and detaching the ligament from the radial styloid insertion point and coursing along the proximal aspect of the scaphoid.

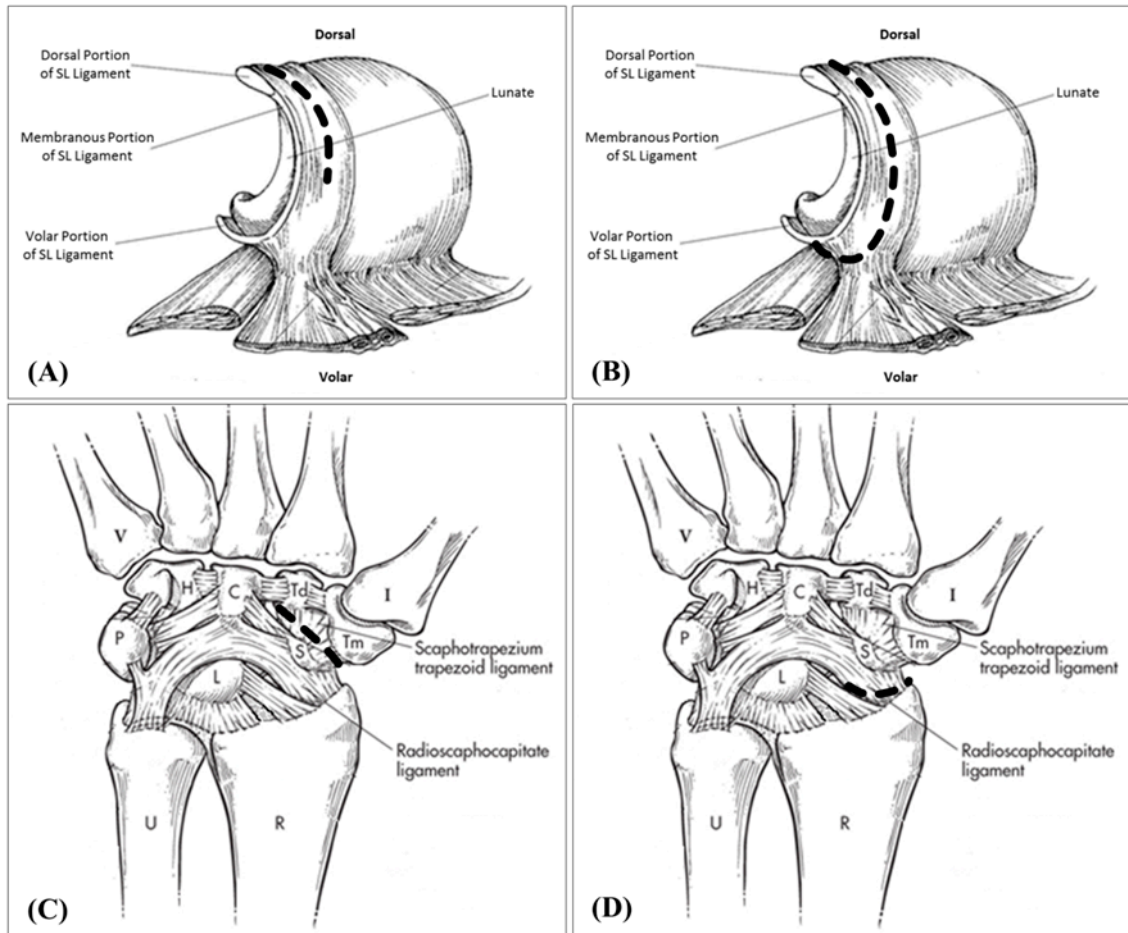


**Figure 3-3: Stages of Sectioning the Scapholunate Ligament and Secondary Stabilizers.** (A) Dorsal-Volar View, Stage II: Sectioning of the dorsal portion and dorsal half of the membranous portion of the SL ligament. (B) Dorsal-Volar View, Stage III: Sectioning of the complete SL ligament. (C) Volar View, Stage IV: Sectioning of the STT ligament. (D) Volar View, Stage V: Sectioning of the RSC ligament.

Extension trials were defined as moving the wrist from flexion to extension, and radial trials were defined as moving the wrist from ulnar to radial deviation. Kinematic data was collected continuously at 15 Hz and extracted in 5° increments for the motion paths. The skin was closed throughout each stage of the testing protocol to maintain specimen hydration. Following testing, the specimen was denuded and the joints were dissected. Each optical tracker mount was inspected to ensure there was no movement that occurred throughout the experiment protocol. The landmarks on the bones of interest: the radius, ulna, third metacarpal, scaphoid and lunate were digitized using a pointed stylus. Neutral wrist position, as defined by ISB, served to form the coordinate system of each bone and was used to calculate the angle of wrist motion throughout testing.<sup>25</sup>

### 3.2.3 *Outcome Variables and Data Analysis*

The rotation of the scaphoid and lunate relative to the distal radius were evaluated for flexion-extension and radial-ulnar deviation motion trials. This permitted the investigation of the relative contribution of each bone to global wrist motion for each of the five different stages of testing. The mean angular difference in carpal bone flexion-extension between each stage of testing was calculated for flexion (0° to 45° FEM), extension (-45° to 0° FEM), and radial-ulnar deviation (10° to 20° RUD) motion trials. Scapholunate intercarpal motion was calculated by subtracting the angle of the scaphoid in the flexion-extension plane from the angle of the lunate in the flexion-extension plane, with respect to the distal radius (Fig. 3-4). Wrist angle was defined as the angle between the long axis of the radius and the long axis of the third metacarpal with respect to the distal radius coordinate system. The coordinate systems for each bone used the ISB recommendations with the origin of the carpal coordinate systems located at the volumetric centroid of each bone (Appendix C).<sup>25</sup> The orientation of the carpal coordinate systems remained parallel with the radial coordinate system when the wrist was in the defined neutral position.<sup>25</sup>

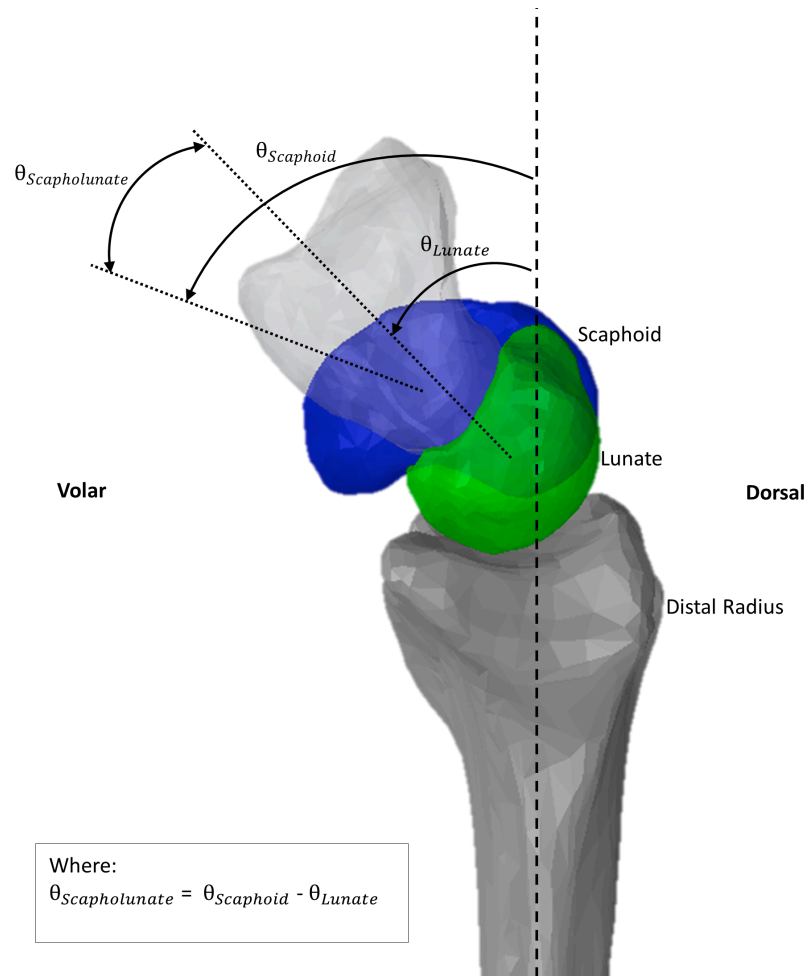


**Figure 3-4: Scapholunate Intercarpal Motion.** The figure shows a sagittal view of the distal radius (grey), scaphoid (blue), lunate (green), and capitate of a left wrist during flexion. Scapholunate intercarpal motion was measured by subtracting the angle of the scaphoid from the angle of the lunate in the flexion-extension plane.

### 3.2.4 *Statistical Methods*

A 2-way repeated measures analysis of variance (ANOVA) was performed using SPSS 17.0 (SPSS Inc., Chicago, IL, USA). The factors (*viz.* independent variables) included: the sectioning stage (intact; dorsal SL cut; SL cut; SL and STT cut; SL, STT, and RSC cut) and wrist motion angle (flexion-extension, radial-ulnar deviation). Individual analyses were performed for the scaphoid and lunate during wrist flexion-extension and radial-ulnar deviation. Statistical significance was set at  $p < 0.05$ .

### 3.3 Results

#### 3.3.1 *Scaphoid and Lunate Kinematics During Wrist Flexion-Extension*

##### 3.3.1.1 *Scaphoid Kinematics During Wrist Flexion-Extension*

In the native state the scaphoid was found to correlate linearly with total wrist motion throughout flexion and extension (Fig. 3-5). During wrist flexion the scaphoid rotated  $71\pm 8\%$  ( $R^2=0.99$ ) of total wrist flexion. During extension, the scaphoid rotated  $85\pm 10\%$  ( $R^2=0.99$ ) of total wrist extension. At  $45^\circ$  of wrist flexion the scaphoid flexed  $30\pm 7^\circ$  and for  $60^\circ$  of wrist extension the scaphoid extended  $41\pm 6^\circ$ .

During wrist flexion statistically significant changes in scaphoid motion were recorded following the incremental sectioning of the SL ligament and secondary stabilizers ( $p=0.01$ ). Each consecutive sectioning stage significantly increased scaphoid flexion compared to the intact wrist [(Stage II  $1.5\pm 1.5^\circ$ ;  $p=0.02$ ) (Stage III  $4.4\pm 3.3^\circ$ ;  $p=0.007$ ) (Stage IV  $4.5\pm 3.8^\circ$ ;  $p=0.01$ ) (Stage V  $4.6\pm 3.7^\circ$ ;  $p=0.01$ )] (Fig. 3-7). There was also a significant increase in scaphoid flexion following the complete sectioning of the SL ligament, the STT ligament, and the RSC ligament compared to when only the dorsal SL ligament was sectioned [(Stage III  $2.9\pm 3.1^\circ$ ;  $p=0.03$ ) (Stage IV  $3.0\pm 3.5^\circ$ ;  $p=0.05$ ) (Stage V  $3.1\pm 3.5^\circ$ ;  $p=0.04$ )] (Fig.3-7).

During wrist extension there were no significant changes in scaphoid motion following the incremental sectioning of the SL ligament and secondary stabilizers when compared to the intact state ( $p=0.7$ ).

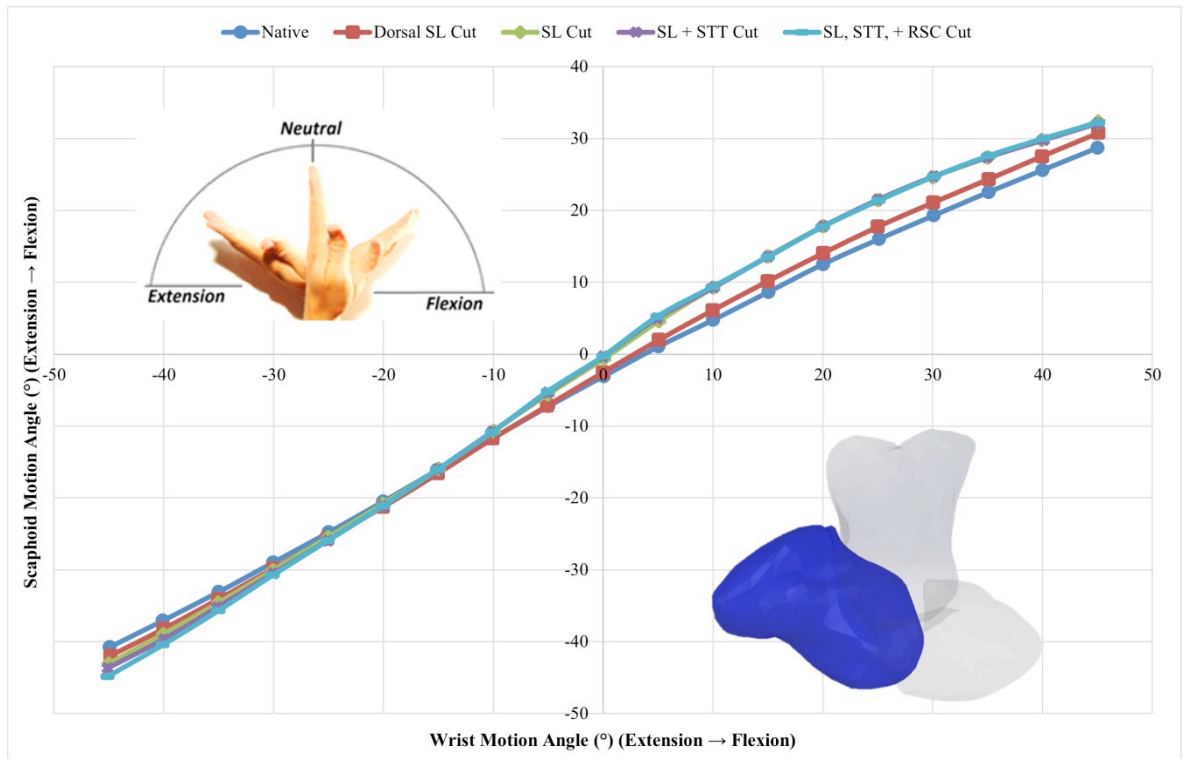


**Figure 3-5: Scaphoid Flexion-Extension Following Sequential Ligament Sectioning During Wrist Flexion-Extension.** The graph shows the mean scaphoid contribution to total wrist motion during wrist flexion-extension in the native state and following the incremental sectioning of the SL ligament and secondary stabilizers (Stage I: Intact State, Stage II: Dorsal SL Cut, Stage III: Complete SL Cut, Stage IV: SL and STT Cut, Stage V: SL, STT, and RSC Cut). Standard deviations were omitted for clarity (Stage I range:  $\pm 4.26^\circ$  to  $\pm 6.72^\circ$ ; Stage II range:  $\pm 5.21^\circ$  to  $\pm 8.31^\circ$ ; Stage III range:  $\pm 5.36^\circ$  to  $\pm 8.34^\circ$ ; Stage IV range:  $\pm 5.43^\circ$  to  $\pm 8.77^\circ$ ; Stage V range:  $\pm 5.15^\circ$  to  $\pm 8.94^\circ$ ).

### 3.3.1.2 *Lunate Kinematics During Wrist Flexion-Extension*

In the intact state the lunate was also found to correlate linearly with total wrist motion during planar flexion and extension (Fig. 3-6). During wrist flexion the lunate rotated  $45\pm 9\%$  ( $R^2 = 0.99$ ) of total wrist flexion. During wrist extension the lunate rotated  $51\pm 26\%$  ( $R^2 = 0.99$ ) of total wrist extension. For  $45^\circ$  of wrist flexion the lunate flexed  $19\pm 3^\circ$  and for  $60^\circ$  of wrist extension the lunate extended  $25\pm 11^\circ$ .

There were significant changes in lunate motion following sequential sectioning of the SL ligament and secondary stabilizers during wrist flexion ( $p=0.01$ ). During wrist flexion there were significant increases in lunate extension following the complete sectioning of the SL ligament, the STT ligament, and the RSC ligament when compared to the native state [(Stage III  $3.5\pm 3.6^\circ$ ;  $p=0.03$ ) (Stage IV  $3.9\pm 3.8^\circ$ ;  $p=0.03$ ) (Stage V  $4.8\pm 4.6^\circ$ ;  $p=0.02$ )] (Fig. 3-7). There was no significant difference in lunate extension following the isolated disruption to the dorsal portion of the SL ligament when compared to the intact state ( $1.2\pm 2.2^\circ$ ;  $p=0.18$ ). There was a significant increase in lunate extension following the complete sectioning of the SL ligament, the STT ligament, and the RSC ligament when compared to only the dorsal portion of the SL ligament sectioned [(Stage III  $2.3\pm 1.8^\circ$ ;  $p=0.008$ ) (Stage IV  $2.7\pm 2.0^\circ$ ;  $p=0.007$ ) (Stage V  $3.6\pm 2.7^\circ$   $p=0.007$ )] (Fig.3-7). There was also a significant increase in lunate extension following the additional sectioning of the RSC compared to the sectioning of the SL and STT ligaments ( $0.9\pm 1.1^\circ$ ;  $p=0.05$ ).

Likewise, in wrist extension there was a number of significant increase in lunate extension following the incremental sectioning protocol ( $p=0.03$ ). Sectioning the STT ligament in addition to sectioning the RSC ligament caused a significant increase in lunate extension when compared to the intact state [(Stage IV  $3.5\pm 4.1^\circ$ ;  $p=0.05$ ) (Stage V  $4.3\pm 4.2^\circ$ ;  $p=0.02$ )] (Fig. 3-7). Likewise, there was a significant increase following sectioning of the complete SL ligament, the STT ligament, and the RSC ligament when compared to the isolated sectioning of the dorsal SL ligament [(Stage III  $2.0\pm 1.8^\circ$ ;  $p=0.02$ ) (Stage IV  $2.3\pm 1.6^\circ$ ;  $p=0.005$ ) (Stage V  $3.1\pm 1.6^\circ$ ;  $p=0.001$ )] (Fig. 3-6). There was also a significant increase in lunate extension following the sectioning of the RSC ligament when compared to the complete sectioning of the SL ligament ( $1.1\pm 1.2^\circ$ ;  $p=0.04$ ) (Fig. 3-7).

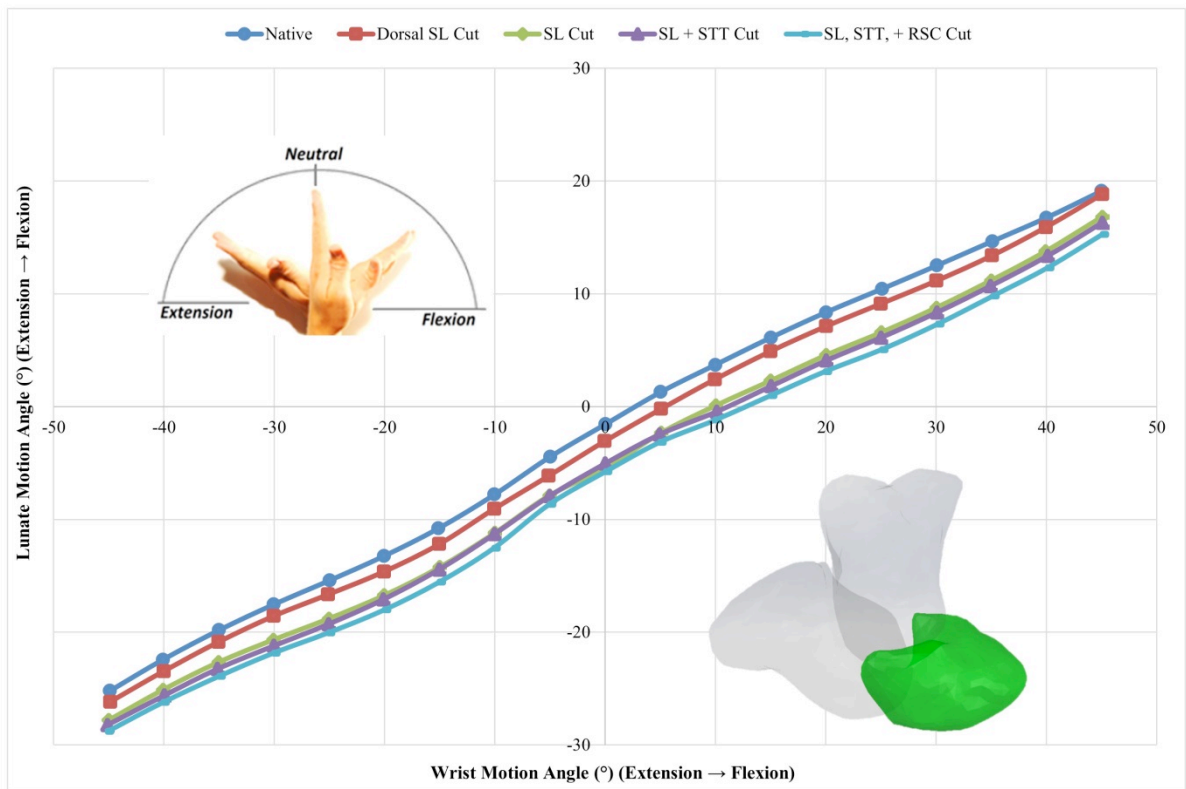


**Figure 3-6: Lunate Flexion-Extension Following Sequential Ligament Sectioning During Wrist Flexion-Extension.** The graph shows the mean lunate contribution to total wrist motion during wrist flexion-extension in the native state and following the incremental sectioning of the SL ligament and secondary stabilizers (Stage I: Intact State, Stage II: Dorsal SL Cut, Stage III: Complete SL Cut, Stage IV: SL and STT Cut, Stage V: SL, STT, and RSC Cut). Standard deviations were omitted for clarity (Stage I range:  $\pm 2.86^\circ$  to  $\pm 10.55^\circ$ ; Stage II range:  $\pm 3.01^\circ$  to  $\pm 12.00^\circ$ ; Stage III range:  $\pm 3.90^\circ$  to  $\pm 13.32^\circ$ ; Stage IV range:  $\pm 4.15^\circ$  to  $\pm 13.51^\circ$ ; Stage V range:  $\pm 4.39^\circ$  to  $\pm 13.55^\circ$ ).



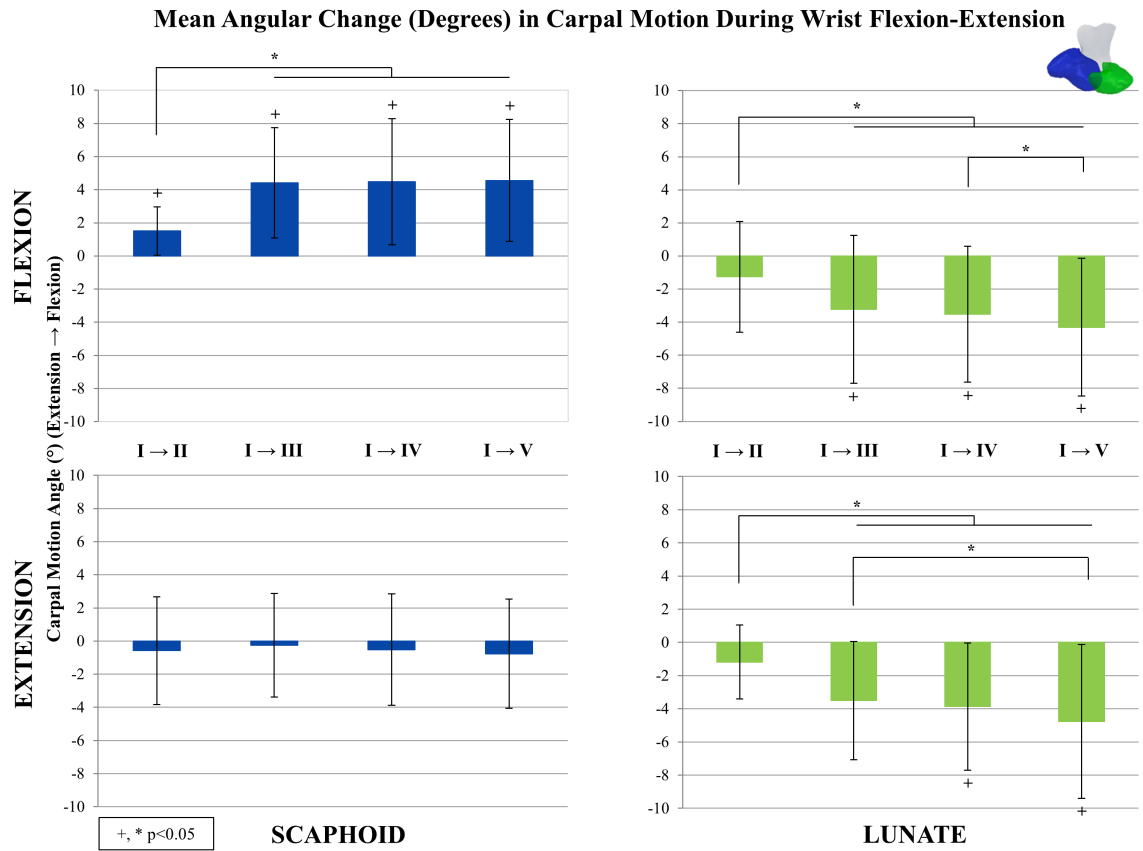


**Figure 3-7: Mean Angular Change in Carpal Motion During Wrist Flexion-Extension.** Mean angular difference in scaphoid and lunate motion during wrist flexion and extension following the incremental sectioning of the SL ligament and secondary stabilizers of the SL joint (Stage I: Intact State, Stage II: Dorsal SL Cut, Stage III: Complete SL Cut, Stage IV: SL and STT Cut, Stage V: SL, STT, and RSC Cut). Each bar represents the stage of the sectioning protocol compared to the intact state.

### 3.3.1.3 *Scapholunate Kinematics During Wrist Flexion-Extension*

Scapholunate intercarpal motion is the measure of the relative flexion-extension angle between the scaphoid and lunate (Fig. 3-4). As the scaphoid and lunate move synergistically throughout wrist motion, SL intercarpal motion is positive during wrist flexion and negative during wrist extension. In the intact wrist at 45° of wrist flexion SL intercarpal motion was measured at  $10 \pm 5^\circ$ , where both the scaphoid and lunate are flexing with wrist motion; and at 45° of wrist extension was measured at  $-16 \pm 8^\circ$ , where the scaphoid and lunate are extending with wrist motion (Fig. 3-5, 3-6, 3-8).

During wrist flexion there were significant changes in SL intercarpal motion following the sequential sectioning of the SL ligament and secondary stabilizers ( $p=0.004$ ). Each additional stage had a significant increase in the relative extension of the lunate with respect to the scaphoid compared to the intact wrist [(Stage II  $2.7 \pm 2.8^\circ$ ;  $p=0.03$ ) (Stage III  $7.9 \pm 5.7^\circ$ ;  $p=0.006$ ) (Stage IV  $8.4 \pm 6.5^\circ$ ;  $p=0.008$ ) (Stage V  $9.2 \pm 6.5^\circ$ ;  $p=0.005$ )]. There was also a significant increase in SL intercarpal motion following complete sectioning of the SL ligament, the STT ligament, and the RSC ligament compared to only the dorsal SL ligament sectioned [(Stage III  $5.2 \pm 4.4^\circ$ ;  $p=0.01$ ) (Stage IV  $5.7 \pm 5.1^\circ$ ;  $p=0.01$ ) (Stage V  $6.5 \pm 5.2^\circ$ ;  $p=0.009$ )]. In addition, there was a significant increase in scapholunate motion following the sectioning of the SL ligament, the STT ligament and the RSC ligament compared to only the sectioning of the SL and STT ligaments ( $0.8 \pm 0.6^\circ$ ;  $p=0.006$ ).

Throughout wrist extension there were significant changes in the SL intercarpal motion following sequential sectioning of the SL ligament and secondary stabilizers of the SL joint ( $p=0.005$ ). There was significant increase in the relative extension of the lunate with respect to the scaphoid following complete sectioning of the SL ligament, the STT ligament, and the RSC ligaments compared to the intact state [(Stage III  $3.0 \pm 2.3^\circ$ ;  $p=0.009$ ) (Stage IV  $3.0 \pm 2.2^\circ$ ;  $p=0.006$ ) (Stage V  $3.5 \pm 2.3^\circ$ ;  $p=0.003$ )]. There was also a significant increase in SL intercarpal motion following the sectioning of the complete SL ligament, the STT ligament, and the RSC ligament compared to isolated disruption of the dorsal portion of the SL ligament [(Stage III  $2.3 \pm 2.7^\circ$ ;  $p=0.05$ ) (Stage IV  $2.3 \pm 2.4^\circ$ ;  $p=0.03$ ) (Stage V  $2.9 \pm 2.9^\circ$ ;  $p=0.03$ )].

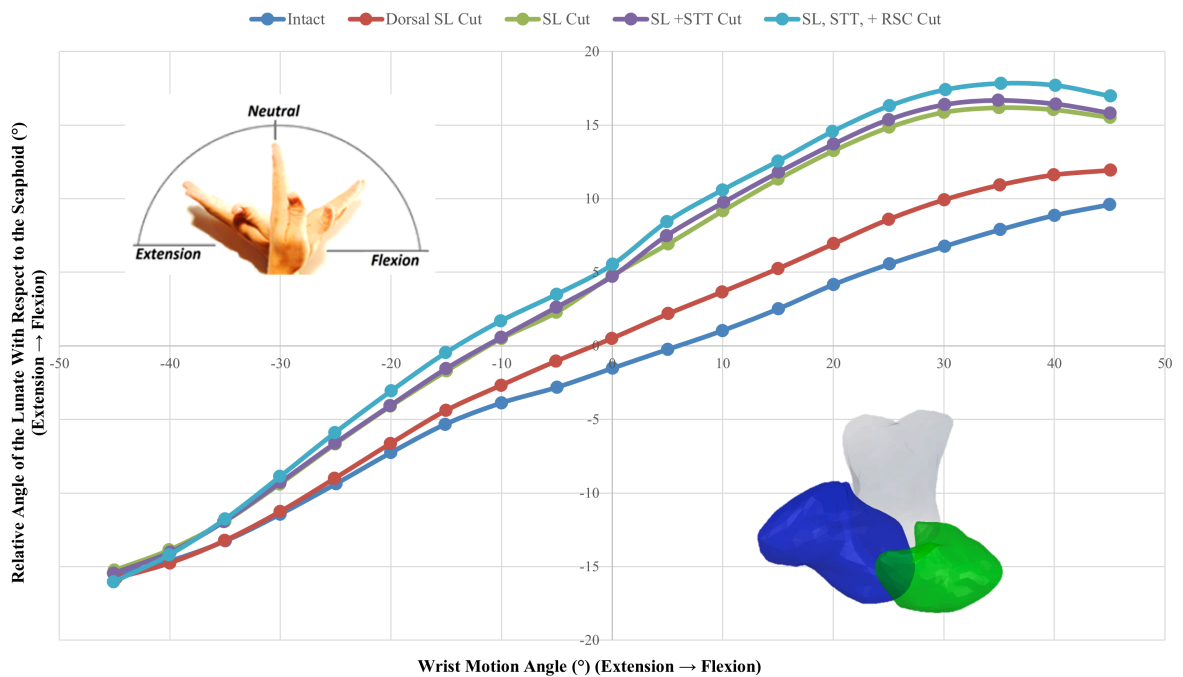


**Figure 3-8: Scapholunate Intercarpal Motion Following Sequential Ligament Sectioning During Wrist Flexion-Extension.** The graph shows the mean SL intercarpal motion during wrist flexion-extension in the native state and following the incremental sectioning of the SL ligament and secondary stabilizers (Stage I: Intact State, Stage II: Dorsal SL Cut, Stage III: Complete SL Cut, Stage IV: SL and STT Cut, Stage V: SL, STT, and RSC Cut). Standard deviations were omitted for clarity (Stage I range:  $\pm 3.31^\circ$  to  $\pm 7.69^\circ$ ; Stage II range:  $\pm 2.53^\circ$  to  $\pm 7.74^\circ$ ; Stage III range:  $\pm 2.35^\circ$  to  $\pm 9.09^\circ$ ; Stage IV range:  $\pm 3.14^\circ$  to  $\pm 9.32^\circ$ ; Stage V range:  $\pm 3.24^\circ$  to  $\pm 9.66^\circ$ ).

### 3.3.2 *Scaphoid and Lunate Kinematics During Wrist Radial-Ulnar Deviation*

#### 3.3.2.1 *Scaphoid Kinematics During Wrist Radial-Ulnar Deviation*

Radial-ulnar deviation motion trial data was obtained for 7 of the 8 specimens (Average age: 73 years).

During wrist radial-ulnar deviation there was no significant changes in scaphoid flexion-extension motion following the incremental sectioning of the SL ligament and secondary stabilizers compared to the intact state ( $p=0.1$ ) (Fig. 3-9, 3-11).

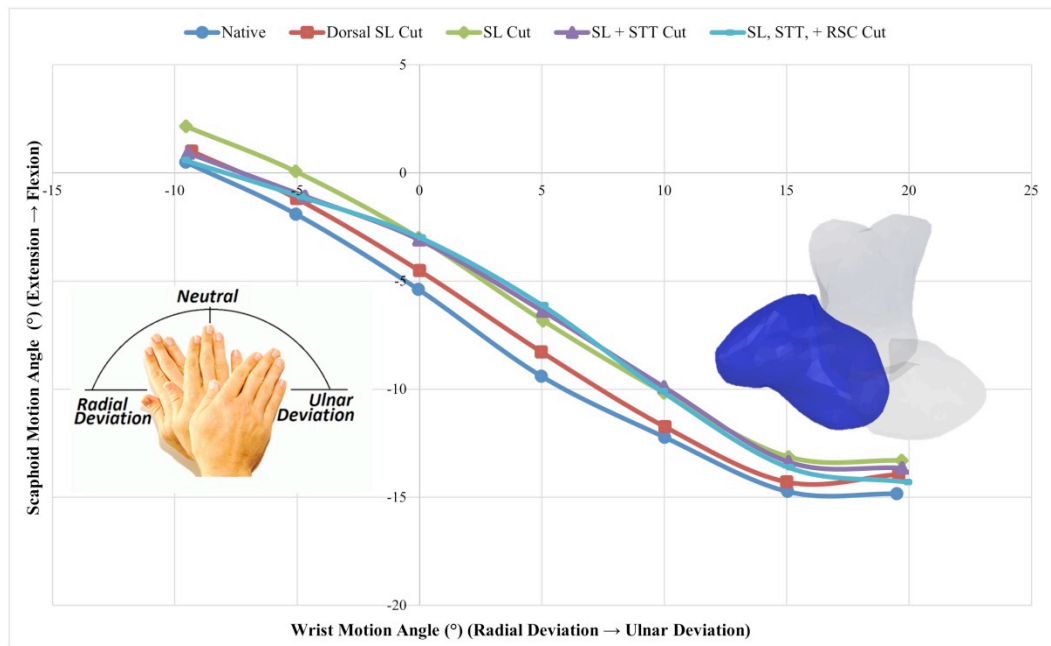


**Figure 3-9: Scaphoid Flexion-Extension Motion Following Sequential Ligament Sectioning During Wrist Radial-Ulnar Deviation.** The graph illustrates scaphoid flexion-extension motion during wrist radial-ulnar deviation in the native state and following the incremental sectioning of the SL ligament and secondary stabilizers (Stage I: Intact State, Stage II: Dorsal SL Cut, Stage III: Complete SL Cut, Stage IV: SL and STT Cut, Stage V: SL, STT, and RSC Cut). Standard deviations were omitted for clarity (Stage I range:  $\pm 3.64^\circ$  to  $\pm 7.70^\circ$ ; Stage II range:  $\pm 3.84^\circ$  to  $\pm 8.25^\circ$ ; Stage III range:  $\pm 2.96^\circ$  to  $\pm 8.16^\circ$ ; Stage IV range:  $\pm 4.73^\circ$  to  $\pm 8.82^\circ$ ; Stage V range:  $\pm 4.67^\circ$  to  $\pm 8.48^\circ$ ).

### 3.3.2.2 *Lunate Kinematics During Wrist Radial-Ulnar Deviation*

Throughout wrist radial-ulnar deviation there were significant changes in lunate flexion-extension motion following the sequential sectioning protocol ( $p < 0.001$ ) (Fig. 3-10). There were significant increases in lunate extension following the complete sectioning of the SL ligament, the STT ligament, and the RSC ligament compared to the intact state [(Stage III  $3.5 \pm 2.3^\circ$ ;  $p = 0.007$ ) (Stage IV  $4.0 \pm 2.4^\circ$ ;  $p = 0.005$ ) (Stage V  $5.8 \pm 2.4^\circ$ ;  $p = 0.001$ )] (Fig. 3-11). Likewise, there was a significant increase in lunate extension following the complete sectioning of the SL ligament, the STT ligament and the RSC ligament compared to the isolated sectioning of the dorsal portion of the SL ligament [(Stage III  $2.2 \pm 1.4^\circ$ ;  $p = 0.006$ ) (Stage IV  $2.7 \pm 1.6^\circ$ ;  $p = 0.004$ ) (Stage V  $4.6 \pm 2.1^\circ$ ;  $p = 0.001$ )] (Fig. 3-11). There was also a significant increase in lunate extension following the sectioning of the STT ligament and the RSC ligament when compared to just the sectioning of the complete SL ligament [(Stage IV  $0.5 \pm 0.3^\circ$ ;  $p = 0.005$ ) (Stage V  $2.3 \pm 1.7^\circ$ ;  $p = 0.01$ )] (Fig. 3-11). Lastly, there was a significant difference in lunate extension following the sectioning of the RSC ligament compared to the sectioning of the STT ligament ( $1.8 \pm 1.5^\circ$ ;  $p = 0.02$ ) (Fig. 3-11).

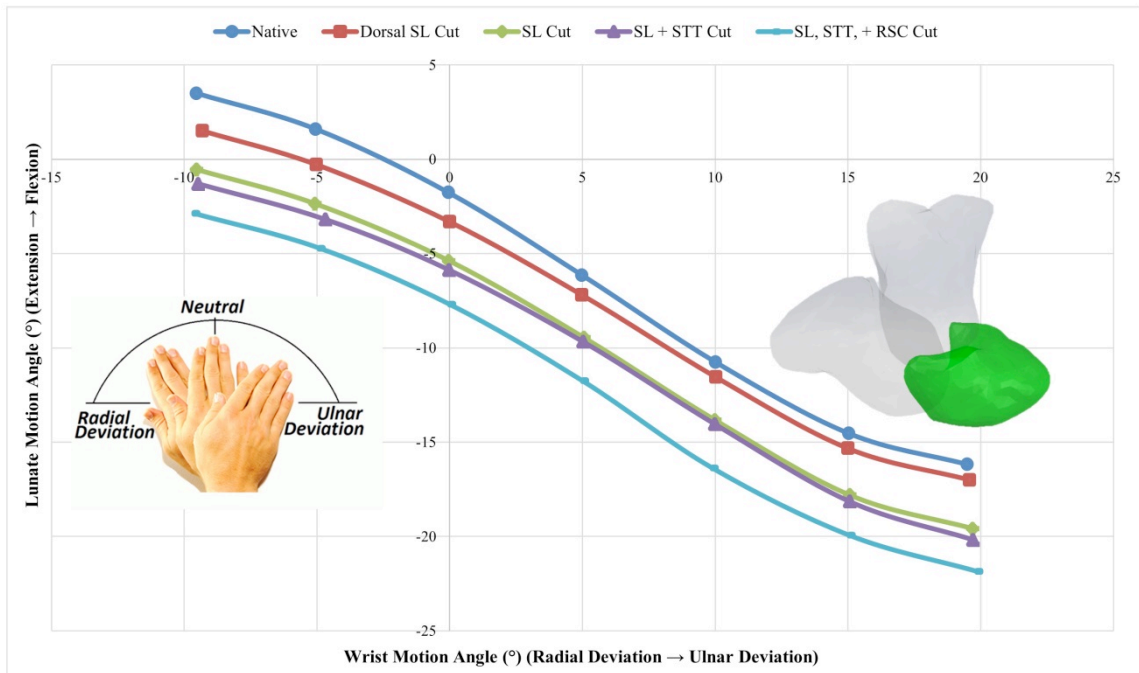


**Figure 3-10: Lunate Flexion-Extension Motion Following Sequential Ligament Sections During Wrist Radial-Ulnar Deviation.** The graph illustrates lunate flexion-extension motion during wrist radial-ulnar deviation in the native state and following the incremental sectioning of the SL ligament and secondary stabilizers (Stage I: Intact State, Stage II: Dorsal SL Cut, Stage III: Complete SL Cut, Stage IV: SL and STT Cut, Stage V: SL, STT, and RSC Cut). Standard deviations were omitted for clarity (Stage I range:  $\pm 6.23^\circ$  to  $\pm 10.37^\circ$ ; Stage II range:  $\pm 6.14^\circ$  to  $\pm 10.64^\circ$ ; Stage III range:  $\pm 7.46^\circ$  to  $\pm 11.82^\circ$ ; Stage IV range:  $\pm 7.23^\circ$  to  $\pm 12.48^\circ$ ; Stage V range:  $\pm 6.76^\circ$  to  $\pm 12.09^\circ$ ).

**Mean Angular Change (Degrees) in Carpal Motion During Wrist Radial-Ulnar Deviation**

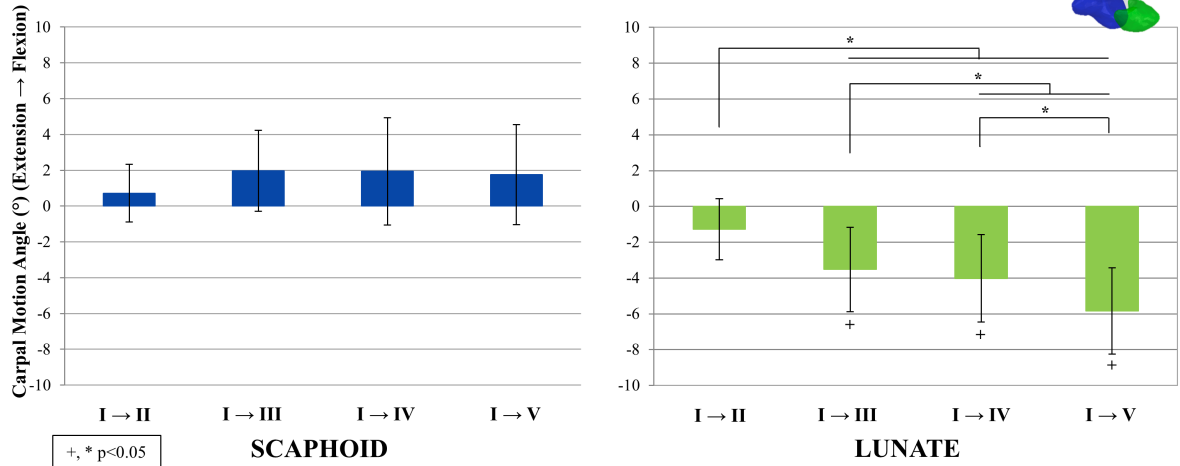


**Figure 3-11: Mean Angular Change in Carpal Motion During Wrist Radial-Ulnar Deviation.** Mean angular difference in scaphoid and lunate motion during wrist radial-ulnar deviation following the incremental sectioning of the SL ligament and secondary stabilizers of the SL joint (Stage I: Intact State, Stage II: Dorsal SL Cut, Stage III: Complete SL Cut, Stage IV: SL and STT Cut, Stage V: SL, STT, and RSC Cut). Each bar represents the stage of the sectioning protocol compared to the intact state.



### 3.3.2.3 *Scapholunate Kinematics During Wrist Radial-Ulnar Deviation*

During wrist radial-ulnar deviation there were significant changes in the intercarpal SL intercarpal motion following the incremental sectioning of the SL ligament and the secondary stabilizers ( $p=0.001$ ). Each stage of sectioning resulted in a significant increase in lunate extension with respect to the scaphoid compared to the intact wrist [(Stage II  $2.0\pm 1.9^\circ$ ;  $p=0.03$ ) (Stage III  $5.5\pm 2.8^\circ$ ;  $p=0.002$ ) (Stage IV  $5.7\pm 3.6^\circ$ ;  $p=0.006$ ) (Stage V  $7.3\pm 4.3^\circ$ ;  $p=0.004$ )]. In addition, there were significant increases in lunate extension relative to the scaphoid following the sectioning of the complete SL ligament, the STT ligament, and the RSC ligament when compared to the sole sectioning of the dorsal SL ligament [(Stage III  $3.5\pm 1.9^\circ$ ;  $p=0.002$ ) (Stage IV  $3.7\pm 2.4^\circ$ ;  $p=0.007$ ) (Stage V  $5.3\pm 3.6^\circ$ ;  $p=0.007$ )].

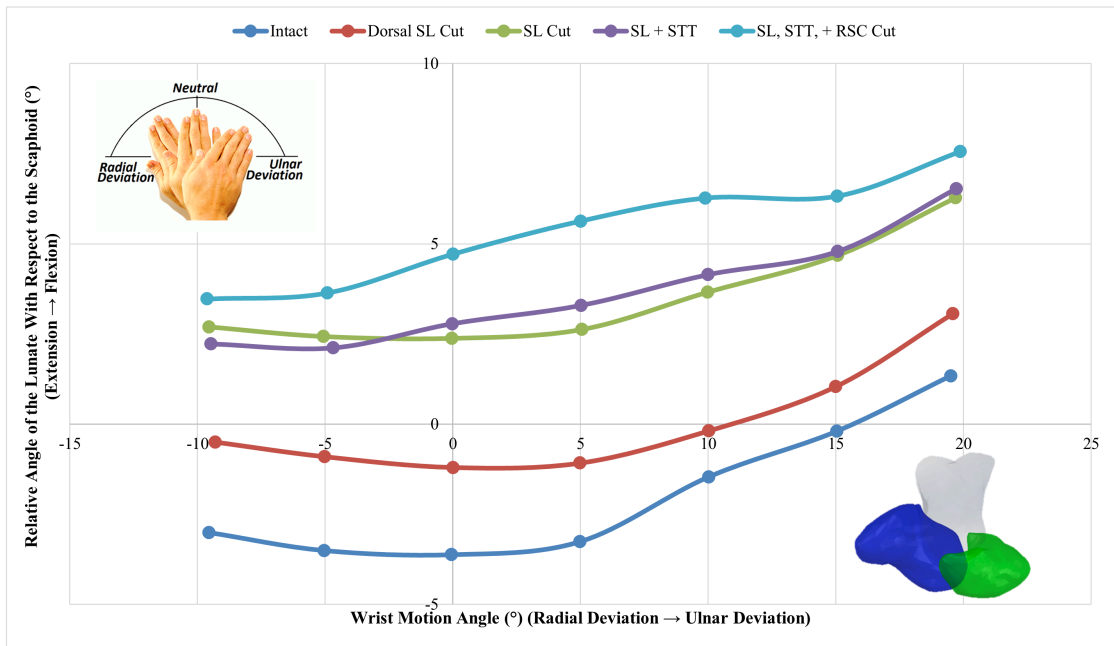


**Figure 3-12: Scapholunate Intercarpal Motion Following Sequential Ligament Sections During Wrist Radial-Ulnar Deviation.** The graph illustrates the lunate angle relative to the scaphoid during wrist radial-ulnar deviation in the native state and following the incremental sectioning of the SL ligament and secondary stabilizers (Stage I: Intact State, Stage II: Dorsal SL Cut, Stage III: Complete SL Cut, Stage IV: SL and STT Cut, Stage V: SL, STT, and RSC Cut). Standard deviations were omitted for clarity (Stage I range:  $\pm 5.13^\circ$  to  $\pm 6.90^\circ$ ; Stage II range:  $\pm 6.20^\circ$  to  $\pm 8.23^\circ$ ; Stage III range:  $\pm 6.90^\circ$  to  $\pm 9.32^\circ$ ; Stage IV range:  $\pm 7.43^\circ$  to  $\pm 9.70^\circ$ ; Stage V range:  $\pm 7.25^\circ$  to  $\pm 10.23^\circ$ ).

### 3.4 Discussion

The SL ligament plays a critical role in preserving scaphoid and lunate stability linking the scaphoid and lunate allowing them to move synergistically throughout wrist motion. The SL ligament is in turn surrounded by a network of secondary ligamentous restraints, each insufficient to cause SL instability following isolated disruption but play a critical role in the maintenance of normal SL kinematics.<sup>2</sup> Following trauma to the wrist, the SL ligament is often damaged leading to wrist instability and carpal dissociation.<sup>4</sup> The secondary ligamentous restraints surrounding the SL joint are often injured concomitantly or may gradually elongate due to attritional failure following SL ligament injury.<sup>2</sup> The ligamentous anatomy has been well recorded yet the relative role and stabilizing function of each structure remains unclear. There is confusion as to which ligament combinations need to be injured to induce specific wrist instability patterns. This study investigated the stabilizing function of the SL, STT, and RSC ligament with respect to scaphoid and lunate kinematics. The mean angular change in carpal bone flexion-extension was recorded following the incremental sectioning of the SL ligament and two of the secondary stabilizers, the STT and RSC ligaments, during planar wrist flexion-extension and radial-ulnar deviation.

During planar wrist flexion-extension the scaphoid and lunate were found to correlate linearly and move synergistically throughout wrist motion. The scaphoid was found to contribute at a greater degree to total wrist motion at all wrist angles when compared to the lunate. During planar radial-ulnar deviation the scaphoid and lunate were found to flex and extend throughout wrist motion. The scaphoid was found to be in neutral flexion-extension when the wrist was radially deviated and began to extend as the wrist entered ulnar deviation. The lunate followed a similar trend but was in a slightly more flexed position during radial deviation.

Isolated sectioning of the dorsal portion of the SL ligament induced changes in the angular position of the scaphoid and lunate during wrist flexion-extension and radial-ulnar deviation. The scaphoid experienced significantly larger angular changes during wrist flexion when compared to extension, flexing more when compared to the intact state. The

lunate experienced similar changes in position following the isolated disruption of the dorsal SL ligament during wrist flexion and extension. The lunate assumed a more extended posture throughout wrist motion, extending more in both wrist flexion and extension. During wrist radial-ulnar deviation there was a slight difference in carpal bone flexion-extension following the isolated disruption of the dorsal SL ligament causing an increase in scaphoid flexion and lunate extension. These results correspond with previously completed *in vitro* biomechanical and histological studies showing that the dorsal component of the SL ligament plays a critical role in SL joint stability.<sup>10,11,16</sup> *Waters et al.*<sup>16</sup> evaluated the stabilizing and functional role of the dorsal and volar portions of the SL ligament with respect to SL kinematics, finding the dorsal portion of the SL ligament induces larger angular changes when sectioned compared to the volar portion. *Berger et al.*<sup>11</sup> investigated the constraint and material properties of the different anatomic regions of the SL ligament concluding that the failure force of the dorsal SL ligament was more than twice the failure force of the volar and four times the force of the palmar SL ligament. The angular changes in carpal posture following the partial sectioning of the SL ligament suggest the dorsal portion of the SL ligament plays a key role in the stability of the SL articulation.

Following the complete sectioning of the SL ligament there were further changes in scaphoid and lunate posture during wrist flexion-extension and radial-ulnar deviation. During wrist flexion there was a significant increase in scaphoid flexion, whereas in extension there were minimal changes in scaphoid posture when compared to the intact state. Similarly, the lunate extended more in wrist extension and significantly more in wrist flexion when compared to the intact state. In radial-ulnar deviation there was an increase in scaphoid flexion and a significant increase in lunate extension when compared to the intact state. The larger angular change in carpal flexion-extension supports the notion that the SL ligament is the primary stabilizer of the SL articulation.<sup>2,12,13,15,26</sup> The results of the current study are in agreement with the work of previously completed *in vitro* biomechanical studies showing that the complete sectioning of the SL ligament resulted in increased scaphoid flexion during wrist flexion and lunate extension during wrist flexion-extension.<sup>12,13,15,24</sup> Our results showed that complete sectioning of the SL

ligament had a larger angular effect on carpal posture during wrist flexion when compared to extension, highlighted by the minimal change in carpal angulation during wrist extension. This suggests that the SL ligament plays a more critical role in scaphoid and lunate stability during wrist flexion when compared to extension. Our results agree with the work by *Short et al.*<sup>12,14</sup> showing an increase in scaphoid flexion and lunate extension during all motion following the complete sectioning of the SL ligament in wrist radial-ulnar deviation.

After the additional sectioning of the STT ligament the carpals underwent further postural changes during wrist flexion-extension and radial-ulnar deviation when compared to the intact state. During wrist flexion there were significant increases in scaphoid flexion and lunate extension while in wrist extension only the lunate experienced significant angular changes when compared to the intact state. During wrist radial-ulnar deviation there was an increase in scaphoid flexion and a significant increase in lunate extension when compared to the intact state. Our results contrast the study completed by *Short et al.*<sup>12</sup> who reported that sectioning of the STT ligament following the SL ligament caused no further changes in scaphoid and lunate kinematics during wrist flexion-extension. We also found that following the sectioning of the STT and SLIL ligament there was a further  $0.5 \pm 0.3^\circ$  significant increase in lunate extension during wrist radial-ulnar deviation. Our results also contrast the *in vitro* study performed by *Short et al.*<sup>15</sup> who sectioned the STT prior to the SL ligament and reported no changes in scaphoid or lunate kinematics following the isolated disruption of the STT. The discrepancies in data could be due to methodology limitations of previous *in vitro* studies<sup>12,15</sup> including the use of less accurate electromagnetic trackers and the more extensive removal of soft tissue structures prior to testing. Overall, our results support the notion that the STT ligament is a secondary stabilizing structure of the SL articulation and does cause further deviation from normal SL kinematics following injury.

Sectioning the SL ligament followed by the STT and the RSC ligament caused supplementary changes in both scaphoid and lunate kinematics. During wrist flexion there was significant increases in scaphoid flexion and lunate extension when compared to the

intact state. We also found in wrist flexion that there was a significant increase in lunate extension following the sectioning of the RSC ligament compared to after the STT was sectioned. While in wrist extension similarly to the previous sectioning stages, the scaphoid underwent minimal postural changes while there was a significant increase in lunate extension when compared to the intact state. During wrist radial-ulnar deviation we found there to be a minimal increase in scaphoid flexion and a significant increase in lunate extension when compared to the intact state. Our results agree with previously completed *in vitro* studies showing that following the sectioning of the SL, STT, and RSC ligaments there is an increase in scaphoid flexion.<sup>12</sup> The *in vitro* study completed by *Short et al.*<sup>14</sup> investigated the effect of sectioning the RSC prior to the SL ligament and showed no changes in carpal kinematics during wrist flexion-extension or radial-ulnar deviation; however did conclude that sectioning the RSC in conjunction with the SL ligament results in angular carpal changes throughout larger portions of wrist motion. Our results show that sectioning the RSC ligament following the disruption of the SL and STT ligament has a significant effect on carpal kinematics particularly during wrist flexion and radial-ulnar deviation. These results support the hypothesis that the RSC ligament does play a secondary stabilizing role of the SL articulation with emphasis on stability of the lunate.

The results of this study have shown that the sectioning of the SL ligament and secondary stabilizers causes a significant increase in scaphoid flexion during wrist flexion and a significant increase in lunate extension throughout wrist flexion-extension and radial-ulnar deviation. Given the angular changes observed in this study are smaller than those commonly encountered clinically, our findings suggest that there are additional soft-tissue secondary restraints that play a role in the stability and maintenance of normal SL kinematics. Currently a range of surgical repair techniques exist for SL ligament injuries including direct repair, capsulodeses, tenodeses, bone-ligament-bone reconstructions, arthrodeses, and SL screws<sup>5,17-19,27-32</sup>; however it is unclear which method of surgical repair effectively restores the native kinematics and range of motion. Our results provide a more accurate representation of how the kinematics of the scaphoid and lunate are altered following injury, providing insight as to which repair technique will optimize the patient's outcomes.

The study presented within this chapter has limitations. In order to maintain reproducibility wrist motion was simulated in planar flexion-extension and radial-ulnar deviation; not accounting for all of the complex multiplanar motions of the wrist. Similarly, the mean angular differences in carpal kinematics were reported solely in flexion-extension not accounting for the rotational or translational motions of the bones following ligament sectioning. Future work will investigate the out of plane angular changes experienced by the scaphoid and lunate following the sequential sectioning of the SL ligament and secondary stabilizers. Additionally, although wrist motion was performed actively and loads were applied within a physiologic range<sup>33</sup> it is an estimation of *in vivo* loading scenarios during simple motions rather than the loading which would be experienced with resisted motions or lifting heavy objects. This study only investigated the stabilizing role of the SL and secondary stabilizing ligaments in one sequence not evaluating the individual role of the STT and RSC ligaments on scaphoid and lunate kinematics. Future studies should reverse the order of sectioning to evaluate the effects of isolated sectioning of these structures. Finally, this study was limited to investigating the role of only two of the secondary stabilizers of the SL articulation. Future studies will investigate the influence of additional secondary stabilizer including the scaphocapitate ligament, short and long radiolunate ligaments, and the dorsal radiocarpal ligament on scaphoid and lunate kinematics.

This study has several strengths. This investigation was able to simulate and analyze a greater range of wrist flexion-extension motion from  $\pm 45^\circ$  compared to similar *in vitro* biomechanical studies only simulating  $30^\circ$  of wrist extension to  $50^\circ$  of wrist flexion.<sup>12,14,15</sup> Additionally, unlike similar studies that reported only the largest angular change in carpal posture following ligament sectioning we reported the mean angular change throughout wrist motion providing a more accurate depiction of the change in kinematics.<sup>12-16</sup> Furthermore, unlike other *in vitro* biomechanical studies, all soft tissue structures were left intact and the incisions were closed throughout testing. This was done to maintain tissue hydration and the soft tissue viscoelastic behavior more similar to an *in vivo* scenario. This study also utilized a highly accurate optical motion tracking system capable of quantifying real time kinematic measurements.

### **3.5 Conclusions**

The current biomechanical study supports the hypothesis that the SL ligament is the primary stabilizer of the scapholunate articulation, and that the STT and RSC are secondary ligamentous restraints. Sectioning the SL ligament caused the largest change in scapholunate kinematics during wrist flexion-extension and radial-ulnar deviation wrist motions. The additional sectioning of the STT and RSC ligaments induced further postural changes in scapholunate kinematics during planar wrist motions. Our results indicate that there are other soft-tissue ligamentous restraints that contribute to the maintenance of normal SL kinematics that were not investigated in this study. A more detailed understanding of the role and stabilizing function of the primary and secondary ligamentous structures surrounding the SL articulation may assist in the development of more effective treatment strategies and patient outcomes following a SL ligament injury.



### 3.6 References

1. Wolfe SW, Neu C, Crisco JJ. In vivo scaphoid, lunate, and capitate kinematics in flexion and in extension. *J Hand Surg Am.* 2000;25(5):860-869.
2. Kitay A, Wolfe SW. Scapholunate instability: current concepts in diagnosis and management. *J Hand Surg Am.* 2012;37(10):2175-2196.
3. Johnson JE, Lee P, McIff TE, Toby EB, Fischer KJ. Effectiveness of surgical reconstruction to restore radiocarpal joint mechanics after scapholunate ligament injury: an in vivo modeling study. *J Biomech.* 2013;46(9):1548-1553.
4. Dimitris C, Werner FW, Joyce DA, Harley BJ. Force in the Scapholunate Interosseous Ligament During Active Wrist Motion. *J Hand Surg Am.* 2015;40(8):1525-1533.
5. Kuo CE, Wolfe SW. Scapholunate Instability: Current Concepts in Diagnosis and Management. *J Hand Surg Am.* 2008;33(6):998-1013.
6. Ruby LK, An KN, Linscheid RL, Cooney WP, Chao EY. The effect of scapholunate ligament section on scapholunate motion. *J Hand Surg Am.* 1987;12(5 Pt 1):767-771.
7. O'Meehan CJ, Stuart W, Mamo V, Stanley JK, Trail I a. The natural history of an untreated isolated scapholunate interosseous ligament injury. *J Hand Surg Am.* 2003;28 B(4):307-310.
8. Landsmeer JM. Studies in the anatomy of articulation. I. The equilibrium of the "intercalated" bone. *Acta Morphol Neerl Scand.* 1961;3:287-303.
9. Cooney WP. *The Wrist: Diagnosis and Operative Treatment.* Vol 8. 2nd ed. (Kluwer W, ed.). Philadelphia, Baltimore, New York, London, Buenos Aires, Hong Kong, Sydney, Tokyo; 2011.

10. Berger RA. The gross and histologic anatomy of the scapholunate interosseous ligament. *J Hand Surg Am.* 1996;21(2):170-178.
11. Berger RA, Imeada T, Berglund L, An K-N. Constraint and material properties of the subregions of the scapholunate interosseous ligament. *J Hand Surg Am.* 1999;24(5):953-962.
12. Short WH, Werner FW, Green JK, Masaoka S. Biomechanical evaluation of ligamentous stabilizers of the scaphoid and lunate. *J Hand Surg Am.* 2002;27(6):991-1002.
13. Short WH, Werner FW, Fortino MD, Palmer AK, Mann KA. A dynamic biomechanical study of scapholunate ligament sectioning. *J Hand Surg Am.* 1995;20(6):986-999.
14. Short WH, Werner FW, Green JK, Masaoka S. Biomechanical evaluation of the ligamentous stabilizers of the scaphoid and lunate: Part II. *J Hand Surg Am.* 2005;30(1):24-34.
15. Short WH, Werner FW, Green JK, Sutton LG, Brutus JP. Biomechanical evaluation of the ligamentous stabilizers of the scaphoid and lunate: part III. *J Hand Surg Am.* 2007;32(3):297-309.
16. Waters MS, Werner FW, Haddad SF, McGrattan ML, Short WH. Biomechanical Evaluation of Scaphoid and Lunate Kinematics Following Selective Sectioning of Portions of the Scapholunate Interosseous Ligament. *J Hand Surg Am.* December 2015.
17. Lavernia CJ, Cohen MS, Taleisnik J. Treatment of scapholunate dissociation by ligamentous repair and capsulodesis. *J Hand Surg Am.* 1992;17(2):354-359.
18. Blatt G. Capsulodesis in reconstructive hand surgery. Dorsal capsulodesis for the unstable scaphoid and volar capsulodesis following excision of the distal ulna. *Hand Clin.* 1987;3(1):81-102.

19. Weiss A-PC. Scapholunate ligament reconstruction using a bone-retinaculum-bone autograft. *J Hand Surg Am.* 1998;23(2):205-215.
20. Watson H, Weinzweig J, Guidera PM, Zeppieri J, Ashmead D. One Thousand Intercarpal Arthrodeses. *J Hand Surg J Br Soc Surg Hand.* 1999;24(3):307-315.
21. Kleinman WB. Long-term study of chronic scapho-lunate instability treated by scapho-trapezio-trapezoid arthrodesis. *J Hand Surg Am.* 1989;14(3):429-445.
22. Wyrick JD, Stern PJ, Kiefhaber TR. Motion-preserving procedures in the treatment of scapholunate advanced collapse wrist: Proximal row carpectomy versus four-corner arthrodesis. *J Hand Surg Am.* 1995;20(6):965-970.
23. Wyrick JD, Youse BD, Kiefhaber TR. Scapholunate ligament repair and capsulodesis for the treatment of static scapholunate dissociation. *J Hand Surg Br.* 1998;23(6):776-780.
24. Werner FW, Short WH, Green JK. Changes in patterns of scaphoid and lunate motion during functional arcs of wrist motion induced by ligament division. *J Hand Surg Am.* 2005;30(6):1156-1160.
25. Wu G, van der Helm FCT, Veeger HEJD, et al. ISB recommendation on definitions of joint coordinate systems of various joints for the reporting of human joint motion--Part II: shoulder, elbow, wrist and hand. *J Biomech.* 2005;38(5):981-992.
26. Short WH, Werner FW, Green JK, Masaoka S. Biomechanical evaluation of the ligamentous stabilizers of the scaphoid and lunate: Part II. *J Hand Surg Am.* 2005;30(1):24-34.
27. Lee SK, Zlotolow DA, Sapienza A, Karia R, Yao J. Biomechanical comparison of 3 methods of scapholunate ligament reconstruction. *J Hand Surg Am.* 2014;39(4):643-650.

28. Rosenwasser MP, Miyasajsa KC, Strauch RJ. The RASL procedure: reduction and association of the scaphoid and lunate using the Herbert screw. *Tech Hand Up Extrem Surg.* 1997;1(4):263-272.
29. Garcia-Elias M, Lluch AL, Stanley JK. Three-ligament tenodesis for the treatment of scapholunate dissociation: indications and surgical technique. *J Hand Surg Am.* 2006;31(1):125-134.
30. Hom S, Ruby LK. Attempted scapholunate arthrodesis for chronic scapholunate dissociation. *J Hand Surg Am.* 1991;16(2):334-339.
31. Aviles AJ, Lee SK, Hausman MR. Arthroscopic reduction-association of the scapholunate. *Arthroscopy.* 2007;23(1):105.e1-e5.
32. Moran SL, Cooney WP, Berger RA, Strickland J. Capsulodesis for the treatment of chronic scapholunate instability. *J Hand Surg Am.* 2005;30(1):16-23.
33. Werner FW, Palmer AK, Somerset JH, et al. Wrist joint motion simulator. *J Orthop Res.* 1996;14(4):639-646.

# Chapter 4

## 4 *General Discussion and Conclusions*

### *Overview*

*This chapter summarizes the objectives and hypotheses outlined in Chapter 1, and the major conclusions of each study. The strengths and limitations are reviewed, as are the testing methods used to investigate carpal kinematics in the intact and injured state. Current and future research directions are discussed.*

## 4.1 Summary

This work was performed to improve the current state of knowledge of scaphoid and lunate kinematics during planar wrist motions in both the intact and injured states. This research elucidates the normal flexion-extension motion of the scaphoid and lunate in the native wrist, as well as following sequential sectioning of the scapholunate ligament and secondary stabilizers. The specific objectives outlined at the beginning of this work have been accomplished with results supporting previous hypothetical predictions, as well as some unexpected results.

The objectives of this thesis were:

1. To determine the normal kinematics of the capitate, scaphoid, and lunate during unconstrained wrist flexion-extension;
2. To determine the effect of the scapholunate (SL) ligament sectioning on scaphoid and lunate motion throughout planar wrist flexion-extension and radial-ulnar deviation and;
3. To determine the effect of the secondary stabilizers including: the scaphotrapezium-trapezoid (STT) ligament and radioscapocapitate (RSC) ligament on scaphoid and lunate kinematics throughout planar wrist flexion-extension and radial-ulnar deviation.

The hypotheses and findings of the studies detailed in Chapter 2 and 3 which sought to fulfill the aforementioned objectives, are reviewed and summarized in the following sections.

#### 4.1.1 *Chapter 2: Biomechanical Evaluation of Carpal Kinematics During Simulated Wrist Motion*

The first objective of this thesis was to investigate the normal kinematics of the scaphoid, lunate, and capitate during unconstrained wrist flexion and extension. The goals of the objective were achieved through the use of a passive wrist motion simulator. The major flexor and extensor muscle groups were tone loaded and an investigator simulated planar wrist flexion-extension by passively moving each specimen through the desired range of motion. Optical trackers were affixed to the bones of interest in order to track wrist motion and capture carpal kinematics.

The results described in Chapter 2 suggest a relative collaboration of the scaphoid, lunate, and capitate throughout planar wrist flexion and extension. Throughout wrist motion, the scaphoid contributed a greater extent to wrist motion when compared to the lunate. Scaphoid and lunate motion was found to correlate linearly with the capitate throughout wrist flexion-extension, with both carpals contributing more during wrist flexion compared to extension. In addition, the results show that the ratio of scaphoid and lunate rotation to wrist rotation decreases as the moves from flexion to extension, suggesting the radiocarpal joint plays a more critical role during wrist flexion and the midcarpal joint plays a larger role in wrist extension. The large magnitude of intercarpal motion between the scaphoid and lunate throughout wrist flexion and extension may account for the high levels of scapholunate ligament injuries relative to other intercarpal ligaments. These results confirm the first hypothesis that the scaphoid and lunate contribute at varying levels throughout wrist flexion and extension as stated in Chapter 1.

#### 4.1.2 ***Chapter 3: Biomechanical Evaluation of the Scapholunate Ligament and Secondary Stabilizers on Scaphoid and Lunate Kinematics***

The second objective of this research was to determine the effect of SL ligament sectioning on scaphoid and lunate kinematics throughout planar wrist flexion and radial-ulnar deviation. Similarly, the third objective of this thesis was to determine the effect of the two possible secondary stabilizers, the STT and RSC ligaments, on scaphoid and lunate kinematics throughout planar wrist flexion-extension and radial-ulnar deviation. The goals of the second and third objective were accomplished using an active wrist motion simulator, different from the simulator used in Chapter 2. Planar wrist flexion-extension and radial-ulnar deviation was achieved via a force-position algorithm to apply force directly to the muscle tendons of interest. Optical trackers were attached to the bones of interest to track wrist motion and capture the kinematics of the scaphoid and lunate throughout wrist motion.

The results discussed in Chapter 3 support the hypothesis, stated in Chapter 1, that the SL ligament is the primary stabilizer of the SL joint, as sectioning this structure caused the largest angular change in SL kinematics during wrist flexion-extension and radial-ulnar deviation. The results also support the hypothesis, stated in Chapter 1, that the STT and RSC ligaments are secondary ligamentous restraints to the SL joint, as sectioning these structures induced further postural changes in scaphoid and lunate kinematics throughout wrist flexion-extension and radial-ulnar deviation. Following sectioning of the SL ligament and secondary stabilizers, the scaphoid flexed significantly more during wrist flexion and the lunate extended more throughout wrist flexion-extension and radial-ulnar deviation. Additionally, there was a significant increase in intercarpal SL motion throughout wrist flexion-extension and radial-ulnar deviation. Each additional stage caused a small but significant increase in the relative rotation of the lunate with respect to the scaphoid in the direction of flexion during wrist flexion-extension and radial-ulnar deviation. As the angular changes recorded were significant but smaller than those encountered clinically, the findings within Chapter 3 suggest that there are likely additional soft-tissue restraints that contribute to the stability and maintenance of normal SL kinematics that were not evaluated in this study.



## 4.2 Strengths and Limitations

Similar to all *in vitro* biomechanical studies, the work presented within this thesis had various strengths and limitations. Both studies had adequate power in spite of the relatively small specimen population likely due to the highly reproducible simulator and the use of a repeated measure ANOVA with multiple measurements acquired for each specimen. The studies presented within Chapters 2 and 3 utilized a highly accurate motion capture system which likely reduced measurement noise and increased reproducibility. Real time kinematic measurements permitted joint angle tracking throughout the entire tested range of wrist motion, which permitted the representation of dynamic wrist motion with a high resolution. Contrasting similar *in vitro* biomechanical studies, the present work maintained all soft tissues structures and any incisions were closed throughout testing, to more accurately mimic *in vivo* conditions. Chapter 2 and 3 were performed using different but both previously validated testing apparatuses accurately simulating planar wrist motions.

The limitations of this thesis are similar to any *in vitro* biomechanical study using cadaveric specimens. To eliminate any unsuitable specimens, all wrists were examined prior to testing to rule out any underlying wrist pathologies using CT scans and fluoroscopy. Both studies only analyzed carpal kinematics during planar wrist motions and did not account for complex multiplanar motions such as dart throw and circumduction. Likewise, carpal kinematics were only considered in the plane of flexion-extension, not taking into consideration the complex three dimensional movements occurring during wrist motion. This study analyzed wrist motion using both active and passive motion simulators. The study in Chapter 2 was performed using a passive motion simulator whereas the study in Chapter 3 was performed using an active motion simulator. The passive motion simulator produced wrist motions with the musculature tone loaded and an investigator passively manipulating the position of the wrist using a guiding track. Applying tone loads provides more clinically relevant results, however the magnitude of tone load which was added may not replicate loads encountered clinically. Additionally, human manipulation may result in varied movements and may result in externally applied forces and moments, affecting the reliability of the results. The active motion simulator

produced wrist motion by actively actuating musculature using physiologically accurate lines of action directly to the muscle tendon of interest. Pulling from the true line of action of the muscle reduces the potential for joint laxity and more effectively reproduces an *in vivo* loading scenario. While this simulator provides more reproducible motion pathways than a passive system it is unlikely that the loads applied precisely reproduce those that occur clinically.

### 4.3 Current and Future Directions

The current studies have achieved the specific objectives outlined at the beginning of this thesis, providing a broad overview of carpal kinematics during planar wrist motions. Future work is needed to further investigate carpal kinematics in both the intact and injured state.

Although the studies outlined in Chapters 2 and 3, measured carpal motion using six degrees of freedom they were limited to analyzing carpal kinematics in one plane, future work will report on the three dimensional rotational and translational carpal movements throughout wrist motion. This information will provide a better indication of how each carpal bone is moving in the intact state and how the kinematics are altered following injury. Similarly, future studies should study more complex multi-planar motions of the wrist joint including dart throw and circumduction; as these motions often occur during *in vivo* wrist motion. Additionally, future efforts should investigate the changes in articular contact at the SL joint following the sequential sectioning of the SL ligament and secondary stabilizers; which may aid in understanding the secondary degenerative outcomes that occur following a SL injury.

Future work should also change the sequence of sectioning should be altered to permit the investigation of the individual stabilizing role of each ligament throughout wrist motion. In addition, future efforts should investigate the relative role of additional secondary scapholunate stabilizers including the scaphocapitate, short and long radiolunate, and dorsal radiocarpal ligaments on scaphoid and lunate kinematics. Additionally, future work should investigate the effect of cyclic loading following the sequential sectioning of the ligamentous structures, offering a more accurate simulation of an *in vivo* loading scenario with ligament attenuation over time. Following further investigation of the effect of the scapholunate ligament and secondary stabilizers on scaphoid and lunate kinematics, different scapholunate ligament repair and reconstruction techniques should be tested and compared.

#### 4.4 Significance

Carpal kinematics have been studied extensively both *in vitro* and *in vivo*, yet there remains no agreement regarding the relative contribution of each bone to total wrist motion. A more comprehensive understanding of carpal kinematics is also essential in the diagnosis and treatment of injuries of the hand and wrist. This information is of paramount interest as many injuries arising within the wrist present as an alteration of intercarpal motion. A more detailed understanding of carpal kinematics allows for a more effective evaluation of the wrist joint under both normal and pathological conditions. In addition, this research may assist in the design and development of prosthetic devices, and assist in improving the outcomes of partial wrist fusions and ligament reconstructions.

Injuries to the scapholunate joint are one of the most common causes of carpal instability, accounting for a considerable degree of wrist dysfunction and pain. Isolated scapholunate ligament injuries often lead to cartilage wear, altered joint kinematics, and additional degenerative changes. Management of scapholunate ligament injuries aims to slow this degenerative process by facilitating ligament healing or reconstructing the ligament in an effort to normalize carpal kinematics and articular loading. As there is currently no definitive standard in treating scapholunate ligament injuries, recommendations often vary and frequently result in poor long-term outcomes for patients. A more thorough understanding of the individual role and stabilizing function of the scapholunate ligament and secondary stabilizers will assist in the development of more effective treatment strategies following scapholunate ligament injuries.

## *Appendices*

### *Appendix A – Glossary*

Active Motion	Muscle forces to move a joint, force applied directly to the muscle group of interest.
Anterior	Directed to the front; opposite of posterior.
Arthritis	A disorder affecting the joints that can have a number of causes including inflammation, degeneration, or post traumatic.
Arthroplasty	The surgical reconstruction or replacement of a joint; restores function.
Articular Surface	Connection made between two bones within the body.
Capsulodesis	Orthopedic technique, joint capsule rigidly attached to a bone to reduce range of motion.
Casting	The act of encasing an extremity in a cast.
Debridement	Process of removing non-living tissue from a wound.
Deviation	Moving away from the midline of the body.
Dislocation	Displacement of a bone from its native articulation within a joint.
Distal	Located away from the origin or line of attachment.
Extension	Motion moving two segments of the body apart.
Fixation	The act of holding, suturing, or fastening an extremity in a fixed position.
Flexion	Motion bringing two segments of the body closer together.
Inferior	Located below, or directed downwards.
<i>In vitro</i>	Latin; an experiment or process conducted outside of a living organism.
<i>In vivo</i>	Latin; an experiment or process conducted within a living organism.
Lateral	Directed away from the midline of the body.

Ligament	Fibrous connective tissue that connects bone to bone; supports and strengthens joints.
Medial	Directed towards the midline of the body.
Osteoarthritis	Degeneration of articular cartilage; results in adaptive bone stiffening and reduces joint functionality.
Posterior	Directed to the back, opposite anterior.
Proximal	Located towards the origin or line of attachment.
Pronation	At the forearm, hand and upper limb turned inwards.
Splinting	The act of encasing an extremity in a splint; rigid fixation technique.
Subluxation	Incomplete or partial dislocation of a joint.
Superior	Located above, or directed upwards.
Supination	At the forearm, hand and upper limb turned outwards.

*Appendix B – Carpal Tracker Mounts*



**Figure B-1: Scaphoid Tracker Mount.** Illustration of the scaphoid tracker mount inserted through a volar incision over the tuberosity. Secured with  $\varnothing$  2.7mm cortical bone screws.



**Figure B-2: Lunate Tracker Mount.** Illustration of the lunate tracker mount inserted through a dorsal incision over the midpoint of the body. Secured with  $\varnothing$  2.7mm cortical bone screws.



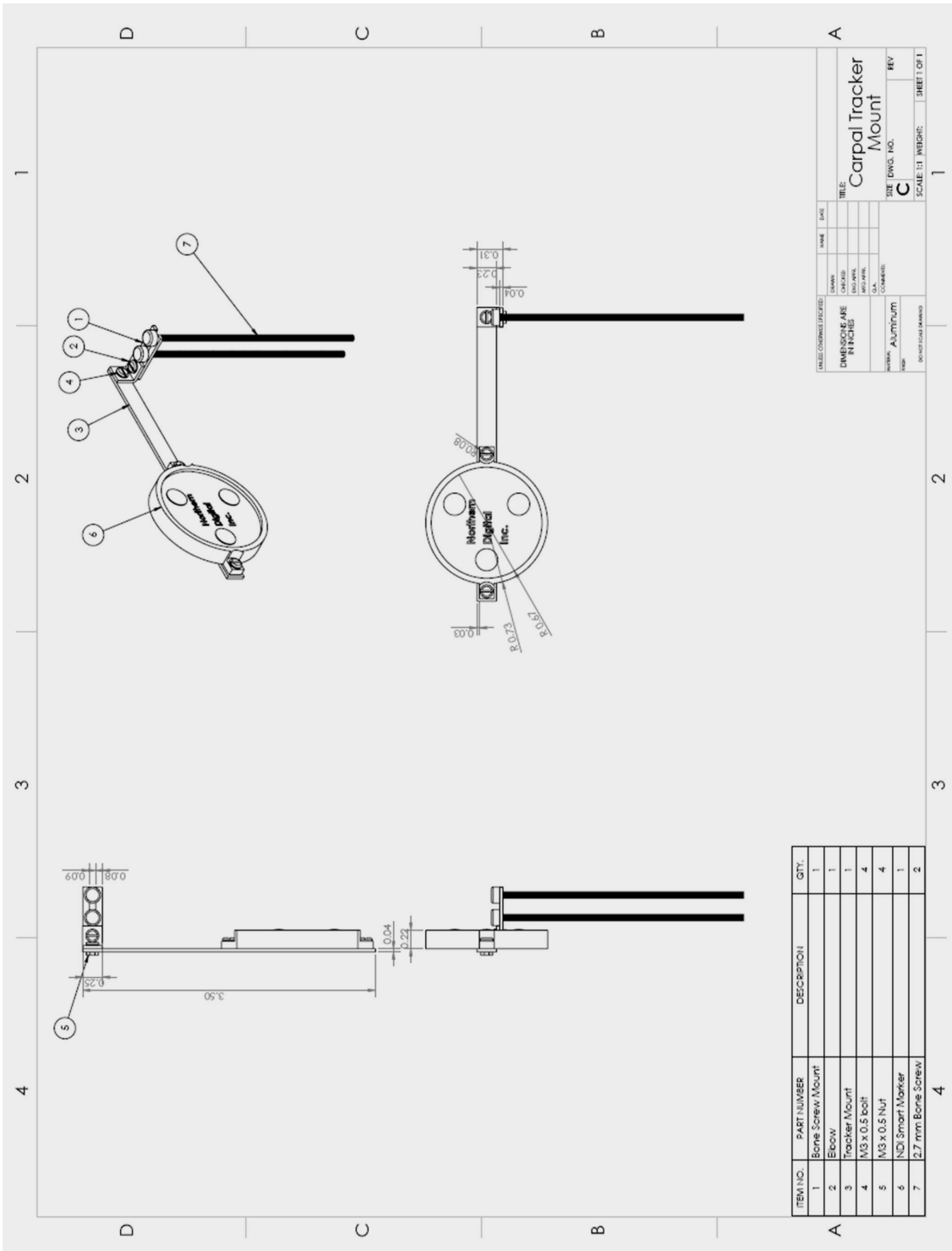


**Figure B-3: Carpal Tracker Mount.** Drawing used to machine the carpal tracker mounts. The mounts were designed with three degrees of freedom allowing for variable set up. Accounts for inter-specimen variability and visibility issues.

## ***Appendix C – Carpal Coordinate System Construction***

### **Background**

The International Society of Biomechanics (ISB) recommends carpal coordinate systems for each bone to be aligned with the radial coordinate system when the wrist is in the neutral anatomical position, when the long axis of the third metacarpal and radius are parallel. The volumetric centroid of the bone is defined as the origin of each carpal coordinate system. This method accounts for the variations between the different carpals, and relates the coordinate systems to the relative geometry of the wrist.

### **Digitization and Registration**

Following the completion of the investigation, the bones of interest were resected and isolated. The surface of the scaphoid, lunate, and capitate third-metacarpal were traced using an optical stylus (Certus Optotrack, Northern Digital Inc., Waterloo, Canada) and saved as a point cloud. A CT scan of each carpal bone was obtained and modified using ParaView, an open source application, to create an equally distributed surface mesh of the surface. Using custom software, the mesh created from the CT scan and the digitization mesh were reoriented and registered into the same frame using a least-squares data fitting algorithm with visual confirmation. All digitization points were discarded and the registered surface mesh was averaged to obtain the volumetric centroid and serve as the origin for each carpal coordinate system.

### **Coordinate Systems Construction**

To report relative carpal kinematics during wrist motion, we determined the transformation required to bias the initial set of carpal data to the neutral reference frame. To construct this transformation, a regressive search algorithm was used to determine the instance of most neutral wrist position, obtained from the third metacarpal with respect to the radius, and a 4x4 transformation matrix was constructed using the origin of the carpal of interest and the 3x3 rotation matrix of the radius (Fig. C-1)

$$\begin{bmatrix} r_{11} & r_{12} & r_{13} & L_x \\ r_{21} & r_{22} & r_{23} & L_y \\ r_{31} & r_{32} & r_{33} & L_z \\ 0 & 0 & 0 & 1 \end{bmatrix}_{radius} \begin{bmatrix} L_x \\ L_y \\ L_z \\ 0 & 0 & 0 & 1 \end{bmatrix}_{carpal} \rightarrow \begin{bmatrix} r_{11} & r_{12} & r_{13} & L_x \\ r_{21} & r_{22} & r_{23} & L_y \\ r_{31} & r_{32} & r_{33} & L_z \\ 0 & 0 & 0 & 1 \end{bmatrix}_{neutral\ carpal}$$

**Figure C-1: Construction of the Neutral Carpal Frame**

Following the construction of the neutral carpal frame, the transformation required to convert the original data from to the neutral frame can be calculated. Both frames share the same origin resulting in a rotation bias to convert one to the other. This transformation was collected for each carpal bone and applied to each frame within the data set.

$$[T_{NC}^G] = [T_C^G][T_{NC}^C]$$

Where:

$[T_{NC}^G]$  → Neutral carpal frame with respect to global

$[T_C^G]$  → Original carpal frame with respect to global

$[T_{NC}^C]$  → Original carpal frame with respect to neutral carpal frame

By rearranging the equation we are able to isolate the necessary transformation, and apply it accordingly:

$$[T_{NC}^C] = [T_C^G]^{-1}[T_{NC}^G]$$

# HELEN STOESSER

---

## EDUCATION

The University of Western Ontario, London, Ontario <b>MESc, Biomedical Engineering, Biomechanics</b>	<b>2014-2016</b>
Thesis: Biomechanical Evaluation of Carpal Kinematics During Simulated Wrist Motion	
The University of Guelph, Guelph, Ontario <b>B.ENG, Biomedical Engineering</b>	<b>2010-2014</b>

## AWARDS AND CERTIFICATIONS

Western Research Graduate Scholarship	<b>2014-2016</b>
Lawson Internal Research Fund	<b>2014-2016</b>
Top Poster Presentation for Orthopaedic Trauma at the 2016 Canadian Bone and Joint Conference	<b>2016</b>
University of Guelph Top Entrance Scholarship	<b>2010</b>
Earl B MacNaughton Entrance Scholarship into the College of Engineering Science Honors	<b>2010</b>

## RESEARCH EXPERIENCE

Roth McFarlane Hand and Upper Limb Centre, St Joseph's Healthcare, London, Ontario <b>Research Assistant</b>	<b>2014-2016</b>
<ul style="list-style-type: none"><li>• Developed a laboratory protocol to assess the effect of sequential sectioning of the scapholunate ligament and secondary ligaments on carpal kinematics</li><li>• Designed and developed, and manufactured carpal bone trackers utilized in <i>in-vitro</i> cadaveric testing protocols</li><li>• Established an integrated a carpal bone coordinate system adhering to the International Society of Biomechanics recommendations</li><li>• Conducted optical motion tracking studies to evaluate post injury joint kinematics</li></ul>	

## TEACHING EXPERIENCE

The University of Western Ontario, London, Ontario **Jan 2016-April 2016**  
**Teaching Assistant- Biomechanics of the Musculoskeletal System**  
Coordinated tutorial sessions; prepared and presented lectures;  
proctored examinations; marked assignments and reports

The University of Waterloo, Waterloo, Ontario **March 2016**  
**Invited Lecturer- Engineering Biomechanics**  
Prepared and presented lecture material for a fourth year  
engineering biomechanics class

The University of Western Ontario, London, Ontario **Sept 2015-Dec 2015**  
**Teaching Assistant – Introductory Engineering Design and**  
**Innovation Studio** **Sept 2014-April 2015**  
Instructed and supervised design studios; prepared and  
presented lectures; proctored examinations; graded  
assignments, laboratory books, and formal reports

The University of Guelph, Guelph, Ontario **May 2014-Aug 2014**  
**Science and Engineering Instructor- Creative Encounters with Science**  
Organized and developed science and engineering workshops; planned  
and facilitated an interactive laboratory exercises to demonstrate  
science and engineering concepts

## PUBLICATIONS

**Stoesser, H.L.**, Padmore, C.E., Nishiwaki, M., Gammon, B., Langohr, G.D.G., Johnson, J.A. Biomechanical Evaluation of Carpal Kinematics During Simulated Wrist Motion. *Accepted to The Journal of Wrist Surgery*

Padmore, C.E., **Stoesser, H.L.**, Nishiwaki, M., Gammon, B., Langohr, G.D.G., Lalone, E.A., Johnson, J.A., King, G.J.W. The Effects of Distal Radius Deformities on Wrist Kinematics - An *In-Vitro* Biomechanical Study. *For Submission to The Journal of Hand Surgery.*

## PEER REVIEW ACTIVITY

*Journal of Biomechanics (Ad-Hoc Reviewer)* **2016**

## CONFERENCE PRESENTATIONS

- Carpal Kinematics During Simulated Wrist Motion*** **June 2016**  
Podium Presentation at the 2016 Annual Meeting of the Canadian Orthopaedic Association/ Canadian Orthopaedic Research Society, Quebec City, QC
- The Effects of Distal Radius Deformities on Wrist Kinematics – An In-Vitro Biomechanical Study*** **June 2016**  
Podium Presentation at the 2016 Annual Meeting of the Canadian Orthopaedic Association/ Canadian Orthopaedic Research Society, Quebec City, QC
- Biomechanical Evaluation of Carpal Kinematics During Simulated Wrist Motion*** **April 2016**  
Poster Presentation at the 2016 Biennial Canadian Bone and Joint Conference, London, ON
- Capitate, Scaphoid, and Lunate Kinematics During Simulated Wrist Motion*** **March 2016**  
Poster Presentation at the 2016 Annual London Health and Research Day, London, ON
- Carpal Kinematics During Simulated Wrist Motion*** **March 2016**  
Podium Presentation at the 2016 Annual Meeting of the Orthopaedic Research Society, Orlando, FL
- The Effects of Distal Radius Deformities on Wrist Kinematics – An In-Vitro Biomechanical Study*** **March 2016**  
Podium Presentation at the 2016 Annual Meeting of the Orthopaedic Research Society, Orlando, FL

## EMPLOYMENT EXPERIENCE

- Sarnia Girls Soccer Club, Sarnia, ON** **Summer 2014**  
*Program Director and Camp Coordinator*
- Sunset Golf, Sarnia, ON** **2011-2014**  
*Facility Management*
- Creative Encounters with Science, Guelph, ON** **Summer 2013**  
*Science and Engineering Instructor at the University of Guelph*

## DESIGN PROJECTS

**Biomedical Engineering Design IV**, University of Guelph, Guelph, ON

**Winter 2014**

*Combination Polypectomy Multi-Tool*

- Designed and constructed an innovative colonoscope combination tool to improve the current medical technology
- Improved procedural time, resources consumed, and polyp extraction techniques for routine colonoscopies

**Clinical Biomechanics**, University of Guelph, Guelph, ON

**Winter 2014**

*Gender Differences in the Biomechanics of the Knee Joint During a Stop Jump Test and the Effects on ACL Loading*

- Investigated the differences in the biomechanics of the knee joint for recreational athletes during a stop jump
- Conducted a clinical biomechanical research study incorporating six test subjects requiring a full technical analysis and discussion

**Biomechanical Engineering Design**, University of Guelph, Guelph, ON

**Fall 2013**

*Wheelchair Seat Cushion Optimization for ALS Patient*

- Redesigned the current wheelchair seat cushion structure utilized by an ALS patient
- Improved the patient's spinal stability, frontal and lateral slippage, and comfort

**Bioinstrumentation Design**, University of Guelph, Guelph, ON

**Fall 2013**

*BatheAssist Assistive Device*

- Designed and constructed an assistive device to detect the temperature and water level of a bathtub within an acceptable range for the elderly and people with dementia
- Integrated a temperature and ultrasonic proximity sensor to alert the user when their bathtub water or temperature is too high

**Engineering Biomechanics**, University of Guelph, Guelph, ON

**Winter 2013**

*Study of Shod Running Versus Vibram Five Finger Shoes*

- Quantified the differences between Vibram Five Finger shoes compared to conventional running shoes with respect to biomechanical efficiency and metabolic economy

## VOLUNTEER EXPERIENCE

**Faculty of Biomedical Engineering, The University of Western Ontario**  
*Graduate Sports Representative*

**2015-2016**

- Organized intramural sports on behalf of the Faculty of Biomedical Engineering
- Facilitated sporting events

**Guelph Engineering Society, University of Guelph**  
*Special Events Coordinator*

**2013-2014**

- Acted as a student representative for the School of Engineering
- Organized and Facilitated charity events
- Participated in weekly meetings resolving issues surrounding the School of Engineering, its students, and its curriculum

**School of Engineering, University of Guelph**  
*Ambassador of Engineering*

**2011-2014**

- Acted as a liaison between prospective engineering students and the School of Engineering
- Facilitated campus tours and led information sessions